THE EFFECT OF PHENOTYPIC HETEROGENEITY ON PANCREATIC CIRCULATING TUMOR CELL CAPTURE AND TUMOR SPHEROIDS

A Dissertation

Presented to the Faculty of the Graduate School

of Cornell University

in Partial Fulfillment of the Requirements for the Degree of

Doctor of Philosophy

by

Fredrik Ivar Thege

January 2017

THE EFFECT OF PHENOTYPIC HETEROGENEITY ON PANCREATIC CIRCULATING TUMOR CELL CAPTURE AND TUMOR SPHEROIDS

Fredrik Ivar Thege, Ph.D.
Cornell University 2017

Pancreatic cancer is the third-leading cause of cancer-related death in the US and represents a difficult challenge to modern medicine, with increasing incidence and modest improvements in treatment outcomes. Pancreatic cancer is characterized by aggressive metastatic progression and high rates of resistance to chemotherapy, and there are currently no reliable biomarkers for early detection. In addition, clinicians are faced with difficult decisions regarding the potential benefit of surgical intervention in high-risk individuals, as pancreatic resection often has serious side effects. As such, there is an acute need for the development of improved biomarkers for early detection and to guide treatment. There is also a need for the development of *in vitro* models to study processes that lead to increased complexity in pancreatic cancer, including processes that lead to increased intra-tumor heterogeneity. The research projects described in this thesis are centered around the question of how phenotypic heterogeneity in pancreatic cancer cells influences the performance of platforms engineered to analyze rare cells in patient blood samples, and the self-assembly of cancer cells into tumor spheroids.

These endeavors were spurred on by our early observation that circulating epithelial cells can be isolated from patients with precancerous pancreatic cyst lesions (Chapter 2), and that analysis of these cell populations may serve as a biomarker to stratify patients for surgical intervention. In later studies

we have strived to optimize capture of pancreatic circulating tumor cells in a microfluidic immunocapture platform (Chapter 3), and elucidate what effect the epithelial to mesenchymal transition (EMT) and the acquisition of chemoresistance has on its performance (Chapter 4). In parallel, we have developed *in vitro* models of resistance to gemcitabine chemotherapy to study how the associated phenotypic changes lead to changed cell-sorting behavior in tumor spheroids, and how this influences the response to chemotherapy of the cancer cell population as a whole (Chapter 5).

In addition to the scientific contributions described in the thesis chapters, this work has resulted in the development of a range of engineering tools, *in vitro* models of EMT and microtumor formation, and the establishment of a large panel of chemoresistant pancreatic cancer cell lines, all of which can be used to enable further research into this area.

BIOGRAPHICAL SKETCH

Fredrik Thege was born and raised in Malmö, Sweden. He graduated with a Master of Science in Biotechnology from Lund University in 2011. During his M.S. studies he conducted research on droplet microfluidics in the laboratories of Dr. Abraham Lee at University of California, Irvine and Dr. Damien Baigl at École normale supérieure, Paris. In the fall of 2011 he started his PhD studies in Biomedical Engineering at Cornell University, supervised by Dr. Brian Kirby. In the summer of 2015 he conducted research on sequencing of vesicle-packaged microRNAs as a Visiting Scientist at the Center for Cell Circuits at the Broad Institute of MIT and Harvard working in Dr. Aviv Regev's laboratory. During his PhD, Fredrik has explored a wide range of research topics, spanning microfluidic immunocapture of pancreatic circulating tumor cells, cancer-cell derived exosomes and microvesicles, 3D models of cancer tumors and molecular chemoresistance mechanisms. While at Cornell University, Fredrik has been supported by the Lester B. Knight, Jr. Scholarship Number Two, a HHMI Med-into-Grad Scholarship and the Lester and Sheila Robbins Scandinavian Graduate Student Fellowship.

Till mina föräldrar,

som jag har att tacka för allt

ACKNOWLEDGEMENTS

Firstly, I would like to thank my advisor Dr. Brian Kirby, for his mentorship and for giving me the freedom to follow my research interests and intuition, sometimes far outside the beaten path. I would also like to thank the other members of my committee; Dr. Claudia Fischbach, Dr. Robert Weiss and Dr. Richard Cerione. Through the years of my PhD studies, I have had crucial interactions with each of my committee members, conversations that have helped me navigate the interdisciplinary field of Biomedical Engineering.

I owe many thanks to Dr. Marc Antonyak, for his amazing patience and generosity, especially during many long conversations regarding my research projects and for training me in several core biological research methods and techniques. Through my PhD studies I have also benefitted greatly from the expertise and guidance from several key collaborators, including Dr. Andrew Rhim and Dr. Tracy Stokol.

The research projects described in this thesis would not have been possible if it was not for the expertise and help from the some of the excellent core facilities at Cornell University, including the Biotechnology Resource Center (BRC), the Nanobiotechnology Center (NBTC) and the Cornell Flow Cytometry Core. In particular I would like to thank Dr. Peter Schweitzer, Dr. Teresa Porri, Penny Burke, Carol Bayles and Dr. Johanna Dela Cruz for all their help and guidance.

I would also like to thank all of my, past and present, co-workers in the Kirby Research Group, especially John Hartman and Dr. Timothy Lannin, for their help and solidarity through the years of graduate school. I also owe much gratitude to my stellar undergraduate students, whose hard work and dedication has been indispensable for my research, in particular I want to highlight the contributions made by Conor Gruber, Ian Cardle and Sophie Cong.

I have made many amazing friends while living in Ithaca, friendships I hope will last for many years to come and without which finishing this degree would not have been possible. Finally, I would like to thank my partner, my family and my friends for their support and care.

PDAC	pancreatic ductal adenocarcinoma
PC	pancreatic cancer
IPMN	intraductal papillary mucinous neoplasm
MCN	mucinous cystic neoplasm
GEDI	geometrically enhanced differential immunocapture
CTC	circulating tumor cell
CEC	circulating epithelial cell
CPC	circulating pancreatic cell
PBMC	peripheral blood mononucleated cell
HUVEC	human umbilical vein endothelial cell
EMT	epithelial-to-mesenchymal transition
CT	computerized tomography
MRI	magnetic resonance imaging
RT-PCR	reverse transcription polymerase chain reaction
qPCR	quantitative polymerase chain reaction
FISH	fluorescence in-situ hybridization
IF	immunofluorescence
WB	Western blotting
MPM	multiphoton microscopy

DNA	deoxyribonucleic acid
RNA	ribonucleic acid
mRNA	messenger RNA
siRNA/siR	small interfering RNA
NDP	nucleoside diphosphate
dNDP	deoxynucleoside diphosphate
CDP	cytidine diphosphate
dCDP	deoxycytidine diphosphate
kb/Mb	kilobases/megabases
kDa	kilo Dalton, kilograms per mole
SNP	single nucleotide polymorphism
CNV	copy-number variation
ABC	antibodies bound per cell
IC50	half maximal inhibitory concentration
FBS	fetal bovine serum
BSA	bovine serum albumin
PBS	phosphate buffered saline
RPMI	Roswell Park Memorial Institute medium
DMEM	Dulbecco's modified Eagle's minimal essential medium
IMDM	Iscove's Modified Dulbecco's Medium
EGF	epidermal growth factor
TGFβ	transforming growth factor beta

CD45	cluster of differentiation 45, protein tyrosine phosphatase receptor type C
HER2	receptor tyrosine-protein kinase erbB-2
EGFR	epidermal growth factor receptor
EpCAM	epithelial cell adhesion molecule
MUC1	mucin 1
hMUC1	hypoglycosylated mucin 1
MUC4	mucin 4
CK	cytokeratin
CEA	carcinoembryonic antigen
Pdx-1	pancreatic and duodenal homeobox 1
KRAS	V-Ki-ras2 Kirsten rat sarcoma viral oncogene homolog
SMAD4	mothers against decapentaplegic homolog 4
MAPK	mitogen-activated protein kinase
ERK	extracellular signalregulated kinases
Zeb1	zinc finger E-box-binding homeobox 1
RNR	ribonucleotide reductase
RRM1	ribonucleoside-diphosphate reductase subunit M1
RRM2	ribonucleoside-diphosphate reductase subunit M2
RRM2B	ribonucleoside-diphosphate reductase subunit M2B, p53R2
dCK	deoxycytidine kinase
STIM1	stromal interaction molecule 1
RhoG	ras homolog family member G
ER	endoplasmatic reticulum
SOCE	store operated calcium entry
dFdC	2′,2′-difluorodeoxycytidine, Gemcitabine
MTT	3-(4,5-dimethylthiazol-2-yl)-2,5-diphenyltetrazolium bromide
DAPI	4′,6-diamidino-2-phenylindole

TABLE OF CONTENTS

LIST OF FIGURES

CHAPTER 1

INTRODUCTION

1.1 Pancreatic cancer

Pancreatic cancer is the third-leading cause of cancer-related death in US and is predicted to become the second-leading cause by 2030[1]. In 2016 an estimated 53,000 new cases were recorded, and nearly 42,000 deaths were attributed to pancreatic cancer, in the US alone[2]. The predicted increase in overall pancreatic cancer mortality in the coming decades is due to increased incidence in combination with only minor improvements in treatment outcomes. Currently the overall 5-year survival rate for pancreatic cancer is approximately 8%[2].

When diagnosed with pancreatic cancer, patents are stratified in Stages I to IV; localized and resectable tumor (Stage I and II, 10% of cases), locally advanced/unresectable tumor (Stage III, 30% of cases) or disseminated disease with one or more metastatic sites (Stage IV, 60% of cases)[3]. 95% of pancreatic cancers originate in the exocrine pancreas and 80% of cases are categorized as pancreatic ductal adenocarcinomas (PDAC)[4], which will be the focus of this thesis. PDAC is characterized by rapid and aggressive progression[5], and a majority of patients develop widely metastatic disease with many secondary lesions[6]. As with other cancer types, metastasis is responsible for a large majority of pancreatic cancer-related deaths.

PDAC pathogenesis occurs through the development of histologically distinct precursory lesions, most frequently through the development of

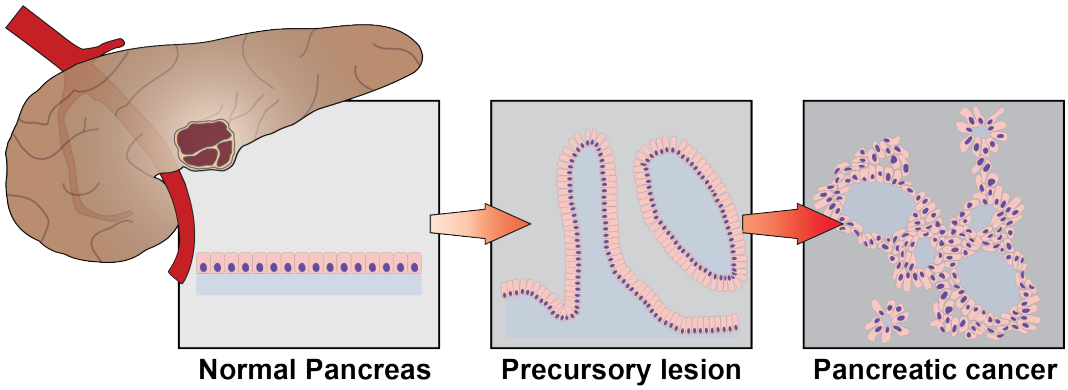

Figure 1.1: Progression of pancreatic cancer through precursory lesions

pancreatic intraepithelial neoplasias (PanINs), see figure 1.1. However, a minority of PDAC tumors develop through intraductal papillary mucinous neoplasms (IPMNs), and mucinous cystic neoplasms (MCNs)[4]. Unlike PanINs, IPMNs and MCNs are in many cases detectable through standard imaging modalities such as CT scans or MRI. PDAC arising from IPMNs and MCNs tend to be less aggressive than PanIN-derived PDAC, and only a subset of IPMNs will progress to invasive carcinomas. IPMNs can be resected, but a significant fraction of resected specimens show no evidence of high-grade neoplasia and resection comes with significant risk and severe side effects (brittle diabetes and exocrine deficiency). Patients with IPMNs thus represent a high-risk population with complicated clinical management and difficult treatment considerations[7].

As 90% of PDAC patients present with unresectable disease, chemotherapy is often the only treatment option. Chemotherapy is typically administered in the form of the nucleoside analog gemcitabine (2',2'-difluorodeoxycytidine, dFdC, Gemzar), although other treatment regimens, such as 5FU or FOLFORINOX, are sometimes used[4]. Recently, a combination therapy of gemcitabine and nab-paclitaxel (abraxane) has shown increased efficiency[8].

However, the response to any pancreatic cancer chemotherapy is typically short-lived and the overall effect on patient survival is modest.

Considering the aggressive nature of metastatic pancreatic cancer and the poor response to chemotherapy, targeting the process of metastasis itself, the metastatic cascade, holds a lot of promise for improving the treatment outcomes of pancreatic cancer.

1.2 The metastatic cascade

The metastatic cascade involves a series of events and processes that result in the spread of a localized cancer tumor to one or more distant, or metastatic, sites. Depending on the type of cancer and the tissue of origin, several routes of metastatic dissemination are possible[9], including dissemination through the lymphatic system, through shedding of cancer cells into tumor-adjacent cavities and dissemination through the blood stream. Here, the discussion will be limited to metastatic spread through the blood stream, referred to as hematogenous dissemination, a schematic of which can be seen in figure 1.2.

In order for a cancer tumor to metastasize through the blood stream, cancer cells have to gain the ability to (1) break down the local environment surrounding the primary tumor, (2) invade into the blood stream, (3) survive the unfamiliar environment of the circulatory system, (4) avoid detection by the immune system, (5) successfully lodge at a distant site, (6) break through the vessel lining into the surrounding tissue (extravasate) and (7) be able to establish a proliferating secondary lesion at a distant site[10].

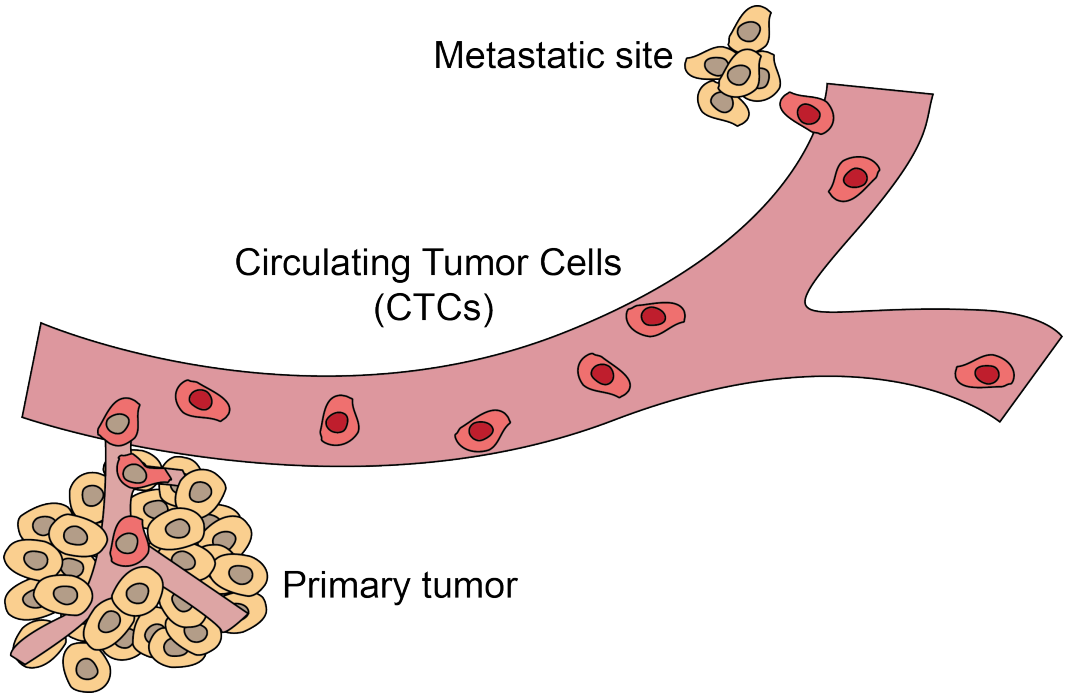

Figure 1.2: The role of CTCs in the metastatic cascade

Consequently, metastasis is a very inefficient process and only a tiny fraction of disseminated cancer cells (<0.01%) are thought to have the ability to form a metastatic lesion[11][10]. The initial steps of the metastatic cascade requires a breakdown of the epithelial characteristics of the tissue of origin, most notably the organization of epithelial cells into tightly regulated epithelial sheets. Several cellular processes are implicated in the development of traits that allow cancer cells to break down this epithelial structure, including the epithelial to mesenchymal transition (EMT)[12].

1.3 The epithelial to mesenchymal transition (EMT) and chemoresistance

The epithelial to mesenchymal transition (EMT) is a process, first observed in the context of embryonic morphogenesis, where epithelial cells lose some or all their epithelial characteristics and develop traits associated with mesenchymal cells[13][14][15]. More specifically, epithelial cells undergoing EMT lose cell polarity, cell-cell junctions, association with a basement membrane, and gain motility, invasiveness, and resistance to anoikis and apoptosis[15]. As such, EMT leads to the breakdown of the highly organized epithelial tissue. EMT is implicated in several pathological processes, including fibrosis[16] and cancer[15]. In cancer, EMT is associated with the onset of metastasis and the development of chemoresistance[11][17].

Numerous studies have shown that EMT can be induced in some non-cancerous epithelial cells and cancer cells *in vitro* by treatment with growth factors, most commonly TGFβ[18][19][20][21][22][23][24]. As EMT allows for cancer cells to free themselves of the cell-cell adhesions that normally keep the integrity of epithelial tissues, EMT is thought to be major contributor to the dissemination of circulating tumor cells (CTCs) into the blood stream, referred to as intravasation[11]. In addition, the development of chemoresistance *in vito*, particularly to gemcitabine, has been associated with the development of cellular EMT-characteristics[25][26][27].

1.4 Circulating tumor cells (CTCs)

Circulating tumor cells (CTCs) are cancer cells that have left the local environment of a primary tumor or metastatic site, and invaded into the blood stream. CTCs are believed to be responsible for seeding metastasis at distant sites[12]. EMT is thought to be necessary for CTC dissemination, and CTCs displaying mixed epithelial/mesenchymal characteristics have been widely observed in patient samples[28][29][30] and mouse models of cancer metastasis[11].

Dissemination of cells from precancerous lesions has been observed in some contexts[11][31], and these cells are typically referred to as circulating epithelial cells (CECs) or circulating pancreatic cells (CPCs) (in the context of pancreatic cysts) rather than CTCs, as they may or may not display carcinogenic traits and their connection with cancer has not been fully determined. However, CEC have also been found in non-cancerous inflammatory conditions[32]. In addition to their proposed mechanistic role in cancer progression, CTCs have been extensively explored as cancer biomarkers for early detection, prognostics and prediction of response to therapy, in a wide range of cancer types, including pancreatic cancer[12].

1.5 CTC isolation methods

The wide range of techniques and platforms have been developed for the isolation of CTCs from patient blood samples[33]. What underpins the technical difficulty in isolating CTCs is their extreme rarity. It is estimated that there may

be as few as 1 CTC in ten billion blood cells in the peripheral blood of a cancer patient[12]. The only FDA approved method for CTC isolation is the CellSearch system. CellSearch uses anti-EpCAM antibody-coated magnetic beads to isolate CTCs from patient blood samples. CTCs are then identified as CD45-negative mono-nucleated cells expressing cytokeratin.

Of particular relevance to this thesis are the microfluidic methods for CTC capture that have been developed over the last decade. Nagrath et al. demonstrated the first microfluidic chip technology for isolation of CTCs from whole blood using an array of microposts coated with antibodies[34]. Since then, countless microfluidic platforms for CTC capture have been developed, most notably the herringbone chip[35], the Vortex chip[36] and the CTC-iChip[37]. The Kirby Research Group has developed a microfluidic platform that uses a combination of size-selection and antibody-antigen recognition to isolate CTC from whole blood, called the Geometrically Enhanced Differential Immunocapture (GEDI) platform[38][39].

1.6 CTCs in the management of pancreatic cancer

The development of CTC biomarkers for clinical use has attracted intense interest in the last decade. This is the direct result of a confluence of developments in the areas of cancer research, clinical care and technical capabilities. Firstly, as the survival-rates of localized and resectable carcinomas has increased across the board, metastasis has emerged as the single process responsible for a vast majority of cancer-related deaths. Biomarkers that are directly linked to the development of metastasis, such as CTCs, have thus come

to the forefront of the collective cancer research consciousness.

Furthermore, personalized medicine has been suggested to be the future of cancer therapy, as patient stratification and targeted therapies have become increasingly important in the clinical management of many cancer types. As such, personalized medicine requires more detailed profiling of each patient than what most standard clinical patient evaluation methods offer. Molecular profiling of patients requires the access to, and analysis of patient samples, most often acquired through biopsies. However, it has become evident that the molecular profile of a patient's cancer is neither static in time nor space, as tumor phenotype has been found to vary within a tumor and through the course of treatment. Fully personalized medicine would thus, require repeated invasive biopsies to be taken from the patient's primary tumor and/or metastatic sites, which is often neither possible nor acceptable to the patient. CTC isolation and analysis has been suggested as an alternative to traditional biopsies[32]. Requiring only the collection of a peripheral blood sample, CTC analysis may serve as a minimally invasive "liquid biopsy". This would allow for CTC biomarkers to be readily incorporated into the clinical care of many cancer patients, as regular blood draws are already part of standard clinical cancer management.

In the case of pancreatic cancer, the limited response to treatment in many patients, and the often very aggressive course of the disease, often prevents attempting multiple therapies in a step-by-step fashion to find an effective treatment[40]. Tumor tissue would be valuable for monitoring patient response to therapy, however the pancreas is inaccessible for biopsy without surgical intervention. In this context, a minimally invasive biomarker that can

help guide clinical decision-making could be transformative. In pancreatic cancer, the correlation between size of the primary tumor and the disease aggressiveness and clinical outcome, is weaker than in many other cancer types[31][11]. It is often observed that patients present with multi-focal metastatic disease with only a small primary pancreatic tumor. Standard imaging modalities that measure static tumor size or tumor load may thus be intrinsically less relevant to pancreatic cancer than biomarkers that incorporate functional information. CTCs represent one such class of real-time biomarkers that are directly linked to the disease mechanism that ultimately leads to patient death.

CTCs are of key disease mechanistic importance, as a subset of CTCs are believed to give rise to distant metastasis[11]. Metastasis is responsible for more than 90% of deaths associated with pancreatic cancer, and a large majority of patients present with metastatic disease. In addition, CTC dissemination has been shown to occur early in pancreatic carcinogenesis in both mouse models and human cancer patients[11]. These factors make CTC biomarkers especially advantageous in the early detection of pancreatic cancer. CTC biomarkers can thus be approached from both the perspective of targeting the small subpopulation of CTCs believed to seed distant metastases, as well as the overall CTC load and phenotype. While the former is relevant to early disease and early detection, the latter may directly measure how active a patient's cancer is and thus be relevant to late stage disease and response to treatment.

1.6.1 Pancreatic CTC biomarkers for screening and diagnostics

CTC capture and identification from patient blood samples could potentially be used to screen patients for carcinogenesis. However, due to the relatively low, albeit rising, incidence of pancreatic cancer, and the cost associated with CTC analysis, a general CTC-based screening approach for pancreatic cancer is currently not feasible. CTC biomarkers may, however, be useful for screening patients with increased risk, complementary to standard imaging modalities such as MRI and endoscopic ultrasound. Unfortunately, relatively few risk factors for pancreatic cancer are known. However, risk factors for pancreatic cancer include a strong history of pancreatic cancer (familial pancreatic cancer) and a few rare hereditary conditions, including Peutz-Jeghers syndrome, hereditary pancreatitis, hereditary p16 mutations, BRCA1 and BRCA2 mutations[41]. As circulating epithelial cells have been found in patients with precancerous pancreatic conditions[31], circulating cell biomarkers may be useful in the monitoring and risk stratification of patients known to be at increased risk. To date, no studies have been published examining the presence of circulating cells in patients with known risk factors for hereditary or familial pancreatic cancer. This is most likely a direct result of these conditions being very rare, and sporadic pancreatic cancer (pancreatic cancer with no known risk factors) accounting for 95% of cases[42].

1.6.2 CTCs as prognostic and predictive biomarkers in pancreatic cancer

CTCs have been found to be prognostic in many human cancers, including breast[43], prostate[44], non-small-cell lung cancer[45] and colorectal cancer[46]. However, CTCs have been proven to be relatively difficult to isolate from pancreatic cancer patients as compared to other cancers, such as breast and prostate cancer. This observation has not been fully explained but the hypovascularization observed in many pancreatic tumors, direct shuttling of pancreatic CTCs to the liver through the portal vein and early onset of EMT, making CTCs undetectable by conventional CTC capture platforms, have been suggested as potential partial explanations.

A number of studies have aimed to determine the prognostic potential of CTCs and disseminated cells in PDAC, with varying and sometimes contradictory results[47][48][49][50][51][52][53][54][55][56][57]. A large portion of this variation can be explained by considering the diverse set of technologies utilized to isolate and analyze CTCs, the variation in the definition of what is considered to be a CTC and the difference in the composition of the patient group studied. Most studies use antibody-antigen recognition or size-based technologies to enrich their samples for CTCs. Downstream of enrichment, CTCs are in many cases identified using immunostaining criteria, or through detection of some CTC surrogate marker, such epithelial-specific mRNA transcripts. The wide range of technologies and CTC identification criteria used make interpreting results of CTC studies challenging, and studies should thus to be compared in the context of that particular technology and

CTC criteria. There is currently no consensus if CTCs are useful prognostic biomarkers in the clinical management of pancreatic cancer. Several studies have aimed to determine if CTC analysis can be used a predictive markers of response to chemotherapy in pancreatic cancer[58][53][40], showing, among other things, that the number and phenotype of CTCs present in blood changed after patients were started on chemotherapy.

1.6.3 Pancreatic CTCs as predictive biomarkers of benefit of resection in precancerous patients

The vast majority (90%) of patients diagnosed with pancreatic ductal adenocarcinoma present with locally advanced or metastatic disease[3]. For the minority of patients that present with localized disease, resection is usually recommended[59]. The decision of whether to resect or not is thus in most cases made only based on if the disease is localized or not, and if the patient is fit enough to benefit from the procedure. There is thus currently no need for a CTC biomarker to guide this decision.

However, there are patient groups where whether or not to resect a pancreatic abnormality is a more ambiguous question. Pancreatic cyst lesions represent a group of cystic abnormalities that are relatively common in the general population, of which a subpopulation will progress into cancer. The two main subtypes are intraductal papillary mucinous neoplasms (IPMNs) and mucinous cystic lesions (MCNs)[7]. IPMN lesions are pre-cancerous lesions that display some cancer like traits such as increased proliferation (neoplasia), and will in some patients develop into invasive ductal carcinoma with poor

patient survival and limited response to treatment. Pancreatic cysts are typically detected in patients during routine imaging procedures, such as CT or MRI scans. To evaluate the risk of progression and thus also the potential benefit of resecting the cyst, a rigorous set of criteria are used[7]. These criteria, known as the Sendai criteria, evaluate the cyst using standard imaging modalities to determine the size and localization of the cyst and weigh in the presence or absence of symptoms. Despite their rigor, the Sendai criteria only predict carcinogenesis in 60% of resected specimens. This means that for a significant portion of patients that undergo resection, no direct benefit can be shown. Bearing in mind that pancreatic resection is an invasive procedure with several common complications, including brittle diabetes and exocrine insufficiency, there is a strong incentive for the development of biomarkers that can predict the presence of carcinogenesis in pancreatic cysts and predict benefit of resection. As mouse model work has shown that CTC dissemination can occur prior to tumor formation[11], CTC biomarkers represent an attractive avenue to explore for the development non-invasive biomarkers in pre-cancerous at-risk patients. A pilot study of circulating epithelial cells in patients with pancreatic cyst lesions is described in Chapter 2.

1.7 Summary of introduction

Pancreatic cancer represents a difficult challenge to modern medicine, driven in large part by the early onset of metastatic disease and high rates of chemoresistance. Gemcitabine chemotherapy is the standard of care but suffers from limited efficacy. Metastasis is responsible for a vast majority of cancer-related deaths. However, the process of metastasis is very inefficient

and requires the interaction of multiple complex processes at different length scales. Circulating Tumor Cells (CTCs) are key players in the metastatic cascade and constitute a rare population of disseminated cancer cells present in peripheral circulating of cancer patients. A small fraction of CTCs are thought to give rise to metastasis by establishing secondary tumors at distant sites. The dissemination of CTCs is thought to require the loss of epithelial characteristics and a gain in mesenchymal traits. This phenotypic switch is thought to in part be orchestrated by a processes called the epithelial-to-mesenchymal transition (EMT). In addition to facilitating CTC dissemination, EMT has been linked to the development of chemoresistance. A wide range of techniques, including the GEDI microfluidic device, have been developed to isolate CTCs from patient samples. CTCs have been explored as biomarkers for pancreatic cancer in a variety of clinical settings. In particular CTCs show promise in the early detection setting and as a potential biomarker of early pancreatic carcinogenesis in high-risk patients. However, the effect of EMT and chemoresistance on the performance of CTC isolation techniques has not been fully investigated. Furthermore, EMT and chemoresistance are known to dramatically alter the phenotype of cancer cells and can thus be expected to influence cancer cell behavior on many levels.

CHAPTER 2

DETECTION OF CIRCULATING PANCREAS EPITHELIAL CELLS IN PATIENTS WITH PANCREATIC CYSTIC LESIONS

This chapter adapted from the article

Andrew D. Rhim, Fredrik I. Thege, Steven M. Santana, Timothy B. Lannin, Trisha N. Saha, Shannon Tsai, Lara R. Maggs, Michael L. Kochman, Gregory G. Ginsberg, John G. Lieb, Vinay Chandrasekhara, Jeffrey A. Drebin, Nuzhat Ahmad, YuXiao Yang, Brian J. Kirby, and Ben Z. Stanger, Detection of Circulating Pancreas Epithelial Cells in Patients With Pancreatic Cystic Lesions. Gastroenterology 119 (2014). doi:10.1053/j.gastro.2013.12.007

2.1 Abstract

Hematogenous dissemination is thought to be a late event in cancer progression. We recently showed in a genetic model of pancreatic ductal adenocarcinoma that pancreas cells can be detected in the bloodstream before tumor formation. To confirm these findings in humans, we used microfluidic geometrically enhanced differential immunocapture to detect circulating pancreas epithelial cells in patient blood samples. We captured more than 3 circulating pancreas epithelial cells/mL in 7 of 21 (33%) patients with cystic lesions and no clinical diagnosis of cancer (Sendai criteria negative), 8 of 11 (73%) with pancreatic ductal adenocarcinoma, and in 0 of 19 patients without cysts or cancer (controls). These findings indicate that cancer cells are present in the circulation of patients before tumors are detected, which might be used in risk assessment.

2.2 Contributions to this chapter

Andrew Rhim and Brian Kirby were responsible for the study concept, analysis, and interpretation of data; Andrew Rhim, Michael Kochman, and Brian Kirby were responsible for the study design; Andrew Rhim, Michael Kochman, Gregory Ginsberg, John Lieb, Vinay Chandrasekhara, Jeffrey Drebin, Nuzhat Ahmad, Trisha Saha, Shannon Tsai, and Lara Maggs were responsible for patient enrollment; Andrew Rhim, Fredrik Thege, Steven Santana, Timothy Lannin, Michael Kochman, Brian Kirby, Trisha Saha, and Shannon Tsai were responsible for the acquisition of data; Andrew Rhim and YuXiao Yang were responsible for the statistical analysis; Andrew Rhim was responsible for the drafting of the manuscript; Andrew Rhim, Fredrik Thege, Michael Kochman, Gregory Ginsberg, Vinay Chandrasekhara, Jeffrey Drebin, YuXiao Yang, Brian Kirby, and Ben Stanger were responsible for critical revision of the manuscript.

2.3 Results and Discussion

A widely accepted paradigm in cancer biology is that epithelial cancers progress in a linear manner whereby cancer-defining properties are acquired sequentially[60]. In this model, cancer cells acquire metastatic potential after large primary tumors are established. However, in pancreatic ductal adenocarcinoma (PDAC), the linear progression model cannot be reconciled with clinical observations. A number of patients undergoing pancreatectomy for chronic pancreatitis will develop disseminated PDAC, although only precancerous pancreatic intraepithelial neoplasias, but no tumors, are found

on histologic analysis[61]. In addition, in patients with small primary tumors (<2 cm) who have no clinical evidence of metastatic disease, 5-year survival after pancreatectomy is less than 18% owing to recurrent metastatic disease[62]. These data suggest that metastatic seeding may occur before the formation of large primary tumors. Moreover, we recently showed that hematogenous dissemination occurs before tumor formation, in a lineage-labeled genetic model of PDAC[11], at which time the pancreas contained only pancreatic intraepithelial neoplasias. Based on the clinical characteristics of PDAC and our findings within a recapitulative mouse model, we hypothesized that bloodstream seeding of pancreas-derived epithelial cells can occur in patients with clinical evidence of only precancerous lesions of the pancreas and no detectable invasive carcinoma. To test our hypothesis, we performed a blinded prospective pilot study of 3 cohorts, as follows: (1) patients with no history of cancer presenting for average-risk, age-appropriate colonoscopy screening and no adenomas detected; (2) patients with precancerous cystic lesions (intraductal papillary mucinous neoplasm [IPMN] or mucinous cystic neoplasms) of the pancreas with no evidence of tumor or metastasis on computerized tomography or magnetic resonance imaging, who did not qualify for surgery using the Sendai criteria[63] (including no evidence of dysplasia or cancer on fine-needle aspiration, if performed); and (3) patients with cytology-confirmed PDAC. Peripheral blood was obtained from patients who consented before the procedure. We analyzed blood samples using geometrically enhanced differential immunocapture (GEDI), a microfluidic platform that has been shown to detect circulating tumor cells from patients with prostate cancers with high sensitivity[38][39]. Here, we functionalized the GEDI device using antibodies to epithelial cell adhesion molecule to capture

circulating epithelial cells (CECs). Captured cells then were stained with 4',6-diamidino-2-phenylindole (DAPI) to visualize nuclei and fluorescently conjugated antibodies to CD45, a universal marker of leukocytes, and cytokeratin 19 (CK), a marker of epithelial-derived cells or pancreatic and duodenal homeobox protein-1 (Pdx-1), a pancreas-specific transcription factor. A blinded observer (B.J.K.) enumerated CECs using the following 2 definitions: (1) CD45-, DAPI+, and (2) CK+,CD45-,DAPI+ using a fluorescence microscope. Definition 1 was confirmed retrospectively with automated cell enumeration and 4-color immunofluorescence for epithelial and pancreas-specific markers.

Table 1. Patient Characteristics

	Age, y	Race	Sex	FHx	BMI	Smoking	EtOH, avg/wk	CA19-9 serum	CEA serum	CEC	Size of cyst/tumor, mm	Cyst type/ cancer stage
Cancer-free controls (n ¼ 19)	53	Cauc	M		35.7	Never	0			0		
	40	Cauc	M		26.3	Never	1			0		
	64	Cauc	F		28.3	Never	0			0		
	61	Cauc	M		31.0	Never	1			0		
	48	Cauc	F		21.0	Never	0			0		
	62	AAM	F		35.4	Never	0			0		
	74	Cauc	F		19.8	Never	0			0		
	56	AAM	F		24.7	Never	0.5			0		
	70	Cauc	M		26.4	Previous	0			0 (CK)		
	51	AAM	F		56.6	Never	0			0 (CK)		
	60	Cauc	M		29.5	Never	0			0 (CK)		
	66	Cauc	M		21.9	Never	1.5			0 (CK)		
	84	AAM	F		29.3	Never	0			0 (CK)		
	53	AAM	F		46.1	Never	0			0 (CK)		
	59	AAM	F		26.6	Never	0			1 (CK)		
	50	AAM	F		36.6	Never	1.5			2 (CK)		
	58	AAM	F		30.2	Never	0			3 (CK)		
	73	AAM	F		26.6	Never	0			0 (CK)		
	50	Cauc	F		24.0	Never	0			0 (CK)		
Mean	59.6				30.3					0.3 – 0.8		
Cystic lesion (n ¼ 21)	67	Cauc	F		31.6	Never	0			0	9	Side-branch IPMN, multiple
	62	Cauc	F	Y	20.2	Never	3		0	0	8	Side-branch IPMN
	64	Cauc	M		34.9	Never	5		86.7	0	16	MCN
	75	Cauc	M		24.3	Never	0			0	15	Side-branch IPMN
	65	Cauc	F	Y	22.4	Never	0			6	9.5	Side-branch IPMN
	60	Cauc	M		28.3	Never	0	1.9	22	16	14	Side-branch IPMN
	72	Cauc	M		21.3	Current	3		< 1	22	10	MCN
	81	Cauc	M		27.7	Never	6			0	15	Side-branch IPMN
	58	Cauc	M		20.7	Current	20			0	5	Side-branch IPMN
	64	Cauc	F	Y	18.0	Never	5	46	3.8	0	20	Side-branch IPMN
	73	Cauc	F		24.6	Never	0			4	14	Side-branch IPMN
	69	Cauc	F		27.8	Previous	4			0 (CK)	11	Side-branch IPMN
	68	Cauc	M		26.3	Previous	7			0 (CK)	3	Side-branch IPMN
	74	Cauc	F		26.6	None	0			19 (CK)	6.5	Side-branch IPMN
	81	Cauc	M		27.5	Previous	7			1 (CK)	25	Side-branch IPMN
	58	AAM	F		32.9	None	0			14 (CK)	5	Side-branch IPMN
	74	Cauc	F		21.7	None	0			0 (CK)	25	Side-branch IPMN
	65	Cauc	F		31.4	None	0			0 (CK)	28	MCN
	79	ASAM	M		21.5	None	0			12 (CK)	23	Side-branch IPMN
	77	Cauc	F		28.5	None	0	19	1.3	0 (CK)	28	Side-branch IPMN
	80	Cauc	M		29.9	None	0			0 (CK)	25	Side-branch IPMN
Mean	69.8				26.1					4.5 – 7.3		

Figure 2.1: Table of enrolled patients

We prospectively enrolled 48 patients (Table 1). Cyst- and cancer-free patients tended to be younger compared with the cystic lesion and PDAC cohorts (P $\bar{0}$.003). However, there were no differences in other demographics.

Table 1. Continued

	Age, y	Race	Sex	FHx	BMI	Smoking	EtOH, avg/wk	CA19-9 serum	CEA serum	CEC	Size of cyst/tumor, mm	Cyst type/ cancer stage
PDAC (n¼11)	92	Cauc	M									
	65	Cauc	M		27.0	Never	0	805	8.2	0	52	Stage I
	76	Cauc	M		33.5	Never	0			12	61	Stage IV
	69	Cauc	M		29.2	Current	3	764	46	59	91	Stage II
	65	Cauc	M		26.1	Current	1	127	39	33	33	Stage IV
	59	AAM	M		37.3	Previous	0	1256		3	23	Stage IIB
	70	Cauc	F		24.8	Previous	0	912		6	15	Stage III
	73	AAM	M		19.9	Previous	0	857		9	17	Stage IV
	62	Cauc	M		22.0	Never	0	410		0	40	Stage IV
	69	Cauc	M		29.4	Current	1	862		24	16	Stage IV
	83	AAM	F		25.5	Previous	1			4 (CK)	40	Stage IV
					27.3	Never	0			5 (CK)	27	Stage IV
Mean	71.2				27.4					14.1 – 18.1		

NOTE. CK, denotes quantification of CECs using definition 2, CKþ/DAPIþ/CD45-. Otherwise, CECs were quantified using definition 1 (DAPIþ/CD45-).
AAM, African American; ASAM, Asian American; Cauc, Caucasian; CEA, carcinoembryonic antigen; FHx, family history; MCN, mucinous cyst neoplasm.

Figure 2.2: Table of enrolled patients, cont'd

Most (85%) cystic lesions were classified as side-branch IPMNs. The size of cystic lesions varied from 5 to 28 mm. Patients with PDAC had a wide range of primary tumor diameters (15-91 mm) and tumor stages (I-IV). Sixteen of 19 cancer-free controls had no CECs by either definition, see figure 2.3B. When CECs were detected, there were no more than 3/mL. Seven of 9 (78%) patients with PDAC had detectable CECs, with an average of 16.2 ± 19.5 CEC/mL blood ($P < 0.0001$ compared with cancer-free patients by the MannWhitney test). Eight of 21 (40%) patients with cystic lesions of the pancreas had detectable CECs, averaging 4.5 ± 7.3 CECs/mL blood ($P = 0.022$ compared with cancer-free patients), and there was a significant difference in CECs across the 3 groups by 1-way analysis of variance ($P = 0.015$). Interestingly, there was no significant difference in the number of CECs detected among cyst lesion patients based on the immunofluorescence definition used (figure 2.3B; black denotes definition 1, red denotes CEC analysis from different patients using definition 2); that is, a similar percentage of cyst lesion patients contained CECs by either definition, and, when CECs were detected in these patients, a similar concentration was found. We found no correlation with CEC count and tumor or cyst size, cancer stage or serum carbohydrate antigen 19-9 (CA19-9) and carcinoembryonic antigen.

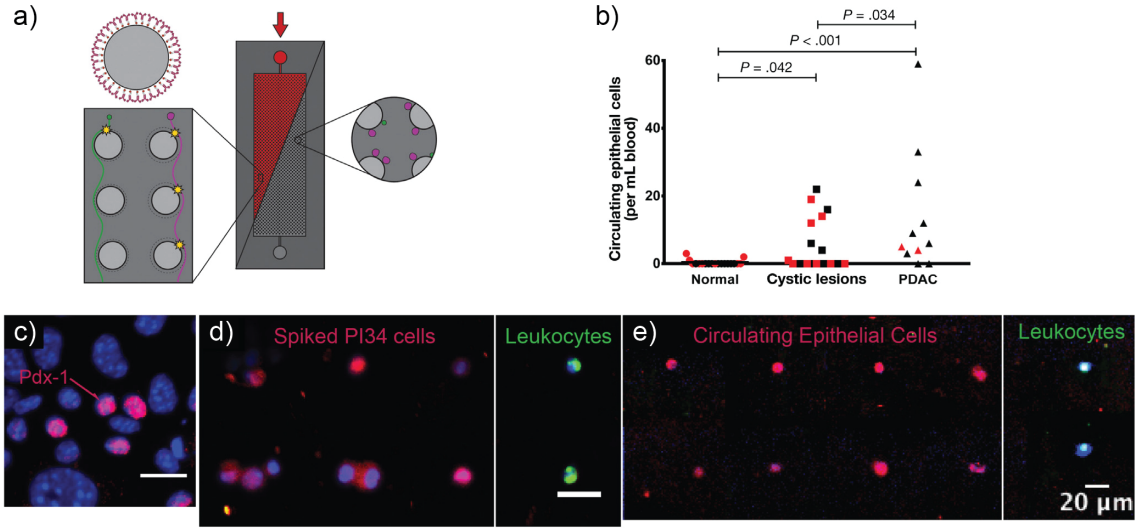

Figure 2.3: Detection of CECs in patients using GEDI. a) Depiction of the GEDI device. b) Vertical scatterplots of CEC concentrations (per milliliter blood) for cancer-free patients (control), patients with cystic lesions of the pancreas without dysplasia or tumor (cystic lesion), and patients with PDAC. Bars indicate statistically significant differences using the MannWhitney test. Representative images of individual GEDI-captured nucleated cells from c) PI34 cells in culture, d) control human blood spiked with PI34 cells and e) blood from a patient with PDAC. Cells were stained for CD45 (green), Pdx-1 (red), and DNA (DAPI, blue). Scale bar: 20 mm.

To confirm the pancreas origin of CECs, we stained cells for Pdx-1, a pancreas-specific transcription factor, expressed in up to 60% of all CECs in mouse models of PDAC4 (figure 2.3B). Adherent and GEDI-captured primary PDAC cells also expressed nuclear Pdx-1 (21% of PI34 and 10.7% of Panc-01; figure 2.3C). However, no nuclear Pdx-1 was detected within human breast (MCF-7) or prostate (LNCaP, CWR22Rv1) cancer cells or CD45+ leukocytes (data not shown). These data suggest that Pdx-1 is a specific marker of pancreas-derived cells. In our analyses, 29% of all CECs showed nuclear Pdx-1 staining (figure 2.3D). These data confirm that at least a portion of all GEDI-captured epithelial cells derive from the pancreas. In conclusion, we report that pancreas epithelial cells can enter the bloodstream in patients

with cystic lesions of the pancreas before the clinical diagnosis of cancer. By using state-of-the-art microfluidic technology and immunofluorescence staining, we confirmed the pancreas origin of captured CECs. Thus, these findings suggest that the ability to seed the bloodstream may precede the formation of detectable tumors, supporting our findings in genetic mouse models of PDAC[11]. These data are supported by the recent finding that 24.6% of resected side-branch IPMNs that do not satisfy Sendai criteria contain regions of high-grade dysplasia or invasive carcinoma[64]. Data from our mouse model predict that these cells represent early, occult cancer cells[11], although we do not yet have evidence to support this in human beings. Studies are underway to interrogate the genomic signature of CECs from cystic lesion patients. If these cells represent the earliest forms of cancer, we predict that they would contain a complement of somatic mutations associated with PDAC. Genomic analyses of CECs represent a technical challenge that recently was addressed elegantly using massively parallel sequencing of RNA from captured tumor cells from patients with PDAC[65]; however, cyst lesion patients contain many fewer CECs, complicating genomic analysis. Furthermore, it is still unknown if patients with CECs are destined to form tumors. If associated with sub-sequent tumor formation, CEC detection could be used as a biomarker for cancer risk stratification in patients at risk for PDAC. Studies underway in this regard will prospectively follow GEDI-analyzed cystic lesion patients to determine if CEC number or genomic analysis are predictive of an eventual diagnosis of PDAC.

CHAPTER 3

MICROFLUIDIC IMMUNOCAPTURE OF CIRCULATING PANCREATIC CELLS USING PARALLEL EPCAM AND MUC1 CAPTURE: CHARACTERIZATION, OPTIMIZATION AND DOWNSTREAM ANALYSIS

This chapter adapted from the article

Fredrik I. Thege, Timothy B. Lannin, Trisha N. Saha, Shannon Tsai, Michael L. Kochman, Michael A. Hollingsworth, Andrew D. Rhim, and Brian J. Kirby, Microfluidic immunocapture of circulating pancreatic cells using parallel EpCAM and MUC1 capture: characterization, optimization and downstream analysis, Lab on a Chip (2014). doi:10.1039/c4lc00041b

3.1 Abstract

We have developed and optimized a microfluidic device platform for the capture and analysis of circulating pancreatic cells (CPCs) and pancreatic circulating tumor cells (CTCs). Our platform uses parallel anti-EpCAM and cancer-specific mucin 1 (MUC1) immunocapture in a silicon microdevice. Using a combination of anti-EpCAM and anti-MUC1 capture in a single device we are able to achieve efficient capture while extending immunocapture beyond single marker recognition. We also detect a known oncogenic KRAS mutation in cells spiked in whole blood using immunocapture, RNA extraction, RT-PCR and Sanger sequencing. To allow for downstream single-cell genetic analysis, intact nuclei were released from captured cells by use of targeted membrane lysis. We have developed a staining protocol for clinical samples, including

standard CTC markers; DAPI, cytokeratin (CK) and CD45, and a novel marker of carcinogenesis in CPCs, mucin 4 (MUC4). We also demonstrate a semi-automated approach to image analysis and CPC identification, suitable for clinical hypothesis generation. Initial results from immunocapture of a clinical pancreatic cancer patient sample show that parallel capture may capture more of the heterogeneity of the CPC population. With this platform we aim to develop a diagnostic biomarker for early pancreatic carcinogenesis and patient risk stratification.

3.2 Contributions to this chapter

Fredrik Thege, Andrew Rhim and Brian Kirby were responsible for study idea. Fredrik Thege was responsible for study design. Andrew Rhim, Michael Kochman, Trisha Saha and Shannon Tsai were responsible for patient enrollment. Fredrik Thege was responsible for the acquisition of data and statistical analysis. Timothy Lannin was responsible for developing automated imaging and image analysis software and code.

3.3 Background and introduction

Pancreatic cancer (PC), the fourth leading cause of cancer-related death in the US and is associated with a poor 5-year patient survival rate of less than 5%. PC is characterized by rapid and often symptom-free progression, resulting in more than 90% of patients being diagnosed with metastatic disease[66], a stage at which there are no effective treatment options. Clinical data show

that the treatment outcome improves dramatically if PC is caught at an early stage, prior to the formation of clinically-detectable metastasis[66][67]. Early detection is thus the most efficient way to improve overall patient survival, but detection is limited by the absence of specific clinical biomarkers and non-invasive screening tests[67].

The formation of metastasis is attributed to the intravasation of cells from the primary site of disease into the blood stream, followed by transport to a secondary site where the cells extravasate, proliferate and form secondary lesions[68][69][70]. These cells are in general referred to as circulating tumor cells (CTCs). Here, we refer to any cell that disseminates from the pancreas into the blood stream as a circulating pancreatic cell (CPC). Recent results in a mouse model that recapitulates human pancreatic carcinogenesis have shown that dissemination of cells from the pancreas occurs prior to tumor formation[11]. Furthermore, we have recently shown that epithelial pancreatic cells can be found in the circulation of patients with pancreatic cyst lesions in the absence of overt tumor formation, making CPCs a more appropriate term for this cell population[31]. In future studies, early dissemination of CPCs could thus offer partial explanation to the rapid and aggressive progression observed in PC patients. Precancerous CPC dissemination also allows for the development of early detection biomarkers of pancreatic carcinogenesis.

CTCs have been shown to be prognostic of patient survival in a number of cancers and are suggested to be of disease mechanistic importance and of diagnostic value[71]. The extreme rarity of CTCs in peripheral circulation makes CTC isolation technically challenging. To allow for their efficient isolation, a range of microfluidic platforms have been developed[33]. These

platforms have explored a range of physical principles and geometries to achieve efficient and pure isolation, including; micropillar arrays[34][38][72], vortex-inducing microgrooves[35], microsieves and filters[73][74], magnetic microbeads[75] and inertial separation[36]. Some techniques rely solely on passive separation of CTCs based on physical parameters such as cell size and stiffness. However, a majority of techniques use an optimized surface capture chemistry to achieve CTC isolation. Immunocapture using surface functionalization of capture antibodies has emerged as the dominant technique for isolating CTCs in microfluidic devices[33] and relies on the collision of target cells with a immunofunctionlized surface. In these devices, the geometry serves to maximize the interaction of target cells with the capture chemistry. We have previously described one such geometry[38][39], that maximizes the cell-capture surface interaction of larger cells, such as CTCs, in combination with an optimized CTC capture chemistry. The choice of capture chemistry influences the resulting population of captured cells and needs to be optimized for each application and disease studied. Antibodies for different cancer and epithelial markers, such as epithelial cell adhesion molecule (EpCAM)[31][34], prostate specific membrane antigen (PSMA)[38][39], Her2[76][29] and EGFR[29] have been used to capture CTCs from a range of cancers. Due to their inherent difference in specificity and binding affinity the choice of antibody clone has been shown to dominate capture performance[77]. In the case of prostate cancer, the use of the tissue specific marker PSMA has been shown to result in superior capture as compared to capture using the commonly used marker EpCAM[39]. The capture chemistry should thus ideally be optimized for each specific application and for a specific cancer type. Here we aim to show that using recognition of a combination of two markers, both upregulated in PC,

we can achieve efficient CPC capture. We also aim to show that the choice of capture chemistry governs the phenotype of captured cells.

As previously stated, EpCAM is the most widely used target for immunocapture of CTCs[34][35][78][38]. However, there is mounting evidence that EpCAM is downregulated in CTCs from some clinical samples[29] and during the cancer-associated process referred to as epithelial-to-mesenchymal transition (EMT)[68], making EpCAM capture alone a potential source of bias for the capture of CPCs. In cancerous and precancerous tissues, EMT results in the development of an invasive phenotype[11][79][80] and has been shown to correlate with cancer progression[29]. On a cellular level, EMT results in the loss of epithelial markers and an upregulation of mesenchymal markers, as well as a gross change in cell morphology[11][79]. Furthermore, because recent PC mouse model data indicate the a vast majority of CPCs display an EMT phenotype, anti-EpCAM capture alone may fail to capture this potentially clinically significant CPC subpopulation. Breast cancer patient CTCs have been shown to express a dynamic range of EMT composition in a way that correlates with treatment outcome[29]. There is thus a pressing need to find alternative and/or complementary, EMT-robust capture modes. In this study we explore parallel anti-EpCAM and anti-mucin capture as a promising novel capture chemistry.

Mucins are a family of high-molecular-weight glycoproteins that are expressed by epithelial tissues, such as the respiratory and gastric linings as well as the ducts of the liver and pancreas, where they protect and lubricate the surfaces[81]. The founding member of this protein family, mucin 1 (MUC1) is expressed at a low level in healthy pancreas tissue, but has

been shown to be strongly upregulated in pancreatic carcinogenesis[81][82]. Furthermore, overexpression of MUC1 has been shown to increase cancer cell invasiveness and motility through the induction of EMT in a PC mouse model[83]. MUC1 expression in CTCs from metastatic pancreatic patients has also been associated with shorter median overall patient survival[50].The cancer-associated post-translational modification of MUC1 differs significantly from MUC1 found in healthy tissues[84]. Cancer-associated MUC1 is typically aberrantly hypoglycosylated[85][86] and the loss of cell polarity that occurs during carcinogenesis results in expression of MUC1 uniformly covering the cell membrane rather than being restricted to the apical side of the epithelial cell[86]. Furthermore, the aberrant expression pattern and hypoglycosylation of MUC1 exposes regions of the protein backbone to antibody binding, allowing for the creation of cancer-specific antibodies that bind minimally to MUC1 from healthy tissues[85][86]. An antibody specific to hypoglycosyled MUC1 (hMUC1) has previously been shown to induce cell adhesion when functionalized to the surface in a E-selectin cell-rolling assay[87]. Although MUC1 has been observed on the surface of some activated T-cells[88], the MUC1 expression level is low and of a distinct glycoform[89], making hMUC1 cancer cell specific in blood samples. Together, the strong upregulation, cancer-specific hypoglycosylation and change in spatial distribution, make hMUC1 an ideal target for the capture of CPCs in early carcinogenesis, allowing for the exploration of the link between capture chemistry and resulting phenotype of early disseminated CPCs.

The clinical implementation of a CPC capture platform relies on the specific and robust identification of captured CPCs and rejection of contaminating leukocytes. Cytokeratin (CK) is an epithelial marker that is frequently used as a

positive marker of CTCs[34]. However, CK has in patient samples been shown to be downregulated more than EpCAM during EMT[90]. Mucin 4 (MUC4) has been shown to be differentially upregulated in pancreatic carcinogenesis; MUC4 is not expressed by healthy pancreatic tissues but strongly upregulated in cancerous and precancerous neoplastic pancreatic lesions[84][91][92]. Since CK expression may be lost during pancreatic carcinogenesis, we suggest using CK and MUC4 as orthogonal positive indicators of CPC identity. The relationship between CK and MUC4 expression level in the CPC population may also be an indicator of the EMT state of the CPCs and thus be of prognostic importance. Since MUC4 expression has been shown to increase progressively in precancerous pancreatic neoplasias[91], the presence or absence of CPC MUC4 expression may be used for risk stratification of patients with precancerous conditions.

Despite the fact that enumeration of CTCs has been shown to be a prognostic biomarker in a number of common cancers, CTC enumeration has not yet been incorporated into standard clinical practice in the management of any cancer[32]. However, the integration of genetic analysis in parallel with cell enumeration may allow for the development of stronger biomarkers and incorporation of these in clinical practice[93]. The genetic analysis of CPCs may reveal early signs of pancreatic carcinogenesis, before any cancer is clinically observable, without requiring an invasive biopsy. Moving beyond CTC enumeration, genetic analysis can provide information about prognosis and disease progression. Genetic mutations in circulating cell populations have shown to be prognostic of treatment outcome in lung cancer[93]. The technical difficulty associated with genotyping circulating cells is considerable, owing to their rarity and the presence of contaminating wild-type genetic

material. Point mutations in circulating cell have been analyzed using mutation-specific qPCR[93]. A drawback of this approach is that it relies on the recognition of known SNPs using mutation-specific primers. As an alternative to genetic analysis, a mutational protein-level approach has recently been described, using an antibody specific to a mutated protein in the lysate from circulating cells[74]. However, this methodology relies on the availability of mutation-specific antibodies, only available for a subset of SNPs. Direct genetic sequencing represents the gold standard for genotyping and requires no previous knowledge of the particular mutation of interest. However, direct sequencing is sensitive to the presence of wild-type genetic material in the sample and can only be used in samples of high purity, i.e. if the number of mutated molecules is comparable to number of the wild-type molecules. In this respect, RNA level analysis may be more feasible than genomic level analysis as the mRNA copynumber of upregulated oncogenes, such as KRAS, can be assumed to be significantly higher in cancer cells compared to the wild-type cells.

Activating KRAS mutations represent some of the most common mutations in human carcinomas[94]. The KRAS gene encodes a small GTPase signaling protein that plays a fundamental role in cell growth regulation. KRAS mutations are found in more than 85% of patients with PC and in approximately 80% of patients with high-risk precancerous cystic lesions[94]. The molecular profiles of activating KRAS mutations are well described and a vast majority of mutations occur in codon 12 and 13 of the KRAS gene[95], which makes them suitable for analysis with RT-PCR-based amplification followed by genetic sequencing.

We have developed a microfluidic platform optimized to capture, identify and genotype CPCs, building on our previously described Geometrically Enhanced Differential Immunocapture (GEDI) device[39][38][72]. In this platform we explore capture chemistry as a design parameter and study its influence on the phenotype of captured cells. Our platform uses a combination of anti-EpCAM and anti-hMUC1 capture and allows for the release of intact cell nuclei and downstream KRAS oncogene genotyping.

3.4 Materials and methods

Device fabrication and functionalization

Devices were fabricated by A.M. Fitzgerald & Associates (Burlingame, CA) according to previously described specifications[38][39]. The silicon device surfaces were functionalized with NeutrAvidin (Thermo Fisher Scientific, Rockford, IL) with a previously described protocol[39]. The devices were functionalized with primary antibodies via biotinylated secondary linker antibodies. NeutrAvidin functionalized devices were (1) incubated with 10 μg/ml biotinylated goat anti-mouse antibody (Santa Cruz Biotechnology, Dallas, TX) and (2) incubated with either 10 μg/ml anti-EpCAM antibody (Clone 158206, R&D Systems, Minneapolis, MN), 10 μg/ml anti-MUC1 antibody (AR20.5) or 5 μg/ml anti-EpCAM and 5 μg/ml anti-MUC1 antibody. Control devices were functionalized with biotinylated normal (non-specific) mouse antibodies (Santa Cruz Biotechnology). All antibodies were prepared in 1% BSA in PBS.

Cell culture

Cell lines (Capan-1, PANC-1 and BxPC-3) were obtained from ATCC (Manassas, VA). All cell lines were cultured in humidified incubators (37 °C and 5% CO_2) using media recommended by ATCC (Capan-1: 20% FBS IMDM, PANC-1: 10% FBS DMEM and BxPC-3: 10% FBS RPMI) and 1X penicillin/streptomycin. Cells were used only below passage number 30 and cells were harvested after 4-6 days of culture at 60-80% confluency.

Quantitative flow cytometry

Cells were trypsinized for 5-10 minutes at 37 °C and then fixed with the Foxp3 fixation/permeabilization kit (eBioscience, San Diego, CA). Staining was performed with 0.5μg primary antibody/10^6 cells and 0.2μg PE-conjugated secondary antibody/10^6 cells in blocking flow cytometry staining buffer (eBioscience). Analysis was performed on a LSRII flow cytometer (BD Biosciences, San Jose, CA) and PE-Quantibrite beads (BD Biosciences) were used to quantify the antibodies bound per cell (ABC) count for this staining protocol. Data processing and calculation of the ABC counts were performed with custom MATLAB software.

Capture experiments

Cells were trypsinized for 5-10 minutes at 37 °C, labeled with 2μg/ml Calcein AM (Santa Cruz Biotechnology) for 45 minutes and resuspended in carrier

solution (1% BSA, 1 mM EDTA in PBS) at approximately 300 cells/ml. Peripheral blood mononuclear cells (PBMCs) were isolated from donor blood using Ficoll centrifugation, labeled with CellTracker orange (Invitrogen, Grand Island, NY) and resuspended at approximately 500 cells/ml. Functionalized silicon devices were mounted with Tygon tubing inlets and outlets in a PMMA holder. Cell capture was achieved by flowing 1 ml cell suspension through the device at 1 ml/h followed by manual cell enumeration using fluorescence microscopy.

Isolation of captured nuclei

Targeted cell membrane lysis and release of nuclei from captured cells was performed using overnight incubation with a modified NST buffer (117mM NaCl, 8 mM Tris base, 0.8mM $CaCl_2$, 38 mM $MgCl_2$, 0.04% BSA, 0.16% NP-40 surfactant in DI water) with and without DAPI (10μg/ml), based previously described method[96].

RNA sequencing

RT-PCR primers were designed to amplify a 249 bp fragment containing codon 12 of human KRAS using the NCBI primer-BLAST tool; forward: GGAGAGAGGCCTGCTGAAAA and reverse: CCCTCCCCAGTCCTCATGTA. The forward primer was designed to overlap on neighboring KRAS exons to increase the RNA specificity of the RT-PCR amplification. Calcein labeled Capan-1 cells were spiked in control blood at 300 cells per ml. The cells were captured using anti-EpCAM GEDI. After washing with PBS and cell

enumeration, RNA was extracted directly on-chip using the RNEasy kit (Qiagen). Extracted RNA from whole blood and Capan-1 cells spiked in PBS served as wild type and positive controls respectively. RT-PCR of extracted RNA was performed using a single tube reaction and the recommended protocol (OneStep, Qiagen); reverse transcription 30 min at 50 °C, PCR activation 15 min at 95 °C, 35 cycles of denaturation 45 s at 94 °C, annealing at 45 s at 61 °C and extension 1 min at 72 °C, followed by final extension 10 min at 72 °C. Successful KRAS cDNA amplification was confirmed using agarose gel separation. RT-PCR products were treated with alkaline phosphatase and exonuclease (ExoSAP-IT, Affymetrix) to remove remaining primers from RT-PCR reaction. Sequencing of GEDI captured samples and whole blood controls was performed by the Cornell Life Sciences Core Facility on an automated 3730xl DNA analyzer (Invitrogen), using Big Dye terminator chemistry, the reverse primer used for RT-PCR as sequencing primer and AmpliTaq-FS DNA polymerase (Invitrogen)

Capture and staining of clinical samples

Blood was obtained through venipuncture of a patient with clinically confirmed pancreatic ductal adenocarcinoma (PDAC). 1ml blood was processed through GEDI devices functionalized with anti-EpCAM, anti-hMUC1 and anti-hMUC1/EpCAM antibodies. Samples were fixed in 2% PFA in 50% PHEM buffer (60 mM PIPES, 25 mM HEPES, 10 mM EGTA and 2 mM $MgCl_2$) for 15 minutes and blocked in 6% BSA and 10% normal goat serum in PBS for 1 hour. After staining of surface markers, the samples were permeabilized with 0.25% (w/w) Triton x-100. The samples were stained

for MUC4 with a primary (ab60720; abcam, Cambridge, MA, USA) and an AlexaFluor 488 conjugated secondary antibody (Invitrogen), for CD45 with a Qdot-800 conjugated antibody (Invitrogen), for CK using a CF543 (Biotium, Hayward, CA, USA) conjugated anti-pan-CK antibody (C11; BioLegend, San Diego, CA, USA) and for DNA/nuclei using DAPI (Invitrogen). Samples were collected, processed, fixed and stained within 48h.

Clinical sample analysis

Stained samples were imaged using a Zeiss LSM Live Confocal Microscope (10x 0.3NA). All cell-sized DAPI+ events with brightness DAPI and CK barely above the background noise were identified using image processing in a custom MATLAB algorithm. The prescreened events were then classified as CPCs or non-CPCs using manual classification. DAPI+/CD45-/CK+, DAPI+/CD45-/MUC4+ and DAPI+/CD45-/CK+/MUC4+ were used as CPC criteria.

3.5 Results and discussion

Expression analysis in model cell lines

A panel of three PC cell lines (Capan-1, PANC-1 and BxPC-3) where used as models for CPCs in the development of the capture methodology. These cell lines represent cells isolated from both primary pancreatic tumors (PANC-1 and BxPC-3) and liver metastasis (Capan-1); cells in different states of

differentiation: Capan-1 (well differentiated), BxPC-3 (moderately to poorly differentiated) and PANC-1 (poorly differentiated); and varying mutation status of key oncogenes (KRAS, TP53, CDKN2A/P16 and SMAD4)[97] as well as distinct levels of MUC1 expression[98].

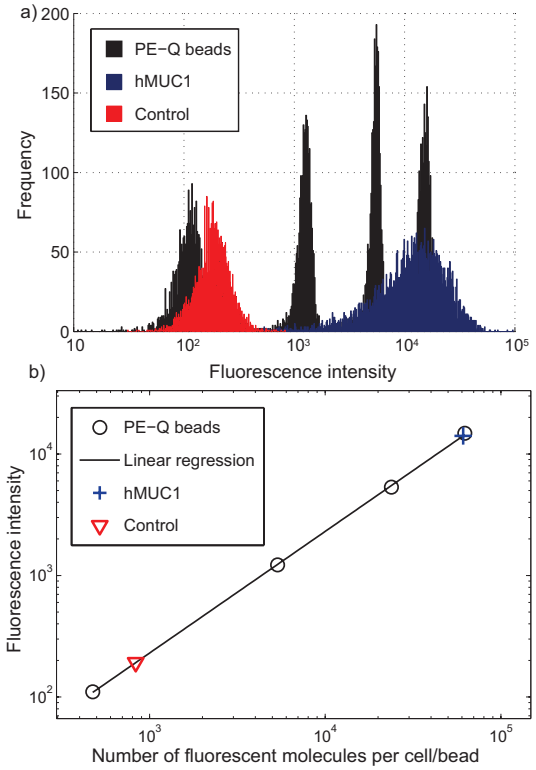

Figure 3.1: Calibration of the antibody bound per cell (ABC) count for determination of antibody binding in PC cell lines, a) histogram showing gated flow cytometry data of phycoerythrin (PE) labeled Quantibrite beads of four intensity levels (black), Capan-1 cells stained with control (red) and hMUC1 (blue) antibodies a) calibration of the ABC count with PE-Quantibrite beads.

The expression level of EpCAM and hMUC1 was determined with quantitative flow cytometry for all three cell lines, as shown in figure 3.1. Quantitative flow cytometry determines the antibodies bound per cell (ABC) count of a population of cells calibrated using beads with known numbers of bound fluorescent molecules. Candidate antibodies for immunocapture were selected based on strong and consistent staining across all three cell lines.

One anti-EpCAM (Clone 158206 mouse mAb, R&D) and one anti-hMUC1 (AR20.5[85] mouse mAb) antibody were identified as promising candidate antibodies for immunocapture. Figure 3.2 shows the resulting ABC counts for these antibodies and cell lines. Since we ultimately aim to determine the influence of capture chemistry design on resulting phenotype of captured cells, the choice of model cell lines is important. In addition to the reasons mentioned above, the flow cytometry results show that this panel of cell lines displays a wide range of expression levels of EpCAM and hMUC1. In our experiments, Capan-1 cells displayed the strongest staining for both EpCAM and hMUC1 whereas PANC-1 stained the weakest for both, with ABC counts ranging from ~10,000 to ~70,000 for the three cell lines. Previous studies have reported EpCAM ABC counts in the range of 2,000 to 500,000 in a variety of cancer cell lines[74]. Interestingly, the relative hMUC1 ABC counts between cell lines do not correlate with previously described mRNA expression levels of these cell lines[98]. We attribute this difference to intrinsic differences in mRNA and surface antigen quantification, the specific fixation protocol used as well as differences in MUC1 glycosylation, accumulation and turn-over. Previous work has highlighted the utility of EpCAM capture[99] for immunocapture of CTCs from many carcinomas, but the role of MUC1 remains less clear. Cocktail capture has been presented in multiple contexts[29]. However, parallel anti-EpCAM/hMUC1 capture has not been implemented in microdevice technology to date and this strategy allows implementation of a novel capture modality in a new device.

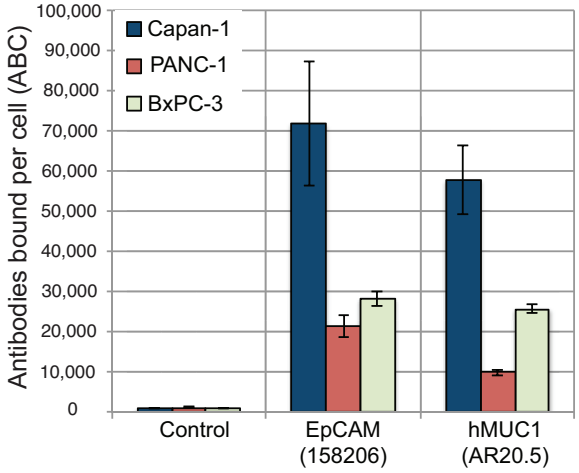

Figure 3.2: Antibody bound per cell (ABC) counts for EpCAM, hMUC1 and PE labeled secondary control antibodies in cell lines Capan-1, PANC-1 and BxPC-3

Microfluidic immunocapture of model cell lines

We have previously described the GEDI capture geometry in detail[39]. In short, the GEDI device[38][39][100] is a microfluidic chip that captures rare cells from blood or cell suspensions, as shown in figure 3.3a. GEDI uses the combination of cancer-specific antibody immunocapture with a micropost geometry that maximizes the collision frequency between the substrate and larger cells (e.g., CTCs), and minimizes collisions of smaller contaminating cells (e.g. leukocytes). We have previously described the GEDI platform in a prostate[39][77], breast [76] and gastric[76] cancer context. We have shown how biotinylated antibodies can be functionalized onto NeutrAvidin coated silicon surfaces[39][77]. However, biotinyation of low concentration antibody samples requires high antibody purity and is typically inefficient. Biotinylated versions of primary antibodies are often not commercially available. As an alternative, we have here developed a protocol that attaches primary antibodies

to silicon surfaces via biotinylated secondary antibody linkers, omitting any modification of the primary antibody. Figure 3.3c shows a schematic of the functionalization chemistry used. Using this approach, we have implemented anti-EpCAM/hMUC1 modalities because of their importance in PC. We expect new anti-EpCAM/hMUC1 devices will enable investigation of questions regarding heterogeneity in CTCs in PC.

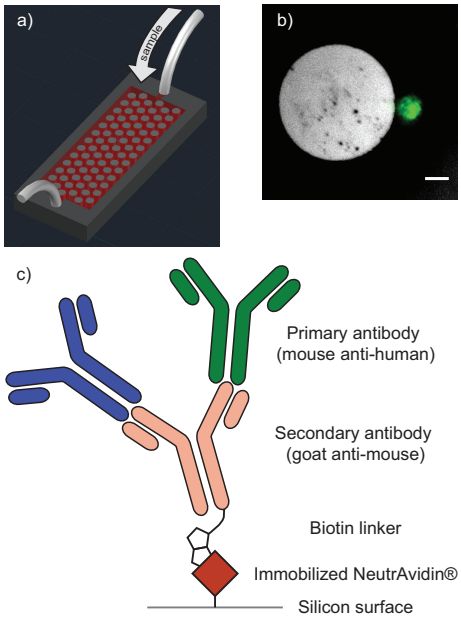

Figure 3.3: a) schematic overview of the GEDI device, modified from Kirby *et al.*[39], microposts not to scale b) calcein-stained (green) PANC-1 cell captured on a GEDI micro post functionalized with a cancer-specific MUC1 antibody. Scale bar: 20 μm c) silicon surface functionalization with primary antibodies and secondary antibody linker chemistry that allows for multiple parallel capture antibodies.

To determine the efficiency of immunocapture in this system, fluorescently labeled cells were resuspended in buffer solution at physiologically relevant levels (300 cells/ml) and processed through GEDI devices, followed by manual counting. A representative image of a PANC-1 cell captured on GEDI micropost can be seen in figure 3.3b. We hypothesize that anti-hMUC1 capture alone or in combination with anti-EpCAM capture will capture a more clinically relevant

population of CPCs as compared to anti-EpCAM capture alone. To evaluate capture performance, we have determined the capture efficiency for all three scenarios, while ensuring that the total amount of antibody in the incubation solution was constant between experiments. As expected, anti-EpCAM alone resulted in efficient immunocapture while anti-hMUC1 capture alone resulted in lower capture efficiencies. However, a 1:1 antibody cocktail of anti-EpCAM and anti-hMUC1 performed indistinguishably from anti-EpCAM capture alone. Figure 3.4a shows the resulting capture efficiencies from EpCAM, hMUC1 and EpCAM/hMUC1 cocktail capture. These results show that for these three cell lines, cocktail EpCAM/hMUC1 capture could replace the current EpCAM gold standard for immunocapture, without reducing capture efficiency. Furthermore, in a clinical scenario where EpCAM expression is reduced as a result of EMT while MUC1 expression is retained or upregulated, as is expected from clinical data[82], the capture performance of the EpCAM/hMUC1 cocktail may result in improved capture performance. Cocktail capture has been explored both for multiple epitopes on a single antigen[77] and for multiple antigens[29]. For single antigens, the data to date shows no synergy[77]. For multiple antigens, the data to date shows potential to capture more of the heterogeneity expected in the CTC population[29]. However to our knowledge, no published study has thoroughly examined the effect of using multiple capture antibodies on the resulting capture efficiency as a function of cellular antigen expression level and cell size.

Our capture data show that Capan-1 and PANC-1 display EpCAM capture efficiencies more than twice that of BxPC-3, despite that fact that PANC-1 cells have lower EpCAM and hMUC1 ABC counts than the corresponding counts for Capan-1 and BxPC-3. This behavior can be explained by considering

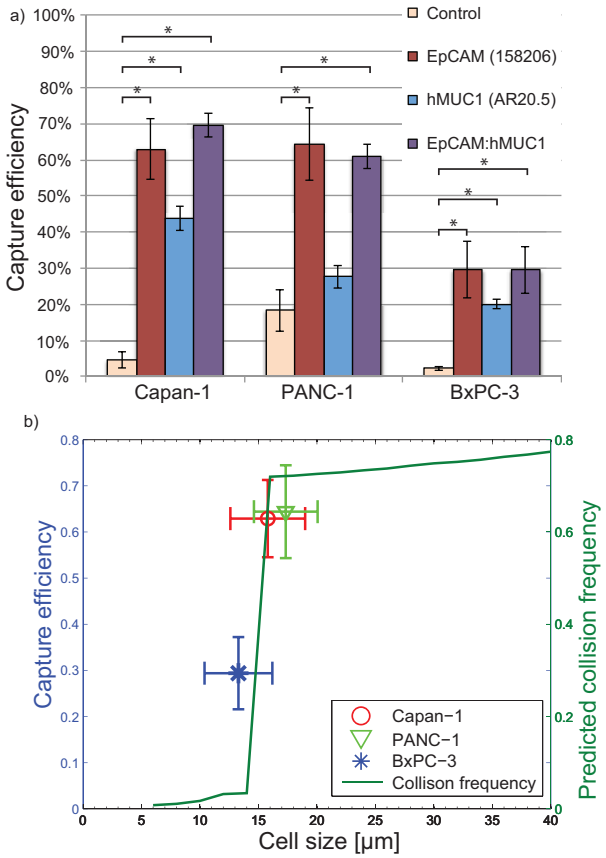

Figure 3.4: a) GEDI microdevice immunocapture of Capan-1, PANC-1 and BxPC-3 cells by anti-EpCAM and anti-hMUC1 antibodies, and an anti-EpCAM/hMUC1 antibody cocktail, b) anti-EpCAM capture efficiencies of Capan-1, PANC-1 and BxPC-3 cells and predicted collision frequency as function of cell size, based on previously described simulations [72]. $*$ indicates statistically significant difference with p=0.05

the size distribution of the cell populations and the predicted size-dependent performance of our device[72]. The predicted collision frequency and the experimentally observed capture efficiencies as function of cell size can be seen in figure 3.4b. Previously described simulations predict a sharp transition from low to high collision frequency for cells larger than 15μm[72]. We have measured the diameter of trypsinized populations of BxPC-3, Capan-1 and PANC-1 cells to be 13.3±2.9 μm,15.8±3.2 μm and 17.3±2.7 μm respectively. The

majority of BxPC-3 cells will thus fall below the cutoff cell size of our device geometry, resulting in low collision rates and capture efficiencies lower than for the two cell lines with mean diameters larger than 15 μm. In the design regime of this platform, size dominates over relative levels of capture target expression provided that the cells express some minimum level of the capture target. Unlike staining for flow cytometry, for which antibodies are freely suspended in solution and can reach sterically obstructed epitopes through diffusion, antibodies for immunocapture are immobilized on surfaces allowing only for binding of epitopes that are pendant on the outer surface of the cell membrane. It is thus expected that some strongly staining antibodies will fail to result in efficient immunocapture. The resulting capture efficiency depends on the abundance and accessibility of antibody binding sites on the target cells. Since the saturation density of antibodies functionalized on the device surface is finite, the use of multiple capture antibodies reduces the surface density of each antibody type. In order for the addition of an additional parallel capture mode to increase capture efficiency, the gain in number and accessibility of possible capture targets has to outweigh the loss of capture efficiency that results of having fewer antibody molecules of each type on the surface. An example of a case where the addition of a second antibody leads to reduced capture efficiency can be seen in a previous capture study, conducted in a Hele-Shaw flow microdevice[77]. In that case, the second antibody was specific to a juxtamembranous epitope on the same target molecule as the first antibody. The total number of available target molecules thus remained unchanged with the addition of the second antibody, but the overall accessibility of binding sites was reduced, resulting in lower overall capture efficiency. In our case, the addition of a hMUC1 antibody to EpCAM capture increases the total number of available

binding sites on each cell, as both EpCAM and hMUC1 are expressed strongly. The net result is that the overall capture efficiency for cocktail capture is retained as compared to anti-EpCAM and increased as compared to anti-hMUC1 capture alone. Given the natural variation in capture marker expression level between cells, the targeting of multiple highly-expressed capture targets will work to increase the robustness of capture to this intercellular variation. We thus conclude that a combined EpCAM and hMUC1 strategy has the potential to increase the robustness of capture to CPC heterogeneity and EMT, without reducing the overall capture efficiency as compared to the gold standard anti-EpCAM capture.

The most common source of cell contamination in microfluidic immunocapture devices is, due to their abundance as compared to rare circulating cells, the nonspecific adhesion of leukocytes[39]. Anti-EpCAM capture is widely used for immunocapture and results in only nonspecific adhesion of leukocytes. To ensure that the same is true for anti-hMUC capture, we conduced capture experiments using isolated donor peripheral blood mononucleated cells (PBMCs) in mixed populations with Capan-1 cells. The results showed that PMBCs adhered to our device at equal and negligible rates for both antibodies.

Isolation of captured cell nuclei

Recent studies have shown that breast cancer CTCs display genetic heterogeneity similar to that of primary and metastatic breast cancer tumors[101]. To analyze the heterogeneity within the CPC population single cell genetic analysis is required. To facilitate the future development of such a methodology we have developed a protocol for the release and isolation of

single nuclei from captured cells on chip. Using targeted cell membrane lysis, followed by elution and retrieval of the nuclei through centrifugation, we have shown successful isolation of intact nuclei from captured cells. Examples of released and isolated nuclei can be seen in figure 3.5a.

Genetic analysis

Genetic analysis of captured CPCs is technically challenging due to the low number of cells present in blood and the presence of background wild-type genetic material from contaminating leukocytes. However, we have previously showed SNP detection of a mutated gene with amplified copynumber in captured cells, spiked in control blood[39]. To show ability to detect mutations in the important oncogene KRAS in small numbers of captured cells in the presence of a whole blood background, we used a PC cell line with known KRAS codon 12 mutation signature (Capan-1, GGT→GTT substitution) spiked in control blood. Calcein labeled cells were spiked in whole blood from a healthy donor (300 Capan-1 cells/ml control blood). RNA from captured cells was extracted directly on chip followed by RT-PCR and Sanger sequencing, the resulting KRAS codon 12 RT-PCR amplicons and Sanger sequences from 250 anti-EpCAM captured Capan-1 cells spiked in blood and buffer as well as whole blood wild type control are shown in figure 3.5b and c. RNA from whole blood showed no evidence of KRAS mutations while RNA extracted on chip from Capan-1 cells captured in buffer and whole blood revealed the expected GGT→GTT SNP in codon 12 of KRAS. In summary, these experiments show our ability to retrieve, amplify and analyze the genetic information from a very small number (<300) of captured cells even in the presence of contaminating

wild-type genetic material.

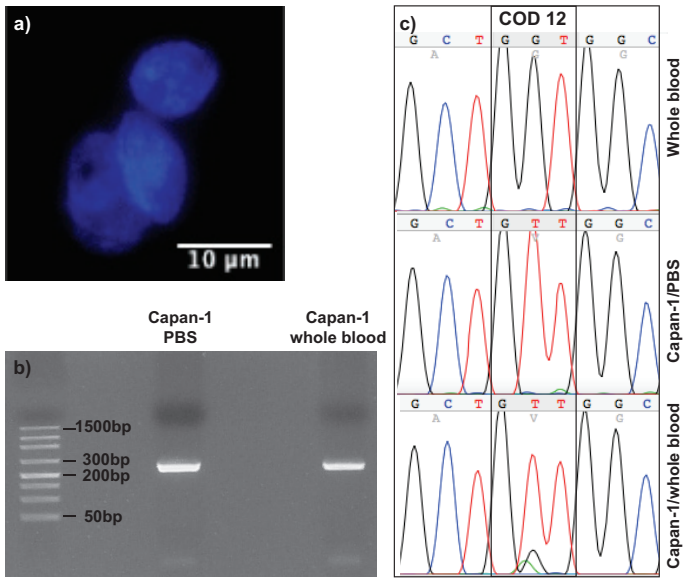

Figure 3.5: a) released and isolated DAPI-stained (blue) Capan-1 nuclei, b) agarose gel with a 249 bp Capan-1 KRAS RT-PCR product from cells spiked in PBS buffer and whole blood, c) Sanger sequencing of the KRAS codon 12 RT-PCR product from whole blood, Capan-1 cells spiked in PBS and Capan-1 cells spiked in whole blood. The whole blood sequence shows the wild type codon 12 genotype (GGT) while RNA extracted from Capan-1 cells spiked in PBS and whole blood show the expected GGT→GTT oncogenic SNP. Note the presence of a small wild-type peak in the spiked blood sample. The presented sense sequences have been converted from anti-sense sequences generated by the Sanger sequencing reaction

Analysis of clinical samples

To show technical capability of capturing CPCs from clinical samples, we analyzed the blood from a patient with clinically confirmed pancreatic ductal adenocarcinoma (PDAC) using anti-EpCAM, anti-hMUC1 and cocktail anti-EpCAM-hMUC1 capture. After processing through the GEDI devices, the samples were fixed and stained. DAPI staining was used to indicate cell nucleus and CD45 antigen staining was used to identify and reject leukocytes,

as previously described[39]. All samples were stained for both CK and MUC4.

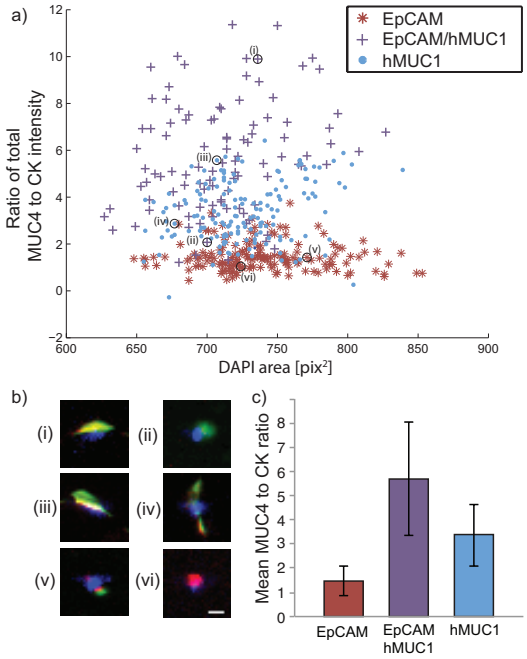

Figure 3.6: Analysis of CPCs from a clinical PDAC patient sample, processed using anti-EpCAM, anti-EpCAM/hMUC1 and anti-hMUC1 GEDI devices, a) ratio of total MUC4 and CK staining intensity versus nuclear DAPI area in events classified as likely CPCs, b) inset images showing representative CPC events, i-ii anti-EpCAM/hMUC1 cocktail capture, iii-iv anti-hMUC1 capture and v-vi anti-EpCAM capture, images i,iii and iv are consistent with cells spread on microposts, DAPI (blue), cytokeratin (red), MUC4 (green). Scale bar: 10 μm c) mean MUC4-to-CK total intensity ratios for all three capture modes, error bars indicate standard deviation within the population of identified CPCs

Nuclear-like DAPI+ events were identified with an automated algorithm. Remaining events were classified manually with CD45-/CK+ and/or CD45-/MUC4+ as CPC criteria, resulting in between 102 and 165 events identified as likely CPCs per milliliter blood in this sample. Figure 3.6 shows that, in this patient sample, events identified as likely CPCs from devices functionalized with anti-hMUC1 and anti-EpCAM/hMUC1 cocktail capture show increased MUC4 to CK intensity ratios relative to anti-EpCAM capture alone. This indicates that, in this sample, anti-hMUC1 capture results in capture

of a cell population that is positive for both CK and MUC4. It is possible that this DAPI+/CD45-/MUC4+/CK+ cell population is of important clinical significance as MUC4 expression correlates with PC progression. Data from this sample shows that the apparent heterogeneity of the captured CPCs, as measured by the range of MUC4 staining in the captured CPCs, is larger in the anti-hMUC1 and EpCAM/hMUC1 samples than in the anti-EpCAM sample. Using this semi-automated approach to image analysis, we generate data suitable for clinical hypothesis generation. The resulting data can be gated and visualized like flow cytometry data and the phenotype of individual cells, as well as cell populations and subpopulations can be analyzed. The automated pre-screening of CPC events also greatly reduces the time and labor required for manual classification.

3.6 Conclusions

We have demonstrated a novel microfluidic platform for the capture and analysis of circulating pancreatic cells. This platform builds on a previously described geometry but incorporates novel anti-hypoglycosylated mucin 1 capture chemistry and explores parallelized EpCAM/hMUC1 capture as a novel capture paradigm. We show that a combination of anti-EpCAM and anti-hypoglycosylated mucin 1 capture performs as well as anti-EpCAM capture alone in model cell lines, while potentially increasing the robustness to variations in marker expression and EMT. To allow for the development of single-cell genetic analysis of circulating cells, we show release and isolation of single nuclei from captured cells. Using on-chip RNA extraction, RT-PCR and Sanger sequencing, we detected a known oncogenic KRAS SNP mutation

in captured cells spiked in whole blood. We have also developed a staining protocol for clinical samples that involves standard circulating tumor cell makers, such as DAPI, CD45 and cytokeratin as well the PC-specific marker mucin 4. In an initial clinical sample, cocktail capture resulted in the capture of a cell population distinct from anti-EpCAM capture. Our approach allows for analysis of single cells and cell populations from patient samples and is suitable for clinical hypothesis generation. In all, we have shown feasibility of this platform for future evaluation in a clinical setting.

3.7 Acknoledgements

The work described was supported by the Cornell Center on the Microenvironment & Metastasis through Award Number U54CA143876 from the National Cancer Institute, the HHMI med-into-grad scholarship (FIT), the Lester and Sheila Robbins Scandinavian Graduate Student Fellowship (FIT), a National Science Foundation Graduate Research Fellowship under Grant No. DGE-1144153 (TBL), Early Detection Research Network U01 CA111294 (MAH), SPORE P50 CA 127297 (MAH), R01 CA057362 (MAH), K08DK088945 from the NIDDK (ADR) and a Career Development Award from the Pancreatic Cancer Action Network and American Association for Cancer Research (ADR)

CHAPTER 4

ELUCIDATING THE EFFECT OF EMT AND CHEMORESISTANCE ON PANCREATIC CTC IMMUNOCAPTURE

4.1 Abstract

Capture and analysis of circulating tumor cells bears promise for improving patient monitoring and guiding treatment in patients with pancreatic cancer. A majority of CTC analysis techniques rely on the recognition of epithelial markers, particularly EpCAM and cytokeratin for CTC identification. As the epithelial-to-mesenchymal transition and acquisition of chemoresistance both have been shown to lead to loss of epithelial markers, the effect of these processes on CTC capture and identification needs exploration. Here, we have developed *in vitro* models of EMT and gemcitabine resistance, and using these models we show that EMT-induction and chemoresistance cells leads to loss of EpCAM capture performance while EGFR capture is more robust to these processes.

4.2 Background and Introduction

Pancreatic cancer is a devastating disease with a 5-year survival rate of about 8%[2] and is predicted to become the second-leading cause of cancer-related death by 2030[1]. Early onset of metastatic disease and high rates of intrinsic and acquired resistance to chemotherapy (chemoresistance) represent major challenges to improving treatment outcomes[102]. A large majority of patients are diagnosed at the metastatic stage, where the tumor has spread beyond

the pancreas and cannot be surgically removed[103], leaving chemotherapy as the only treatment option. Consequently treatment of pancreatic cancer is hampered by the lack of early detection modalities and biomarkers to guide treatment.

Capture and isolation of circulating epithelial cells (CECs) has been proposed as a potential biomarker of early pancreatic carcinogenesis[11]. We have previously shown that CECs are disseminated into the blood stream in some patients with precancerous pancreatic cyst lesions and can be isolated using anti-EpCAM immunocapture in our Geometrically Enhanced Differential Immunocapture (GEDI) platform[31][104]. Furthermore, we have shown that anti-EpCAM capture can be used in combination with other capture modalities, such as anti-MUC1, to capture a wide range of pancreatic cancer cells[104]. However, the question of which CTC markers are ideal for CTC immunocapture remains to be determined. Anti-EpCAM immunocapture remains the gold standard for CTCs capture, despite growing evidence that CTC EpCAM expression is heterogeneous and in many cases absent[105][39].

One process that has been linked to loss of EpCAM expression in carcinoma cells is the epithelial-to-mesenchymal transition (EMT)[106]. EMT involves the downregulation of epithelial markers (e.g. E-cadherin and cytokeratin) and upregulation of mesenchymal markers (e.g. vimentin and N-cadherin), as well as the acquisition of a fibroblast-like morphology and a gain in migratory and invasive traits[15]. EMT is controlled by transcription factors, including Zeb1, Snail, Twist and can be triggered by stimulation of growth-factors (e.g. TGFβ and EGF) in some cancer cells[18][107][23]. As EMT results in the loss of epithelial markers, such as CTC markers EpCAM and cytokeratin, it has

significant implications on the performance of CTC capture techniques that rely on these markers.

The remarkably early onset of the epithelial-to-mesenchymal transition (EMT) in pancreatic cancer is thought to contribute to the early metastasis observed in most patients[11]. EMT is thought to be necessary for intravasation of carcinoma cells into the blood circulation[11] and to contribute to pancreatic chemoresistance[17][102]. The role of EMT in pancreatic cancer is still debated and a recent study suggested that the main contribution of EMT to cancer progression is due to its connection to chemoresistance rather than by enabling metastasis[17].

The canonical definition of a CTC as a nucleated, EpCAM-expressing, cytokeratin positive and CD45 negative cell in circulation makes CTC isolation susceptible to processes that influence the expression of these markers. There is a growing body of evidence showing that patient CTCs display significant heterogeneity and this strict CTC-definition likely leaves many CTC populations undetected[106]. Although purely epithelial or mesenchymal CTCs are present in patient samples, CTCs displaying mixed epithelial and mesenchymal phenotypes are often found[28][29][30]. It has been hypothesized that since EMT represents a key step in the metastatic cascade, CTCs displaying some degree of EMT-induction or mixed phenotype may have increased clinical and pathological significance[108]. In addition, the current understanding of the importance and prevalence of EMT in CTCs is biased as a majority of isolation methods used in previous studies rely on recognition of markers known to be lost during EMT.

Heterogeneity of EpCAM and cytokeratin expression has been observed

in patient CTCs, across several cancer types[105][39]. We have, for example, previously identified CTCs lacking EpCAM expression in samples from prostate cancer patients, captured using anti-PSMA GEDI[39].

In addition, the EMT status of CTCs has been observed to change over time and in response to treatment. In particular, the mesenchymal CTC subtype has been shown to correlate with cancer progression[29]. To accurately monitor a patient's cancer using CTC analysis, the CTC isolation and identification platform thus has to capture this variation in CTC phenotype and not be sensitive to changes in CTC EMT status. One approach to overcome the issues with single-marker capture is to use a combination of markers for CTC capture[104], a combination of EpCAM, HER2 and EGFR has been used successfully in breast cancer[29]. Although, the use of markers other than EpCAM and using several markers in combination may increase the robustness to variations in CTC marker expression, the effect on the performance of a CTC isolation platform of using such markers has yet to be thoroughly evaluated.

Another process know to profoundly change the properties of cancer cells and the expression of surface markers is the acquisition of chemoresistance. For a large majority of patients with pancreatic cancer, chemotherapy in the form of gemcitabine mono- or combination-therapy is the only treatment option, with only a modest positive effect on patient survival[102]. Gemcitabine (Gemzar, 2',2'-difluorodeoxycytidine, dFdC) is a nucleoside analog that induces cell death by terminating DNA replication and inhibiting ribonucleotide reductase (RNR), a key enzyme required for DNA synthesis[109]. The gemcitabine molecule is a prodrug that requires intracellular activation to become biologically active. Intracellular activation occurs through the sequential phosphorylation

of gemcitabine into the corresponding mono-, di- and triphosphates (dFdCMP, dFdCDP and dFdCTP), of which the first and rate-limiting phosphorylation reaction is catalyzed by the enzyme deoxycytidinekinase (dCK)[109]. Previous studies have shown that loss of dCK expression results in strong gemcitabine resistance in vitro[110].

Although multiple different resistance mechanisms are indicated in gemcitabine resistance, acquired resistance to gemcitabine has in some cases been correlated with the acquisition of an EMT-like phenotype[26][27]. Furthermore, recent work has shown the importance of EMT in the development of chemoresistance in pancreatic cancer, suggesting an intrinsic connection between EMT and chemoresistance[17].

In summary these observations emphasize the need for a better understanding of how the phenotypic heterogeneity of cancer cells, induced by processes such as EMT and acquisition of chemoresistance, influences CTC capture and identification platforms. Here, we describe the development of an *in vitro* model of EMT-induction and acquired gemcitabine resistance in pancreatic cancer cells. Using this model we evaluated the performance of anti-EpCAM and anti-EGFR immunocapture in the GEDI microfluidic CTC immunocapture platform. Our results show that anti-EGFR is more robust to EMT and acquired resistance to gemcitabine as compared to anti-EpCAM capture.

4.3 Materials and Methods

Cell culture

PANC-1, BxPC-3, MIAPACA-2 and Capan-1 cells were acquired from ATCC and were cultured following ATCC recommendations; PANC-1 and MIAPACA-2 in DMEM with 10% FBS, BxPC-3 in RPMI-1640 with 10% FBS, and Capan-1 in IMDM with 20% FBS. All cells were cultured with 100 units penicillin, 0.10 mg streptomycin and 0.25 g amphotericin B per ml in a 5% CO2, 37°C humidified incubator.

EMT induction

For EMT-induction, cells were seeded at 500,000 cells per 60mm dish and allowed to grow for 48h. Cells were then replated at 6,000 cells/cm2 and treated with 10ng/ml TGF-beta (R&D Systems) and/or 20ng/ml EGF (R&D Systems) in media supplemented with 2.5% FBS over a period of 7 days, replacing the media every other day.

Generation of gemcitabine resistant cell lines

Gemcitabine resistant sub-clones of PANC-1 cells were generated by exposing naive cells to low doses of gemcitabine over a total of 10 months. Emerging resistant clones were isolated and subcultured.

Immunofluorescence

Cells were grown in optical-bottom 96-well plates (Thermo). Following washing with PBS, cells were fixed with 2% formaldehyde in a PBS/PHEM buffer (60 mM PIPES, 25 mM HEPES, 10 mM EGTA, 2 mM MgCl2). Cells were then blocked with 10% normal donkey serum for 45 minutes at room temperature, followed by permeabilization with 0.1% saponin for 5 minutes. Cells were permeabilized only when staining for intracellular markers or with cocktails of EMT marker antibodies. Following permeabilization, cells were incubated overnight at 4°C with anti-N-cadherin (R&D Systems), anti-vimentin (Santa Cruz, Santa Cruz, CA), anti-E-cadherin (CellSignaling, Beverly, MA), anti-pan-CK (BioLegend, San Diego, CA), anti-EpCAM (R&D) and anti-EGFR (C225, Millipore) antibodies. Cells were then incubated with Alexa Fluor 488, 568 or 647-conjugated secondary antibodies (Life Technologies, Grand Island, NY) for 1 hr at room temperature. Cells were counterstained with 1ug/ml DAPI (Sigma-Aldrich, St. Louis, MO) for 15 minutes. Representative images were then acquired using a Nikon Eclipse TE2000-U fluorescent microscope.

Spreading assay

Cells were seeded sparsely in 96-well plates. When small colonies (5-10 cells) had formed, 10 ng/ml TGF-beta was added to the culture media. The individual colonies were then followed over 72h and spreading was assed by manual inspection.

Western blotting

Cells were seeded in at 500,000 cells/60mm in tissue culture treated dishes 48h prior to harvest of protein lysates. Before lysis, cells were washed with ice-cold PBS followed by complete removal of the supernatant. 100ul lysis buffer (50 mM Tris, 1% (v/v) Triton X-100, 150 mM NaCl, 2mM PMSF, 1mM sodium orthovanadate and 1X protease inhibitor cocktail from Santa Cruz Biotechnology) was then added per plate. Cells were lysed by mechanical disruption using a cell scraper. Lysates were pipetted 10 times with a 1000ul pipettor to homogenize. Lysates were then incubated on ice for 20 min with constant rocking and intermittent vortexing. Insoluble cellular components were removed by spinning the raw lysates at 15,000xg, for 9 minutes at 4°C. The lysates were then stored at -80°C or used right away. Following protein quantification with the DC protein assay (Bio-Rad), lysates were heat treated in Laemmli sample buffer (2% SDS, 2% 2-mercaptoethanol, 0.1% bromophenol blue, 10% glycerol, 62.5 mM Tris-HCl) in a dry bath set to 98°C for 5 minutes. 10-15 ug total protein per well was then loaded in 4-20% Tris-Glycine gradient polyacrylamide gels (Thermo). The Bio-Rad Kaleidoscope protein ladder was used as positive control. SDS-PAGE ran at 160V on ice for approximately 1h and 45min in running buffer (25 mM Tris-HCl, 190 mM glycine, 0.1% SDS). Proteins were then transferred to 0.45um PVDF blotting membranes (Millipore) by electrophoresis at 400mA for 1h and 45 min in transfer buffer (25 mM Tris-HCl, 190 mM glycine, 0.1% SDS, 20% methanol) with constant water cooling. Following protein blotting, the membranes were washed in TBST buffer (20 mM Tris-HCl, 150 mM NaCl, 0.1% (v/v) Tween 20) and blocked for 2h in 3% BSA-TBST. Staining with primary antibodies over night

at 4°C with constant rocking. Primary antibodies used: anti-RRM1 (EPR8483, abcam), anti-RRM2 (N1C1, GeneTex), anti-dCK (Bethyl), anti-β-actin (D6A8, abcam). Following washing, the membranes were stained with HRP-conjugated secondary antibodies for 1h at room temperature. Blots were developed with Western Lightning Plus Enhanced Chemiluminescence Substrate (Perkin Elmer) and autoradiographical film (add company).

Flow cytometry

Cells were seeded in at 500,000 cells/60mm in tissue culture treated dishes, 48h prior to flow cytometry. Following trypsinization, cells were blocked on ice for 30 minutes in 2% FBS in PBS. For EpCAM and EGFR, cells were then incubated with 1ug primary antibody/1e6 cells for 1 hour on ice, followed by washing and incubation with 1ug/1e6 cells PE-conjugated goat anti-mouse secondary antibody (SCBT) in 2% FBS in PBS for 1 hour on ice. Antibodies bound per cell (ABC) counts were determined with PE Quantibtite beads (BD) according to manufacturers description. For cytokeratin staining, cells were fixed for 15 min in 4% PFA in PBS. Following washing, cells were incubated with 1ug/1e6 cells CF568-conjugated (Biotium) pan-reactive cytokeratin antibody (C11, Biolegend) in a buffer containing 2% FBS and 1mg/ml saponin in PBS for 1 hour on ice.

Immunocapture

GEDI microdevices were functionalized with anti-EpCAM (R&D Systems) or anti-EGFR (C225, Millipore) antibodies using a previously described protocol[104]. Briefly, silicon devices were manufactured by AM Fitzgerald

and Associates with Bosch etch on SOI substrates and functionalized with antibodies using consecutive incubation with 4% (v/v) 3-(mercaptopropyl) trimethoxysilane (Sigma) in ethanol, 0.28% (w/v) GMBS (Sigma) in ethanol, 25ug/ml Neutravidin (Thermo) in PBS, 10ug/ml biotinylated goat anti-mouse antibody (SCBT) in 1%BSA in PBS and 10 ug/ml EpCAM or EGFR antbody in 1%BSA in PBS. For capture performance and cell enumeration experiments cells were labeled with 4μM Calcein AM for 30min prior to spiking in running buffer. Approximately 300 cells/ml were spiked in PBS containing 1% BSA and 1mM EDTA, and subsequently captured in GEDI devices, followed by manual counting of calcein positive cells.

4.4 Results and Discussion

Expression of CTC markers in pancreatic cancer cell lines

Efficient CTC immunocapture relies on the recognition of surface markers expressed by CTCs but not by other cells present in blood. The epithelial cell marker EpCAM is the most commonly used capture marker for CTCs, but other markers such as EGFR[29], MUC1[104] and HER2[76] have also been used[29]. Following capture using positive selection, CTCs are typically distinguished from white blood cells using staining for cytokeratin (CK), a family of epithelial-specific cytoskeletal proteins and CD45, a pan-leukocyte marker absent on epithelial cells. EpCAM and CK expression have been shown to vary greatly in patient CTCs[105][39][90][51][30], and certain cancer-related processes, such as EMT and acquired chemoresistance, have been shown to

influence the expression of these markers[106][11]. Here, we measured the baseline expression of EpCAM and CK in three pancreatic cancer cell lines, as well as in the context of EMT and chemoresistance. In addition, we explored EGFR as a possible alternative capture marker, or complement to anti-EpCAM capture.

First, we determined the baseline expression of EpCAM, EGFR and CK in a panel of pancreatic cancer cell lines that span the range from epithelial-like to mesenchymal-like morphology and marker expression, see figure 4.1a. BxPC-3 cells display pronounced epithelial-like traits (epitheloid morphology and colony formation, high E-cadherin expression, low vimentin and low N-cadherin expression), whereas MIAPACA-2 cells display a mesenchymal phenotype (spindle-like morphology, undetectable E-cadherin , high vimentin and high N-cadherin expression), see figure 4.1a. PANC-1 cells display a mixed phenotype with epithelial and mesenchymal traits (some epithelial colony formation, heterogenic E-cadherin expression, high vimentin and N-cadherin expression).

As can be seen in figure 4.1b, BxPC-3 cells display the highest level of EpCAM expression whereas MIAPACA-2 cells lack detectable EpCAM expression, consistent with these cells exhibiting epithelial and mesenchymal phenotypes, respectively. An intermediate level of EpCAM expression was found on PANC-1 cells, which is consistent with an intermediate EMT-status. All three cell lines were found to express significant levels of EGFR, whereas PANC-1 expressed markedly more than the other cell lines. The level of EGFR expression did thus not correlate with baseline EMT status in these cell

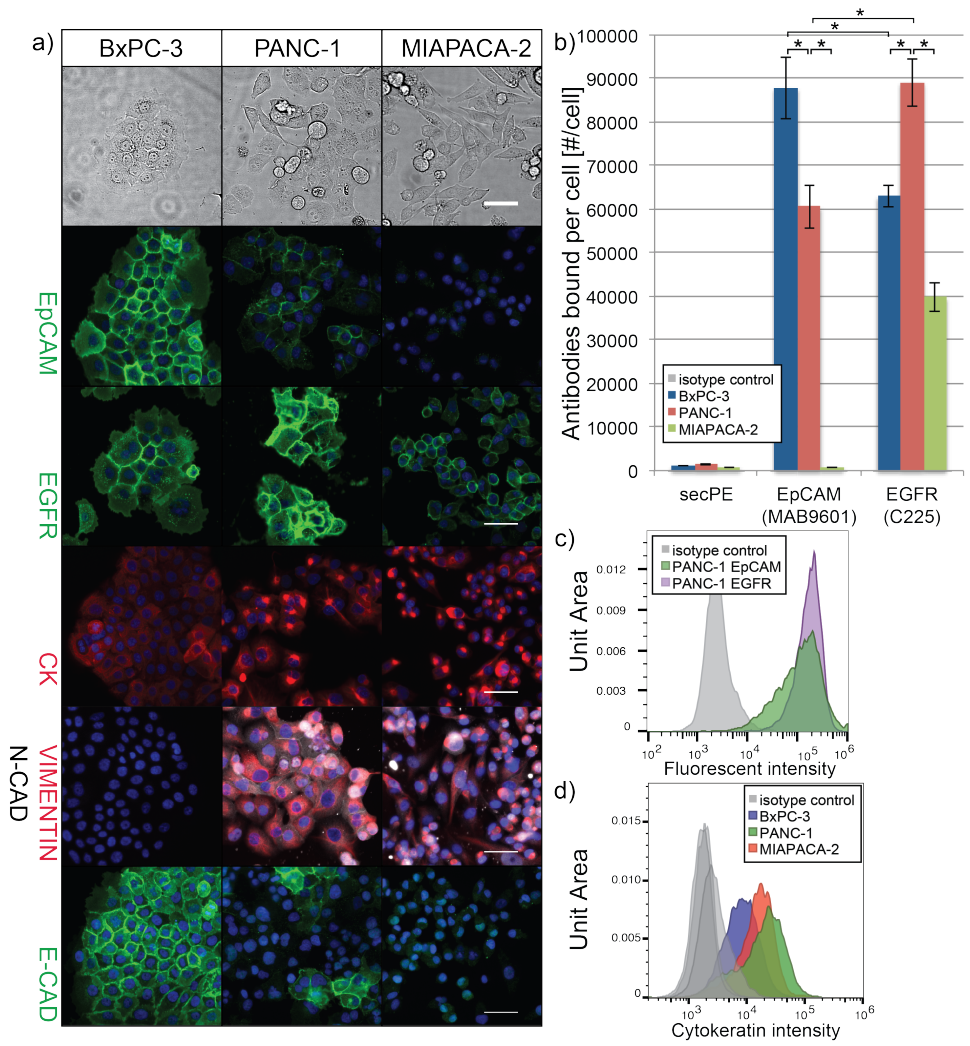

Figure 4.1: a) immunofluorescence staining reveal widely varying cellular phenotypes in the panel of pancreatic cancer cell lines studied: BxPC-3, PANC-1 and MIAPACA-2, b) quantitative flow cytometry shows that all cell lines expressed significant levels of EGFR, whereas EpCAM expression was detected in BxPC-3 and PANC-1 but not in MIAPACA-2 cells, c) EpCAM expression is more variable within the cellular populations tested, as indicated by a wider histogram of EpCAM expression, as compared to EGFR expression, d) cytokeratin expression does not correlate with epithelial-like phenotype as MIAPACA-2 cells express higher levels of cytokeratin than PANC-1 and BxPC-3

lines. Interestingly, we found that in all cell lines the intercellular variability of EpCAM expression was greater than for EGFR, an example of which can be seen as a broader EpCAM flow cytometry histogram in figure 4.1c. Considering that EGFR was present on all the cell lines tested, and that EGFR expression showed

less intercellular variability than EpCAM in these cell lines, indicates that EGFR may be a more universal capture marker for pancreatic CTCs. All cell lines were found to express cytokeratin, however, the level of cytokeratin expression did not correlate with baseline EMT-status. PANC-1 cells expressed the highest level of cytokeratin as measured by flow cytometry, followed by MIAPACA-2 and BxPC-3, see figure 4.1d.

EMT is thought to be a dynamic and in some cases reversible process[15]. Growth factor signaling in the tumor microenvironment could potentially trigger transient EMT induction[15], leading to intravasation of CTCs into the blood stream. However, the effect of growth factor-induced EMT on the expression of CTC markers EpCAM, EGFR and cytokeratin has not to be determined in these cell lines. It is well established that EMT can be induced by growth factor stimulation in some cancer cell lines, potentially allowing for the creation of an in vitro EMT-induction model and the determination of the effect of EMT on CTC marker expression.

Development of an EMT induction protocol

To determine the effect of EMT on CTC marker expression and immunocapture, we developed an *in vitro* EMT-induction protocol using growth factor treatment. Based on results reported by others[107][23], cells were treated with TGFβ, alone or in combination with EGF. For these experiments we used a panel of epithelial-like or mixed-phenotype pancreatic cancer cells: Capan-1 (epithelial-like), BxPC-3 (epithelial-like) and PANC-1 (mixed phenotype). As can be seen in figure 4.2, we evaluated EMT-induction with staining for E-cadherin (epithelial marker), vimentin and N-cadherin (mesenchymal

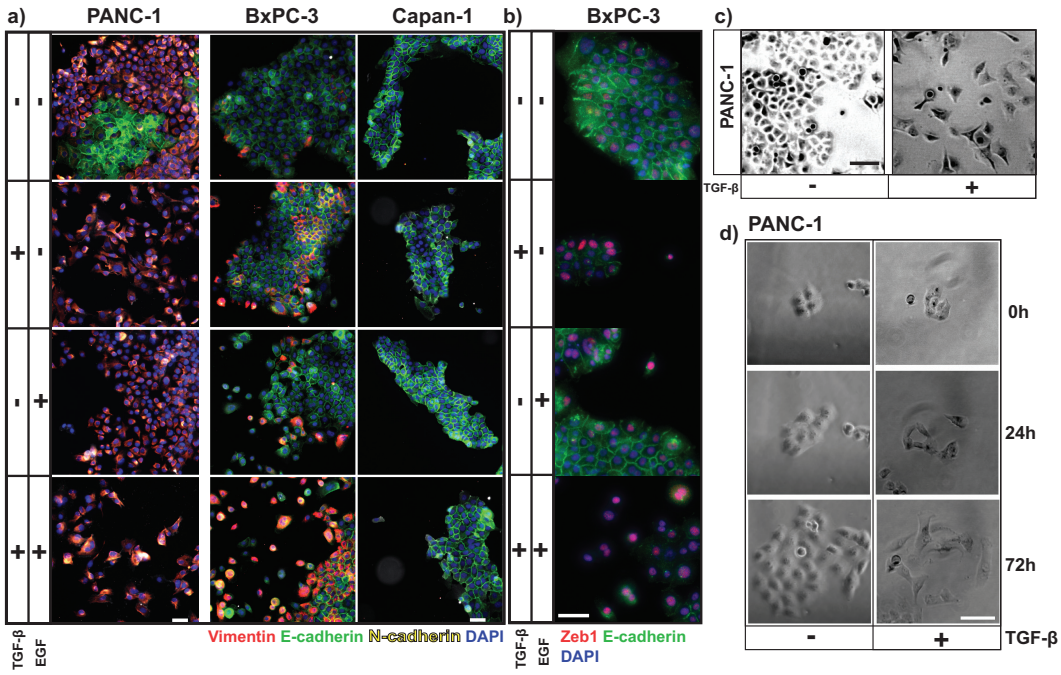

Figure 4.2: a) EMT-induction was observed in PANC-1 and BxPC-3 cells following treatment with TGFβ alone or in combination with EGF, b) TGFβ and EGF stimulation resulted in upregulation of nuclear Zeb1 expression in BxPC-3 cells, c) TGFβ-treatment dramatically alters the morphology of PANC-1 cells, leading to an acquisition of a mesenchymal morphology, d) colony spreading was observed in PANC-1 cells following stimulation with TGFβ

markers), using immunofluorescence. Functional EMT was confirmed with a previously described colony-spreading assay[18].

In concordance with other studies[18], we found that TGFβ alone induced distinct EMT in PANC-1 cells. In these cells, TGFβ treatment led to a near complete loss of epithelial-like colony formation and acquisition of a pronounced mesenchymal-like phenotype, as well as a near-complete loss of E-cadherin expression and increased expression of vimentin. In this population, EMT-induction was observed in nearly all cells, as determined by manual inspection, see figure 4.2a. TGFβ treatment alone did not noticeably alter the morphology of BxPC-3 or Capan-1 cells, although some upregulation of vimentin and N-cadherin was observed in BxPC-3 cells, see figure 4.2a. These

results are consistent with the expected results considering the previously determined cell line genotypes. PANC-1 cells harbor an activating KRAS mutation and wt SMAD4, whereas BxPC-3 cells are KRAS wt and SMAD4 deficient, and Capan-1 cells are KRAS activated and SMAD4 mutated[97]. Previous studies have shown that active MAPK/ERK signaling is necessary for TGFβ induced EMT[21][18], suggesting that BxPC-3 cell may be able to undergo TGFβ-induced EMT if simultaneously stimulated with EGF. Potent induction of EMT following treatment of epithelial cells with TGFβ and EGF has been described previously[107][23], to our knowledge not in the context of pancreatic cancer. Indeed, we found that BxPC-3 cells could be induced to undergo EMT when stimulated with TGFβ in combination with EGF, despite reportedly lacking SMAD4 expression[97]. However, EMT-induction was observed in only a fraction of cells and some epithelial-like colonies persisted in the cell population, see figure 4.2.

Although TGFβ signaling is mediated by several pathways down-stream of ligand/receptor binding, canonical TGFβ signaling occurs through a SMAD4, mediated pathway[111]. SMAD4 (also known as Deleted in Pancreatic Carcinoma Locus 4, DPCL4) is often mutated or deleted in pancreatic cancer, underscoring the importance of the anti proliferative/tumor suppressor role of TGFβ signaling in early carcinogenesis. However, late in tumor progression TGFβ is thought to play a role in the metastatic cascade by inducing EMT, contributing to the dissemination cells from the primary tumor[111]. However, our finding that BxPC-3 cells can be induced for EMT despite lacking SMAD4 expression is consistent with the increasing appreciation of non-canonical (SMAD-independent) TGFβ signaling[112][113]. In line with our hypotheses and the presence of KRAS activating mutations in Capan-1 cells, the addition

of EGF did not lead to EMT-induction in these cells, potentially due to disrupted TGFβ signaling. As PANC-1 cells display a mixed EMT phenotype and responded the strongest to EMT-induction with TGFβ treatment alone, we decided to use PANC-1 for our future studies of the effect of EMT and chemoresistance on CTC marker expression and immunocapture.

Development of gemcitabine-resistant subclones

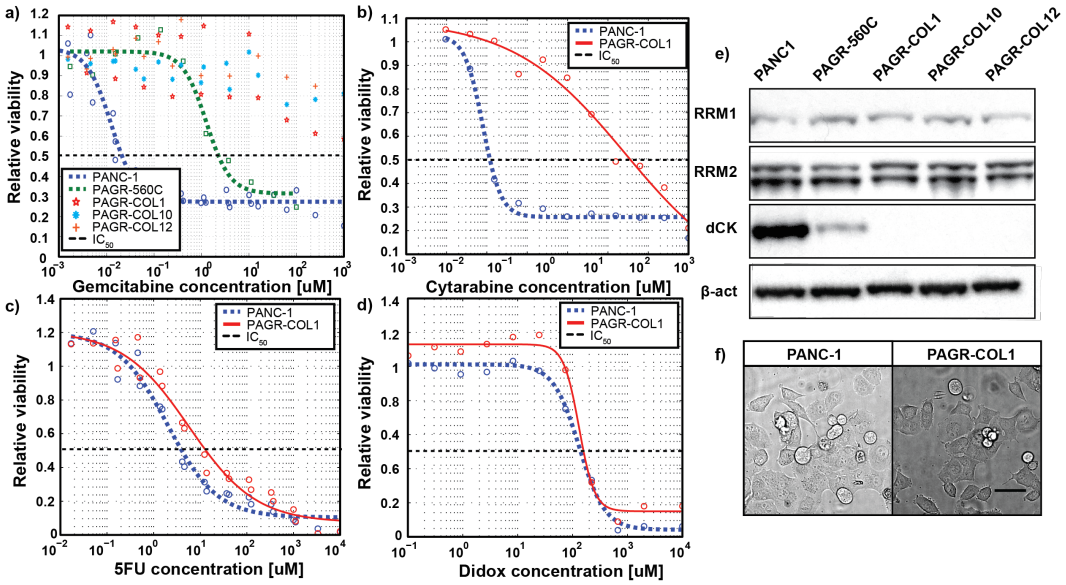

Figure 4.3: a) gemcitabine resistant PANC-1 subclones were generated using long-term drug exposure and display significantly increased gemcitabine resistance, as indicated by increased IC_{50}-values, PAGR-560C represents a heterogeneous mix of resistant and non-resistant cells, PAGR-COL1, COL10 and COL12 represent isolated resistant subclones with IC_{50}-values higher than 1mM, b) PAGR-COL1 cells display significant cross-resistance with cytarabine, c-d) no significant 5FU or didox cross-resistance was observed in PAGR-COL1 cells, e) PAGR subclones display decreased expression of the gemcitabine activating enzyme deoxycytidine kinase (dCK), expression level of RRM1 and RRM2 was unaltered in resistant cells, f) PAGR-COL1 cells display a phenotype similar to parental PANC-1 cells, scale bar 50μm

Acquisition of gemcitabine resistance has been shown to alter the phenotype and EMT status of cancer cells *in vitro*. Several studies have found that

development of gemcitabine resistance results in the acquisition a migratory phenotype, with or without increased expression of EMT markers[25][26][27]. With this in mind we aimed to determine what the effect of acquired gemcitabine resistance is on the expression of CTC markers and CTC immunocapture of pancreatic cancer cells. First, gemcitabine resistant subclones of the pancreatic cancer cell line PANC-1 were selected by exposing cells to increasing levels of gemcitabine, over a course of 10 months. Several highly resistant subclones (PAGR-COL1-12) were isolated from a heterogeneouspopulation of resistant cells treated with 560nM gemcitabine (PAGR-560C). Acquisition of a resistant phenotype was confirmed with MTT viability assays, see figure 4.3. These clones displayed more than 50,000 fold increased IC_{50} values as compared to the parental cells.

In order to determine possible resistance mechanisms, we performed Western blotting for key activators and targets of gemcitabine; RRM1, RRM2 and dCK. All gemcitabine-resistant PANC-1 clones tested (PAGR-COL1, COL-10 and COL-12) were found to have lost expression of the enzyme deoxycytidine kinase (dCK), see figure 4.3e. dCK catalyzes the rate-limiting step in activating the gemcitabine prodrug into its phosphorylated derivatives (dFdC to dFdCMP). Loss of dCK expression as a mechanism of gemcitabine resistance has been described previously, and has been found to result in strong gemcitabine resistance[110]. In normal cells, dCK catalyzes the conversion of dC to dCMP. However, dCK is a relatively promiscuous enzyme with little substrate specificity, and as a result dCK is responsible for the phosphorylation of gemcitabine as well as several other nucleoside analogs. Since we observed the same resistance mechanism in all clones, PAGR-COL1 was chosen for further detailed studies. PAGR-COL1 cells displayed strong

cross-resistance with the dCK-dependent nucleoside analog cytarabine, little cross resistance with 5FU and no cross resistance the RRM2-targeting drug didox, see figure 4.3b-d. As can be seen in figure 4.1, PAGR-COL1 were found to be morphologically similar to the parental PANC-1 cells.

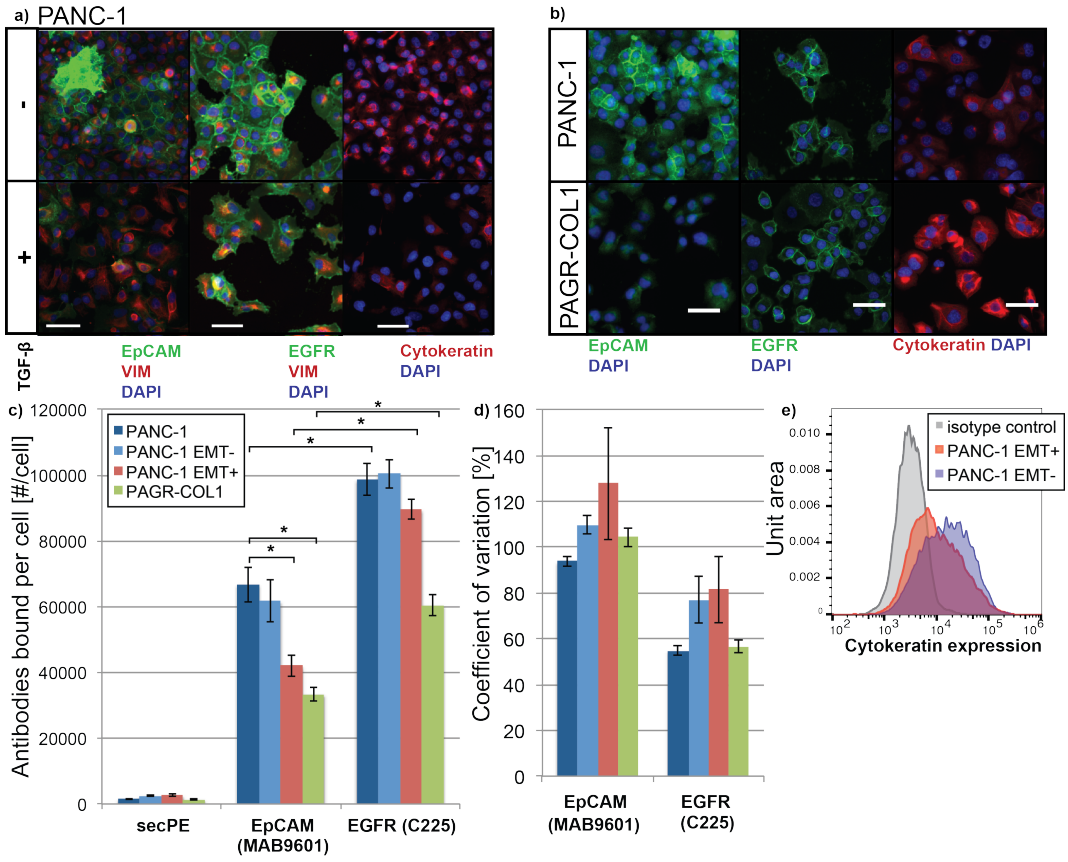

Figure 4.4: a) immunofluorescent staining shows that reduced EpCAM and cytokeratin expression is found in TGFβ treated/EMT-induced PANC-1 cells, whereas EGFR expression was retained, b) loss of EpCAM expression is detected in gemcitabine resistant PAGR-COL1 cells, c) quantitative flow cytometry reveals significant loss of EpCAM expression in EMT-induced and gemcitabine resistant cells, EGFR expression was reduced significantly in gemcitabine resistant cells but only minimally in EMT-induced cells, d) EpCAM expression displayed higher variability than EGFR expression in all conditions. EMT-induction led to increased variability of EpCAM and EGFR expression as well as higher experiment-to-experiment variability, e) flow cytometry reveals reduced cytokeratin expression in EMT-induced PANC-1 cells

EpCAM, EGFR and cytokeratin expression in EMT-induced and gemcitabine resistant cells

After having defined an EMT-induction protocol for PANC-1 cells and derived gemcitabine resistant subclones from the same cell population, we set out to determine the effect of these processes on the expression of CTC markers. The changes in the expression of EpCAM, EGFR and cytokeratin in EMT-induced and gemcitabine resistant PAGR-COL1 cells was determined using immunofluorescence and flow cytometry, see 4.4. We observe a significant down-regulation of EpCAM, both in cells stimulated to undergo EMT (PANC-1 EMT+) and cells with acquired resistance to gemcitabine (PAGR-COL1). Growth-factor restriction (PANC-1 EMT-) was not observed to significantly change the expression of EpCAM or EGFR. As expected, we observe down-regulation of cytokeratin in EMT-induced cells, however, not in PAGR-COL1 cells, see figure 4.4. More cell-to-cell, and experiment-to-experiment variability was observed for EpCAM relative to EGFR in all samples, which manifests in an increased EpCAM Coefficient of Variation (CoV), see figure 4.4. This shows that EpCAM expression is more variable than EGFR expression within the cell populations, and indicates that EGFR may be a preferable marker for capture. The CoV also increased from both EpCAM and EGFR in EMT induced samples relative to non-induced samples, indicating that the EMT induction increased the heterogeneity of marker expression in the cell populations.

In summary, these results indicated that TGFβ mediated EMT-induction recapitulates several of the key phenotypic features observed or hypothesized

for EMT in CTCs; namely loss of cytokeratin and EpCAM-expression, and increased heterogeneity of marker expression. As EpCAM and cytokeratin are widely used to capture and identify CTCs, our results support the notion that EMT presents a potential problem for CTC isolation and identification. EGFR expression was significantly reduced in chemoresistant PAGR-COL1 cells but not in EMT-induced cells.

Immunocapture of EMT-induced and gemcitabine-resistant cells

Having determined what effect EMT-induction and acquired gemcitabine resistance had on the expression of CTC capture markers EpCAM and EGFR in PANC-1 cells, we next set out to determine the effect on microfluidic capture performance. PANC-1 cells, EMT-induced PANC-1 cells or gemcitabine resistant PAGR-COL1 cells were captured using anti-EpCAM, anti-EGFR or non-specific antibodies using the microfluidic GEDI platform. The results, see figure 4.5, show that anti-EpCAM and anti-EGFR immunocapture performed equally well in naive PANC-1 cells. However, EMT-induction and acquired chemoresistance resulted in significant loss of EpCAM capture performance. EGFR capture performance was reduced in EMT-induced cells but performed equally well in PAGR-COL1 cells as in PANC-1 cells. The loss of EpCAM expression observed by flow cytometry is thus resulted in as a loss of anti-EpCAM capture performance in both EMT+ and PAGR-COL1 cells. However, the loss of EGFR-capture in EMT+ cells is not directly explainable by considering protein expression levels as EMT+ cells did not display a loss of median EGFR expression. However, we observed an increased variability of both EpCAM and EGFR expression in these cells, likely contributing to the loss

of capture performance.

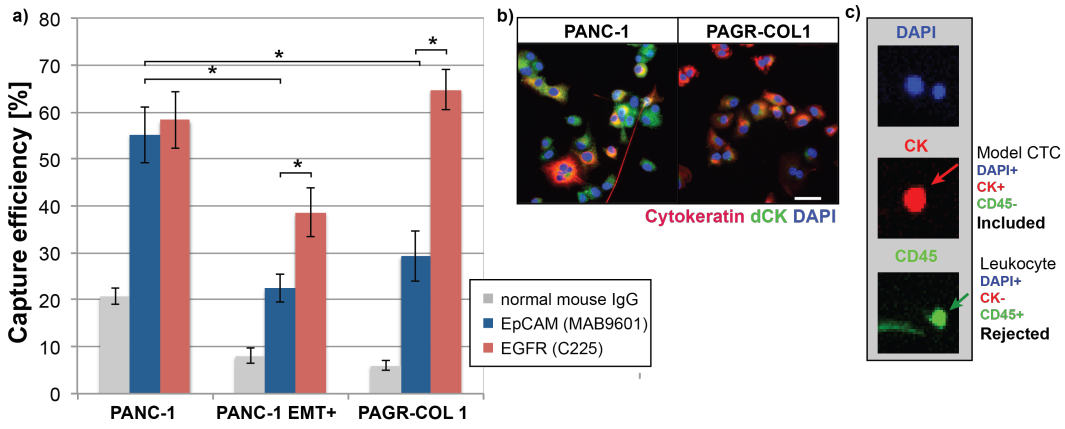

Figure 4.5: a) EMT-induced PANC1 cells and gemcitabine resistant PAGR-COL1 cells display significantly reduced anti-EpCAM capture in the GEDI microdevice, reduced anti-EGFR capture was observed in EMT-induced cells. Overall EGFR capture performed more robustly than EpCAM capture, b) immunofluorescent resistance phenotyping by staining for cytokeratin, dCK and DAPI, c) automated imaging of cells captured on chip allows for CTC phenotyping

Capture performance is thus not a simple linear function of the level of expression. There is likely a threshold expression level below which the adhesive strength generated by antibody-antigen interaction is too weak to immobilize the cells on the surface of the device microposts under the shear imposed by the fluid flowing through the device, which is consistent with our previous findings[104]. The capture performance is thus dependent on the fraction of cells expressing a capture marker level above this threshold. This can explain why the significant loss of EGFR expression in PAGR-COL1 cells does not translate to a significant loss in capture performance despite being on the same relative order as the downregulation of EpCAM in these cells. anti-EGFR capture performance is retained as the absolute EGFR expression level remains high in PAGR-COL1 cells. Other potential explanations include

changes in the distribution and clustering of EpCAM and EGFR receptors on the cell surface as a result of growth factor treatment and chemoresistance. As the loss of dCK expression can be detected using fluorescent staining, see figure 4.5, it would be possible to perform resistance profiling of captured CTCs on chip. Using automated imaging and cell phenotyping, discussed in more detail elsewhere[104][114], we could potentially phenotype captured cells according to the expression of gemcitabine resistant phenotypes, i.e. reduced dCK expression, see figure 4.5.

4.5 Conclusions

EMT-associated loss of epithelial markers (EpCAM and cytokeratin) in cancer cells has important implications for CTC capture modalities that rely on recognition of these markers for cell isolation and identification. Here, we found that TGFβ-induced EMT recapitulates several key aspects of EMT observed in patient CTCs. In particular, we observed loss of EpCAM and cytokeratin expression. We also found a significant loss of EpCAM expression in cancer cells with acquired gemcitabine resistance. These changes in protein expression resulted in loss of anti-EpCAM immunocapture performance. We also identified anti-EGFR capture as a potentially EMT-robust capture mode. EGFR was expressed by all pancreatic cancer cells and culture conditions tested. Future work is necessary to compare the performance of anti-EpCAM and anti-EGFR CTC capture in clinical pancreatic cancer samples.

CHAPTER 5

ACQUIRED CHEMORESISTANCE CHANGES CELL-SORTING OF PANCREATIC CANCER CELLS AND RESULTS IN TUMOR SPHEROID CHEMOPROTECTION

5.1 Abstract

The acquisition of chemoresistance has been shown to lead to changes in cancer cell phenotype and behavior. Here we show that the acquisition of resistance to gemcitabine due to a copy-number amplification of RRM1 in pancreatic cancer cells leads to dysregulation of cell-cell junctions and actin cytoskeleton regulation. This results in altered cell-sorting behavior in tumor spheroids and spheroid chemoprotection.

5.2 Background and Introduction

Although most cancers are thought to be clonal in origin, i.e. stemming from a single cell, it is now well established that over the course of carcinogenesis, multiple cellular clones typically emerge giving rise to significant intratumor heterogeneity as well as heterogeneity between a primary tumor and metastases. The polyclonality of cancer tumors and the resulting heterogeneity is thought to contribute to the resistance to chemotherapy[115][116]. Fully developed pancreatic cancer tumors have been found to be polyclonal[6] and metastatic pancreatic cancer has been shown to display persistent genomic instability, sometimes resulting in the emergence of multiple metastasis-competent clones in the same patient[117] or mouse[118].

Research has also shown that pancreatic tumors are composed of multiple cellular subpopulations. A small subpopulation of pancreatic tumor cells have been found to display cancer stem cell characteristics, including ability to seed metastasis and high intrinsic resistance to chemotherapy[119][120][121]. These cells have in some cases been observed to localize towards the invasive edge of pancreatic cancer tumors[120]. Pancreatic cancers are characterized by having a significant stromal component[5] but relatively little vascularization and invasion of immune cells. Histologically, pancreatic tumors typically appear as tumors where ”regions of duct-like epithelium are interspersed with less differentiated epithelial cells contained within a sea of proliferative stroma”[5]. Pancreatic tumors should thus be regarded as complex tissues, where multiple cell populations are interacting.

The emergence of the structural components of tissues, and the organization of cells into layers and domains has been studied extensively in the context of embryogenesis[122][123][124]. Although the structure of cancer tumors is thought to arise partially as a result of loss of tissue structure and organization, the same rules that guide tissue organization in embryogenesis have to be assumed to apply to tumors. It as been observed that in many cases when different populations of cells are mixed, domains preferentially containing only one of the cell populations spontaneously emerge, a result of a process referred to as ”cell-sorting”. Cell-sorting is a widely observed physiological processes, such as embryogenesis[122][123][124], pathological processes, such as the formation of cancer tumors, as well as in *in vitro* tissue engineering systems[125][126]. The spontaneous organization of mixtures of two cell populations into core-shell type aggregates, where one cell type dominates in the core and the other dominates the shell have been observed in a variety

of contexts[125][126]. What governs cell-sorting behavior is still debated and a number of hypotheses have been put forward, most prominently the differential adhesion hypothesis[125][122][124]. Although no hypothesis has so far been able to fully explain all types of sorting behavior observed, there appears to be a consensus that cell-sorting is driven by the differences in cell-cell adhesion, actomycin contractility and how cellular adhesions link to the cytoskeleton[124][125]. The theoretical models of cell-sorting often assume that, like molecules in a Newtonian fluid, the cells are able to sample enough of the global energy landscape to find an organization that minimizes to total free energy of the system[125]. In real systems this cannot be assumed to be true, and non-equilibrium processes, such as jamming[127] likely plays a significant role in determining the final structure of many cellular systems.

Considering the increasing appreciation for the cross-talk between regulation of cell-cell junctions and remodeling of the cytoskeleton[128], in part mediated by Rho-family small GTPases[129][130], it is not surprising that cell-cell adhesion and contractility both appear to play a role in governing cell-sorting behavior. Interestingly, the difference in expression of cadherins, key mediators of cell-cell adhesions in tissues[124], and differences in adhesive strength were recently shown to not predict the final cell-sorting state of breast cancer co-cultures of cells spanning the range from epithelial- to mesenchymal-like cancer cells[125]. These observations also support the idea that if cell-cell adhesions are dysregulated between two cell populations it can lead to mechanical polarization of cells and increased tension along the borders between the cell types[124][125].

One process that is known to in some case profoundly change the

phenotype of cancer cells is the development of chemoresistance. The acquisition of resistance to the nucleoside analog gemcitabine (difluoro deoxycytidine, dFdC), for example, has been shown to result in dramatically altered cellular phenotypes of cancer cells *in vitro*, often with development of EMT-like characteristics such as increased migratory and invasive cellular behavior[25][26][27]. As a major target of gemcitabine cytotoxic activity, the ribonucleotide reductase (RNR) subunit RRM1, has been associated with the development of chemoresistance. Over-expression of RRM1 has been linked to resistance to gemcitabine chemotherapy both *in vitro*[131][132] and in patients[133]. Interestingly, RRM1 expression is associated with longer survival in cancer patients, presumably due to its role as a tumor suppressor, however it is a predictive biomarker of poor response to gemcitabine treatment[133]. RRM1 over-expression may thus act as mediator of chemoresistance specific to the context of gemcitabine therapy. Gemcitabine (dFdC) inactivates RNR by reacting with the active site of an RRM1 protein in an active RNR complex. The reaction results in the covalent bond between the ribose sugar of dFdC to the active site of RRM1, making dFdC an irreversible suicide inhibitor of RNR. There is evidence that the presence of an excess of RRM1 can result in the reactivation of RNR[134], and that the accumulation of inactivated RRM1 can be detected in cells by western blotting[135].

Here we show that the acquisition of resistance to the small molecule drug gemcitabine in pancreatic cancer cells is caused by a copy-number amplification of the resistance-mediating protein RRM1 and results in a phenotypic switch that changes the cell-sorting behavior of drug-resistant and sensitive cells when grown in spheroid co-cultures. The preferential localization of resistant cells to the surface of spheroids, in combination with the over-expression of RRM1 in

the resistant cells, results in chemoprotection of co-culture spheroids.

5.3 Materials and Methods

Cell culture

BxPC-3 and PANC-1 cells were obtained from ATCC (Manassas, VA). Cell lines were cultured in a humidified incubator (37 °C and 5% CO_2) using media recommended by ATCC (BxPC-3: 10% FBS RPMI and PANC-1: 10% FBS DMEM) with 100 units penicillin, 0.10 mg streptomycin and 0.25 g amphotericin B per ml (Sigma).

Western blotting

Cells were seeded at 500,000 cells/60mm in tissue culture treated dishes, 48h prior to harvest of protein lysates. Before lysis, cells were washed with ice-cold PBS followed by complete removal of the supernatant. 100ul lysis buffer (50 mM Tris, 1% (v/v) Triton X-100, 150 mM NaCl, 2mM PMSF, 1mM sodium orthovanadate and 1X protease inhibitor cocktail from Santa Cruz Biotechnology) was then added per plate. Cells were lysed by mechanical disruption using a cell scraper. Lysates were pipetted 10 times with a 1000ul pipettor to homogenize. Insoluble cellular components were removed by spinning the raw lysates at 15,000xg, for 9 minutes at 4°C. The lysates were then frozen down at -80°C or used right away. Following protein quantification with the DC protein assay (Bio-Rad), lysates were heat-treated in Laemmli sample

buffer (2% SDS, 2% 2-mercaptoethanol, 0.1% bromophenol blue, 10% glycerol, 62.5 mM Tris-HCl) in a dry bath set to 98°C for 5 minutes. 10-15 ug total protein per well was then loaded in 4-20% Tris-Glycine gradient polyacrylamide gels (Thermo). The Bio-Rad Kaleidoscope protein ladder was used as positive control. SDS-PAGE ran at 160V on ice for approximately 1h and 30min in running buffer (25 mM Tris-HCl, 190 mM glycine, 0.1% SDS). Proteins were then transferred to 0.45μm PVDF blotting membranes (Millipore) by electrophoresis at 400mA for 1h and 45min in transfer buffer (25 mM Tris-HCl, 190 mM glycine, 0.1% SDS, 20% methanol) with constant water cooling. Following protein blotting, the membranes were washed in TBST buffer (20 mM Tris-HCl, 150 mM NaCl, 0.1% (v/v) Tween 20) and blocked for 2h in 3% BSA (w/v) in TBST. Blots were stained with primary antibodies over night at 4°C with constant rocking. Primary antibodies used: anti-RRM1 (EPR8483, abcam), anti-RRM2 (N1C1, GeneTex), anti-RRM2B (AF3788, R&D Systems), anti-dCK (Bethyl), anti-E-cadherin (24E10, CST), anti-STIM1 (Bethyl), anti-RhoG (1F3 B3 E5, Biolegend), anti-β-actin (D6A8, abcam). Following washing, the membranes were stained with HRP-conjugated secondary antibodies for 1h at room temperature. Blots were developed with Western Lightning Plus Enhanced Chemiluminescence Substrate (Perkin Elmer) and imaged on a Chemigenius bio-imager.

MTT cytotoxicity assay

For determining the IC_{50} values for gemcitabine and other drugs using MTT cytotoxcity assays, cells were first seeded at 500,000 cells per 60mm dish. After 48 hours of culture, cells were trypsinized and seeded at

5,000 cells per well in 200ul complete media in 96-well plates. Cells were allowed to adhere over-night and media was then replaced with 150ul/well of a 11-point dilution curve of each drug in complete media with 6 replicate wells per condition, including untreated cells and media-only controls. After 96 hours of culture, 16ul of 5mg/ml sterile filtered MTT (3-(4,5-dimethylthiazol-2-yl)-2,5-diphenyltetrazolium bromide), Affymetrix) was added per well. Plates were incubated for 4 hours to allow for the cells to metabolize MTT into purple formazan crystals. Plates were then centrifuged at 1000xg for 5 min to pack formazan crystals on the well bottom. Media was removed by inverting the plates and was replaced by 200ul of acidified isopropanol (50mM HCl and 0.1% Triton X-100 in isopropanol). The solution was pipetted up and down vigorously to dissolve formazan crystals, and plates were left on an orbital shaker set for 37C for 15 min, plates were then inspected for poorly mixed wells. Plates were then read at 560nm and 690nm using a plate reader (Biotek). The relative viability of each drug concentration was calculated by subtracting absorbance at 690nm from 560nm, normalizing to the untreated wells, and averaging the 6 replicates. Sigmoidal kill-curves were fitted to the MTT data using Matlab and IC_{50}-values were calculated as were the interpolating function crosses 50% relative viability.

qPCR copy-number amplification assay

DNA was isolated from pellets containing one million cells for each biological replicate using a DNA micro kit (Qiagen), following the supplier protocol, with the addition of an RNase A treatment step. Isolated DNA was stored at -80C prior to copy-number analysis. Immortalized HUVEC E4 cells were

included in the experiment as a diploid control. A predesigned TaqMan RRM1 qPCR CNV assay (Hs02671698cn, Thermo) was used with an TaqMan RNseP qPCR CNV internal reference assay (Thermo). Copy-number analysis was performed using a ViiA 7 qPCR machine, following the suppliers instructions. Each sample was analyzed with three technical replicates per analysis and each analysis was repeated three times (three biological replicates). To determine the RRM1 copy-number for each cell line and sub-clone, the Ct value for each sample and assay was extracted from the amplification plots. A ΔCt value was determined for each sample ($\Delta Ct = Ct_{RRM1} - Ct_{RNaseP}$), and by assuming exponential amplification, a relative copy-number was then calculated from the ΔCt-value ($n_{rel}=2^{-\Delta Ct}$). An absolute copy-number was calculated by normalizing to the HUVEC diploid control ($n_{abs,subcloneX}=n_{rel,subcloneX}/n_{rel,HUVEC}*2$). The amplification plots were consistent with a diploid copy-number of 2 for RNseP in all samples, indicating that it is an appropriate control for the assay.

siRNA knock-down

For siRNA-mediated knock-down cells were seeded at 400,000 cells/6-well and allowed to adhere over-night. Media was then replaced with 2ml complete media. Cells were then transfected with 125pmol siRNA per 1e6 cells using Lipofectamine RNAiMAX (Thermo). For Western blotting the cells were allowed to incubate with the transfection agent for 72 hours, followed by lysis and Western blotting with the standard procedure described above. Pre-designed Steath siRNAs (Thermo) were used for knock-down: RRM1 (HSS109388, 5'-AAGAUCUGCUUAUUCAGUAACUGGG-3').

Immunofluorescence

Cells were seeded in tissue-culture treated optical-bottom 96-well plates (Thermo) and allowed to grow for 24 hours. Following washing with PBS, cells were fixed with 2% formaldehyde in a PBS/PHEM buffer (60 mM PIPES, 25 mM HEPES, 10 mM EGTA, 2 mM MgCl2) for 15 minutes. Cells were then blocked with 10% normal goat serum for 45 minutes, followed by permeabilization with 0.1% saponin for 5 minutes, when necessary. Following permeabilization, cells were incubated with primary antibodies overnight at 4°C: anti-N-cadherin (R&D Systems), anti-vimentin (RV202, Santa Cruz Biotechnology), anti-E-cadherin (24E10, CST). Cells were then incubated with Alexa Fluor 488, 568 or 647-conjugated secondary antibodies (Life Technologies, Grand Island, NY) for 1 hr at room temperature. For phalloidin staining, cells were incubated with phalloidin conjugated to CruzFluor488 (Santa Cruz Biotechnology, Santa Cruz, CA). Cells were then counterstained with 1ug/ml DAPI (Sigma-Aldrich, St. Louis, MO) for 15 minutes. Representative images were then acquired using a Nikon Eclipse TE2000-U fluorescent microscope or using a Zeiss i880 confocal/multiphoton microscope.

Attachment-free spheroid cell culture

1.5% (w/v) agarose was dissolved in deionized water by heating on a hot plate with constant stirring. When the agarose is completely dissolved, the solution was sterilized by autoclaving at 121°C for 25 minutes. Sterile agaose was then aliquoted and stored at 4°C for later use. To create cell-attachment-free wells, agaose was re-melted by placing the tubes in boiling water until completely

melted. 50ul melted agarose was then pipetted into sterile 96-well plates and plates were swirled to ensure even coverage of the well bottoms. Agarose was allowed to cool down and solidify to at least 30 minutes before adding cells. When solidified, 100ul cell-containing media was then added per well. A total of 2,000 cells were used per spheroid. When appropriate 5μM of the store operated calcium entry inhibitor SKF96365, or 5μM of the Rac1 inhibitor EHop-016 was added.

Spheroid viability assay

48h-old spheroids were treated for 6 days in complete media with or without gemcitabine. Spheroids were labeled by adding propidium iodide and Calcein-AM in serum-free RPMI to spheroid-containing 96-wells. Spheroids were incubated for 30 min and then placed on ice for 10 min, before imaging using a Nikon Eclipse TE2000-U fluorescent microscope.

Multiphoton microscopy

Cells were seeded in complete media at 100,000 cells/24-well and were allowed to adhere over-night. The supernatant was replaced with either CellTracker Green or CellTracker Red (Thermo) at 10μM in serum-free RPMI, and was allowed to incubate with cells for 30 min. After washing with complete media, spheroids were seeded normally. Spheroids were imaged on using a Zeiss i880 confocal/multiphoton microscope.

Spheroid cryosectioning and immunofluorescent staining

For cryosectioning spheroids were collected and allowed to settle in microcentrifuge tubes on ice. Following washing with ice cold PBS, spheroids were fixed in 4% formaldehyde in a PBS/PHEM buffer (60 mM PIPES, 25 mM HEPES, 10 mM EGTA, 2 mM MgCl2) for 20 minutes. Spheroids were stained with 1% methylene blue to make spheroids visible when cryosectioning. Methylene blue-stained spheroids were embedded in Tissue-Tek O.C.T Compound and flash frozen in liquid nitrogen. Spheroids were stored for a minimum of 48h in -80°C before cutting. 8μm spheroid sections were cut onto glass slides. Following removal of embedding matrix by dipping in deionized water and PBS, slides were stained following the standard immunofluorescence protocol described above.

5.4 Results and Discussion

Pancreatic cancer cells with acquired resistance to gemcitabine over-express RRM1

To investigate the relationship between cancer cell phenotype and acquisition of chemoresistance, we first generated gemcitabine-resistant subclones derived from the human pancreatic cancer cell line BxPC-3. The subclones were generated by exposing BxPC-3 cells to increasing concentrations of gemcitabine over a 10-month period. Cell treatment was started at 16nM, as this concentration had been determined to be just below the 96-hour gemcitabine

IC_{50} value for the parental BxPC-3 cells. Transiently increased resistance was observed in the cultures up to about 90nM, where treatment resulted in complete loss of viability. By treating multiple flasks at 80nM we were able to generate a resistant sub-clone emerging from one of the flasks. This clone, referred to as BxGR-80C (for BxPC-3 Gemcitabine Resistant, 80nM, Constant exposure) was isolated and subculured for further experiments. A second resistant clone (BxGR-360C) was isolated from BxGR-80C cells treated with 360nM gemcitabine, following near complete loss of viability in the treated flasks. The gemcitabine resistance of these clones was observed to be stable, as the cells retained resistance after having been grown without gemcitabine for more than 20 passages.

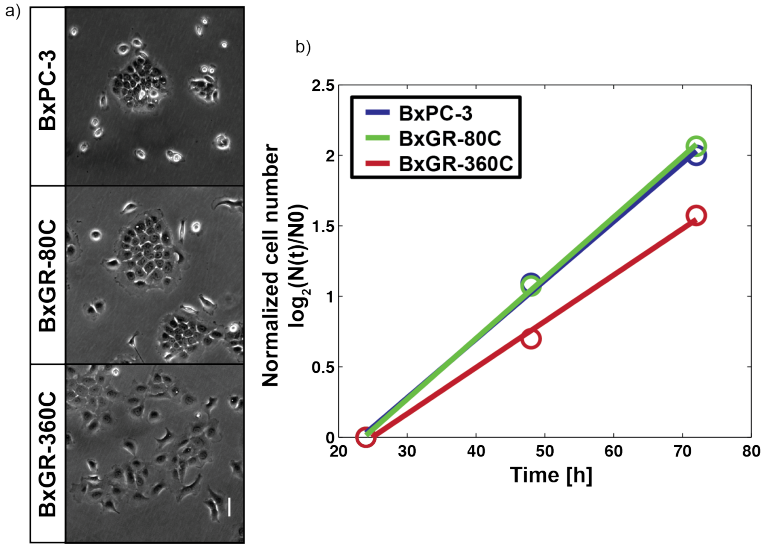

Figure 5.1: a) phase contrast imaging of the pancreatic cancer cell line BxPC-3 and the gemcitabine resistant sub-clones BxGR-80C and BxGR-360C, b) BxGR-360C cells display decrease proliferation rate as compared to BxPC-3 and BxGR-80C cells, doubling times were estimated to be approximately 24h for BxPC-3 and BxGR-80C and 30h for BxGR-360C

The gemcitabine IC_{50}-values (96h treatment) were determined to be approximately 11nM, 200nM (18-fold increase) and 3300 nM (200-fold increase), for BxPC-3, BxGR-80C and BxGR-360C cells respectively, see figure 5.2a. The

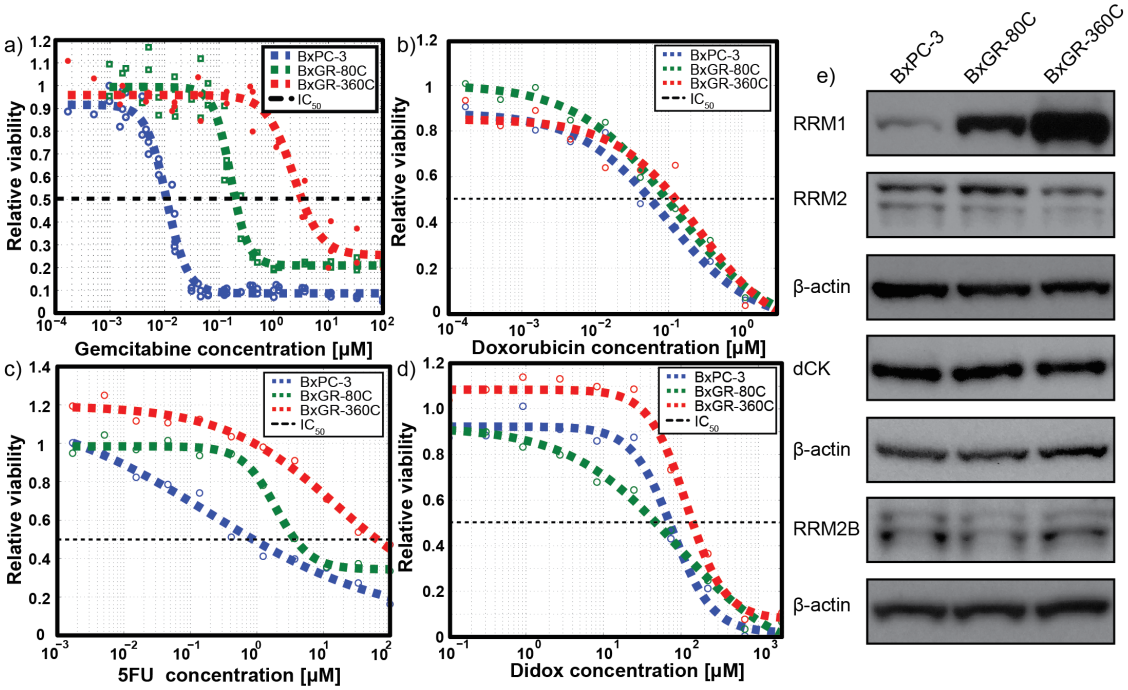

Figure 5.2: a) BxGR-80C and BxGR-360C display significantly increased resistance to gemcitabine as indicated by increased IC_{50} values compared to BxPC-3 cells, b) no doxorubicin cross-resistance was observed in gemcitabine resistant cell lines, c) some cross resistance was observed with 5FU, d) no significant didox cross-resistance was observed, e) Western blotting analysis reveal upregulation of RRM1 in gemcitabine resistant BxPC-3-derived cell lines BxGR-80C and BxGR-360C, no significant changes in RRM2, RRM2B or dCK expression was observed

BxPC-3 and BxGR-80C cells were observed to display similar morphologies and growth behavior in standard 2D culture, including the formation of distinct epithelial colonies in culture, see figure 5.1.BxGR-360C cells were observed to display a more fibroblast-like morphology, with less pronounced colony-formation and a slightly slower growth rate.

To determine potential resistance mechanisms, we measured the expression of known gemcitabine resistance mediators and major targets of gemcitabine, using Western blotting, see figure 5.2e. This protein panel consisted of RNR subunits RRM1, RRM2 and RRM2B, as well as the key gemcitabine-activating

enzyme deoxycytidine kinase (dCK). Using this approach, we found that the BxPC-3-derived sub-clones over-express RRM1. The expression of the other proteins assayed were all unchanged. Using quantitative Western blotting we determined the over-expression of RRM1 to be approximately 20 and 120-fold, in BxGR-80C and BxGR-360C cells, respectively, see figure 5.3b.

To further characterize the resistance of BxGR-80C and BxGR-360C we tested their cross-resistance with other mechanistically related or unrelated small molecule inhibitors. The results of these studies were consistent with an RRM1-mediated resistance mechanism as gemcitabine resistant cells displayed increased resistance to the RRM1-targeting drug clofarabine, but to not to the RRM2-targeting drug didox or to the DNA-targeting drug doxorubicin, see figure 5.2. Interestingly, we observed some cross-resistance with 5-FU. BxGR-360C but not BxGR-80C cells displayed cross-resistance with the structurally similar, but RNR non-targeting drug cytarabine.

Copy-number amplification of RRM1 has been reported to be responsible for RRM1 over-expression in gemcitabine resistant cells. Using qPCR, we determined BxGR-80C and BxGR-360C to have accumulated RRM1 copy-number amplifications of approximately 10- and 60-fold, respectively. The modal RRM1 copy-number of BxPC-3 was determined to be 1, see figure 5.3c.

The RRM1 over-expression thus correlated directly with the observed copy-number amplification in the respective cells, indicating that the amplification likely is a direct cause of the protein over-expression. Furthermore, the gemcitabine IC_{50}-values were observed to correlate directly with RRM1 protein expression and copy-number, indicating that the level of resistance is directly proportional to the amount of RRM1 present in the

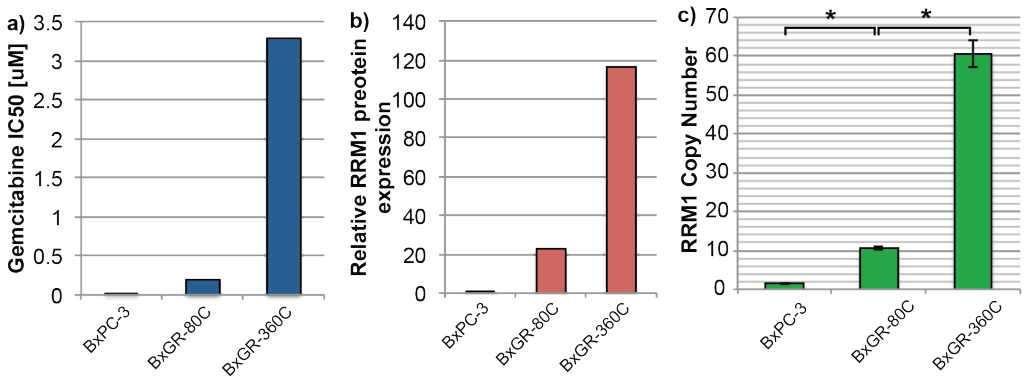

Figure 5.3: a) BxGR-80C and BxGR-360C display 20- and 300-fold increased gemcitabine IC_{50}-values as compared to BxPC-3 cells, respectively, as determined by MTT cytotoxicity assays b) BxGR-80C and BxGR-360C display 20- and 120-fold RRM1 protein expression as compared to BxPC-3 cells, respectively, as determined by quantitative Western blotting c) BxPC-3, BxGR-80C and BxGR-360C cells were determined to have modal RRM1 copy-numbers of 1, 11 and 61, respectively, as determine by qPCR CNV analysis

cells. We therefore conclude that at least two events leading to copy-number amplification of the region of chromosome 11 containing the gene encoding the RRM1 protein have occurred in the BxPC-3 cells, giving rise to the BxGR-80C and BxGR-360C sub-clones respectively.

RRM1 over-expression leads to gemcitabine resistance

To functionally test if RRM1 over-expression is responsible for the observed gemcitabine resistance, we performed siRNA mediated knockdown of RRM1 in BxGR-360C. siRNA knock-down resulted in dramatic resensitization of BxGR-360C cells, see figure 5.4. Following about 40% knock-down of RRM1, as estimated from Western blotting, the gemcitabine IC_{50} value was decreased by 90% in BxGR-360C cells, indicating significant loss of gemcitabine resistance. Over-expression of RRM1 directly leading to acquisition of gemcitabine

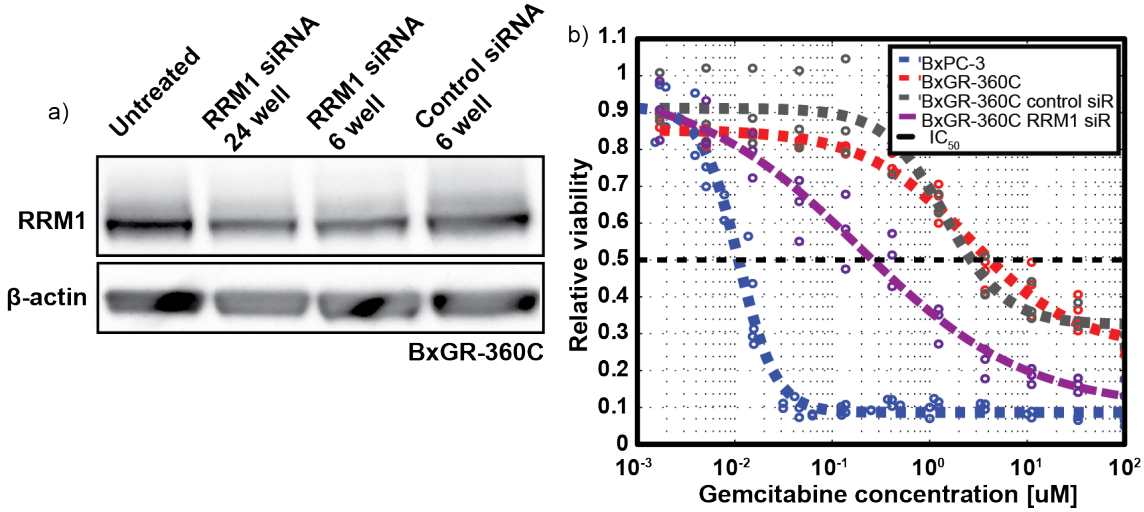

Figure 5.4: a) western blotting of untreated, RRM1 siRNA-treated and control siRNA-treated BxGR-360C cells reveals partial RRM1 knock-down, b) knock-down of RRM1 using siRNA interference results in significant sensitization of BxGR-360C cell to gemcitabine, RRM1 and control siRNA-treated BxGR-360C cells display gemcitabine IC_{50} values of 0.26 and 2.68μM, respectively

resistant is consistent with previous knowledge. The diphosphorylated metabolite of gemcitabine (dFdCDP) is known to inhibit RNR by reacting with the assembled and active RNR complex, forming a covalent bond between the sugar of gemcitabine and the RRM1 subunit of RNR[134]. Although, the inactivated RNR-complex is thought to be stabilized*in vitro*, results support the idea that the presence of an excess of RRM1 can lead to the reactivating of RNR, presumably by functional RRM1 replacing inactivated RRM1 (RRM1*) in the RNR complexes[134].

RNR is an evolutionarily conserved enzyme complex that controls the balance of NDPs and dNDPs in all living cells[134]. Aberrantly low or high levels of RNR activity would likely lead to loss of cell viability as a disrupted NDP/dNDP balance would have severe consequences for a cell. In healthy

cells, RNR activity is primarily controlled by the expression level of RRM2, which is highest during S phase[136]. As we observed the expression of RRM2 to be unchanged in the RRM1-overexpressing sub-clones and as the level of RNR activity is primarily determined by the level of RRM2 present, the excess of RRM1 will thus likely not disturb the NDP/dNDP balance in the cells. Despite observing a 120 fold increase in the amount of RRM1 in our BxGR-360C cells, we only observe a moderately decreased growth-rate. It has previously been described that the reaction of dFdCDP in vitro and in vivo leads to the formation of an inactivated form of RRM1 (RRM1*)[134][135] with an apparent molecular mass of about 110-120kDa, rather than the normal 90kDa, when analyzed by western blotting[135].

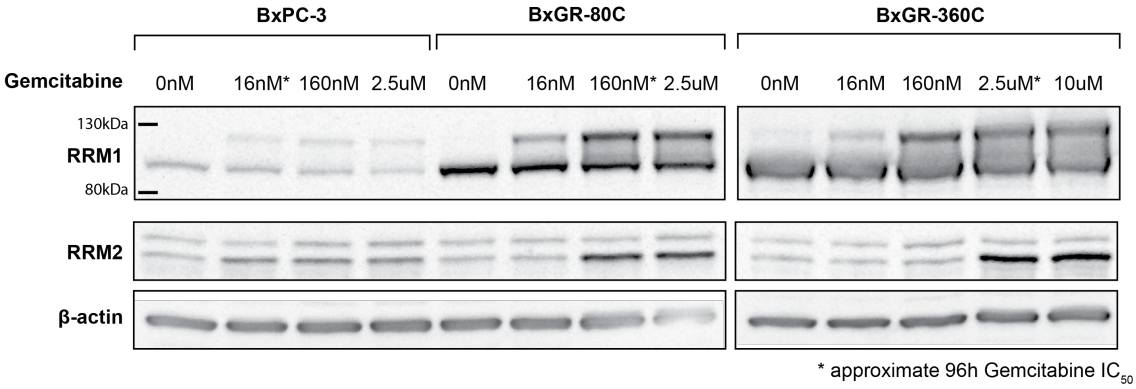

Figure 5.5: Western blotting reveals dose-dependent response to gemcitabine treatment in BxPC-3, BxGR-80C and BxGR-360C. Dose-dependent induction of a RRM1 conformation migrating as an approximately 120kDa protein was observed in gemcitabine treated cells, the intensity of this band was observed to reach a maximum at concentrations around the gemcitabine IC_{50}-value for each cell line. Induction of RRM2 expression was observed at gemcitabine concentrations around the IC_{50}-value for each cell line

In our resistant cells, we observe a dose-dependent induction of a higher molecular weight RRM1 band with an apparent mass of about 120kDa in cell treated with gemcitabine, see figure 5.5. Furthermore, we observe that the ratio between the higher and lower molecular weight RRM1 bands correlates with

the observed IC_{50} values of the respective cell lines. Specifically, the higher molecular weight RRM1 band increases in intensity up until a gemcitabine concentration that correspond to the IC_{50} concentration of the respective cell lines is reached. At gemcitabine concentrations above the approximate IC_{50} value, the band intensity appears unchanged, indicating a maximum accumulation of RRM1*. This observation strengthens our hypothesis that the observed gemcitabine resistance in these cells is a direct result of a presence of excess RRM1, as the saturation value of the ratio between the RRM1* and RRM1 bands likely represents a state where the cells have exhausted their stores of excess RRM1. RRM1 upregulation thus likely leads to gemcitabine resistance by two mechanisms, the presence of excess RRM1 allows cells to (1) maintain enough RNR activity to sustain cell viability despite dFdCDP mediated inactivation of RRM1 by switching out inactivated with functional RRM1, and (2) detoxify gemcitabine by providing enough RRM1 for it to react with, reducing the amount of free and active gemcitabine. In addition, we observe induction of RRM2 expression when the cells are exposed to gemcitabine concentrations above the IC_{50}-value, likely a result of an accumulation of cells in S-phase or a compensatory upregulation of RRM2, in response to lack of RNR-activity.

Gemcitabine resistant cells display evidence of cell-cell junction and cytoskeleton dysregulation

From other studies we know that the acquisition of gemcitabine resistance in pancreatic cancer cells has been linked with an upregulation of mesenchymal markers and the development of an EMT-like phenotype[25][26][27]. As we

observe a markedly altered morphology in BxGR-360C cultures, these initial observations appear to support these findings. To characterize the EMT and cytoskeletal phenotypes of the resistant cells, we performed immunofluorescent staining, in some cases followed up by western blotting for markers involved in these processes. Our results show that BxGR-360C cells express a higher level of filamentous vimentin, a mesenchymal intermediate filament, as compared to parental BxPC-3 cells, see figure 5.6c. No significant difference was observed for the EMT-marker N-cadherin in these cells. BxGR-360C cells were observed to form fewer E-cadherin cell-cell junctions as compared to BxGR-80C and BxPC-3 cells, however, the total amount of E-cadherin present in the cells was observed to be the same for all three cell lines in western blotting, see figure 5.6a and b. BxPC-3 and BxGR-80C cells displayed similar phalloidin staining patterns, whereas BxGR-360C showed a markedly altered intracellular actin distribution and structure. BxGR-360C cells were found to display markedly increased number and size of lamellipodia and cell membrane-associated actin filament formation, as judged by phalloidin staining, see figure 5.6a. BxGR-80C show evidence of somewhat increased filamentous actin expression as compared to BxPC-3 cells, but the difference was subtle. Overall, the resistant cells display evidence of dysregulation of adherens-junction and actin cytoskeleton, most pronounced in the BxGR-360C cells.

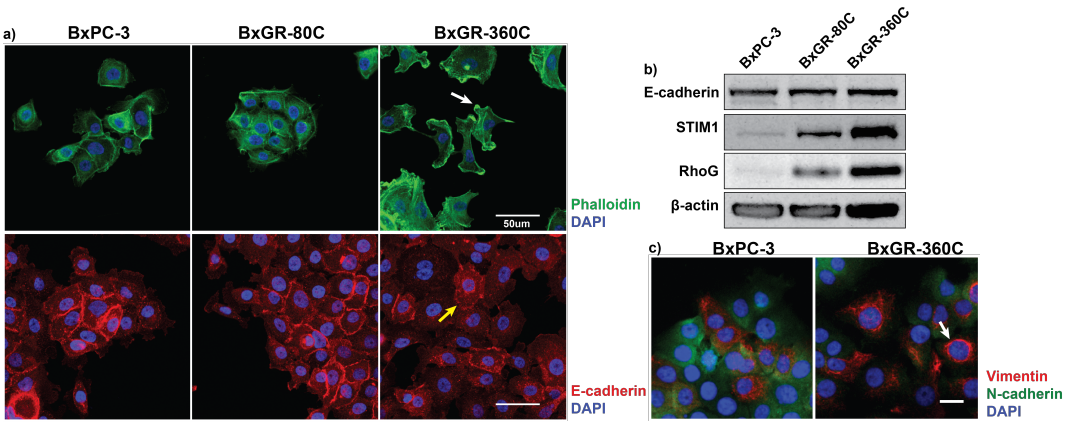

Figure 5.6: Gemcitabine resistant cells display evidence of cell-cell junction and cytoskeletal dysregulation, a) BxGR-360C cells display remodeled actin cytoskeleton, including increased lamellipodia formation (white arrow), and loss of E-cadherin localization to cell-cell junctions (yellow arrow), b) western blotting reveals similar expression of E-cadherin in all sub-clones but over-expression of STIM1 and RhoG associated with a genetic amplification in the chromosome 11p15.4 genomic region, c) BxGR-360C display increased filamentous vimentin (white arrow) expression as compared to BxPC-3 cells

Gemcitabine resistant cells over-express proteins associated with a RRM1 copy-number amplification of a region of chromosome 11p15.4

As discussed previously, we determined the RRM1 over-expression to result from a copy-number amplification of the RRM1 gene, located in the chromosome 11p15.4 region in the human genome. To determine if other genes in this genomic region were also over-expressed in these cells, we performed western blotting for the RhoG and STIM1 proteins, located within 300kb of the RRM1 start codon. The 3′ end of the STIM1 gene is located in a head-to-tail configuration only 1.6 kb from the 5′ end of the RRM1, whereas the RhoG is located 270 kb upstream of the RRM1 gene, on the complimentary DNA strand.

Both proteins were observed to display the same pattern of over-expression in the resistant cells as RRM1, see figure 5.6b. These results strengthen the conclusion that the RRM1 over-expression results from a copy-number amplification and offers an explanation of the alterations in cell phenotype observed as potentially being caused by passenger amplifications of genes functionally unrelated to RRM1 but located in the same genetic region. This result may thus also explain observations of altered phenotype in gemcitabine resistant subclones of BxPC-3 cell made by others[25][26][27]. The discrepancy of phenotypic alterations observed to result from gemcitabine resistance in different pancreatic cancer cell lines may thus be a result of alternative resistance mechanisms being driven by different genetic alterations (RRM1 copy-number amplification, dCK deletion). However, it is remarkable that the acquisition of a more migratory phenotype has repeatedly been observed, in our work and in the work by others.

RhoG is a small GTPase in the Rho family, with significant structural similarity with Rac1[137]. The role of RhoG in healthy and cancerous cells is still debated as early results indicated RhoG as major regulator of Rac1 localization and activity[138][139], however, this observation has been challenged by several newer studies[140]. However, RhoG does appear to play a part in the regulation of actin cytoskeleton cell membrane structure[141][142][143][144], and has been linked to cell migration and invasion[145][146]. STIM1 is a major component of the regulatory part of store operated calcium entry (SOCE) and functions as a endoplasmatic sensor of Ca^{2+}, and signals to its calcium channel partner Orai when the ER is depleted of Ca^{2+}. STIM1 signaling results in the assembly and opening of Orai calcium channels and calcium entry into the cytoplasm[147]. STIM1

has also been linked to migration[148][149][150][151][152], contractility[151], invadopodia formation[148] and metastasis[152].

Rac1 inhibition during spheroid formation was observed to prevent cell-sorting and negatively effect spheroid formation while no effect was observed from SOCE inhibition, see figure 5.10b.

Resistant sub-clones retain ability to form tumor spheroids in attachment-free culture

The phenotypic alterations observed as result of gemcitabine resistance observed by us and others, spurred us to inquire what potential effect these alterations would have on the behavior of gemcitabine resistant cells grown in 3D tumor models as opposed conventional 2D cell culture on rigid plastic substrates. Using an attachment-free culture method we found that the resistant cells retained the ability to form tumor microspheroids, see figure 5.7a. In contrast, the mixed epithelial/mesenchymal phenotype cell line PANC-1 was unable to form spheroids under the same conditions. Spheroid formation was typically observed within 24 hours of seeding cells and spheroids were observed to contract somewhat over-time, see figure 5.7b. No significant spheroid growth, as measured by spheroid diameter was observed over time in attachment free cultures. However, significant spheroids growth was observed when spheroids were encapsulated in matrigel (data not show).

As can be seen in figure 5.7c, the level of gemcitabine resistance, as determined by calcein/propidium iodide staining in gemcitabine treated spheroids was observed to be greatly increased in 3D culture as compared

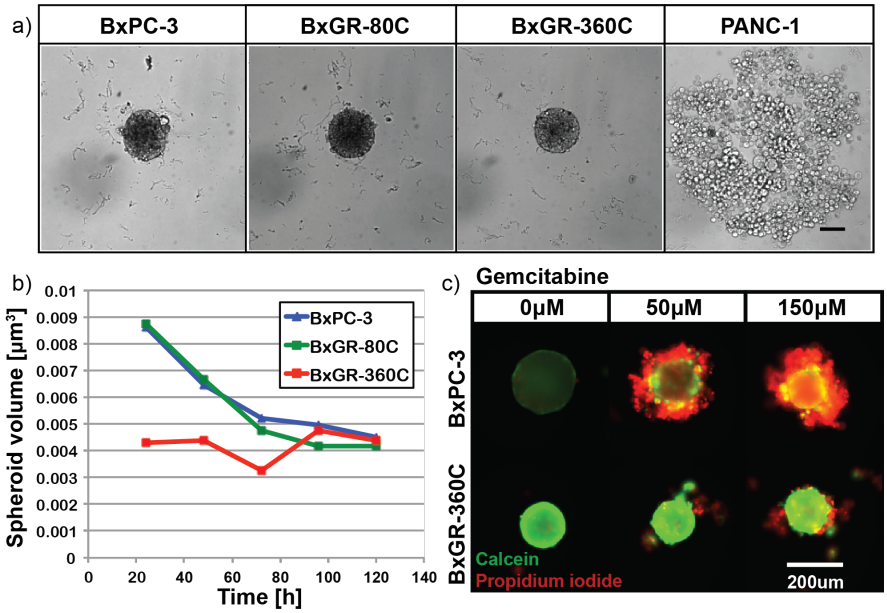

Figure 5.7: a) all BxPC-3-derived cells retain the ability to form tumor spheroids in attachment-free culture, whereas PANC-1 cell do not, scale bar 100μm, b) no signifcant growth is observed in spheroids after initial formation and spheroids are observed to contract over time, c) estimation of spheroid resistance to gemcitabine using calcein and propidium iodide to label live and dead cells, respectively, BxGR-360C cells appear to tolerate gemcitabine 50-fold higher than the 2D IC_{50} value when cultured as tumor spheroids

to conventional 2D culture, consistent with previous literature. We attribute this effect to be the result of the decreased cellular growth-rate observed in 3D culture and the limited drug mass transport into the spheroids.

Resistant cells preferentially localize the outer layer of spheroid co-cultures

To look at the internal cellular structure of heterogenous tumor spheroids we generated co-culture spheroids by mixing BxPC-3 and BxGR-360C cells. Using multiphoton microscopy (MPM) we were able to image the entire cross-section

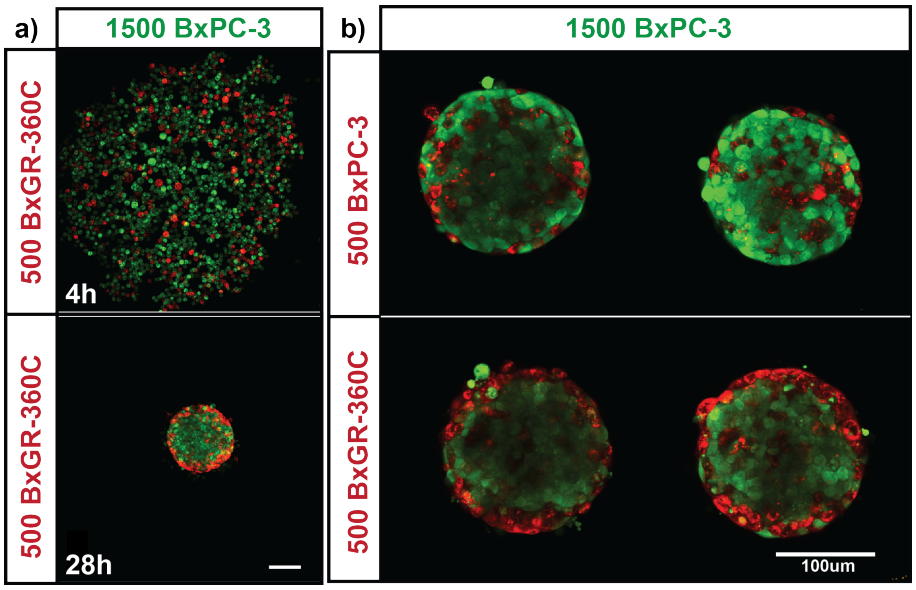

Figure 5.8: a) (top) within 4 hours of seeding cells, a lose network of mixed gemcitabine resistant (BxGR-360C) and sensitive cells (BxPC-3) forms, (bottom) at 28 hours the cellular network has contracted into a spheroid with the resistant cells localized to the surface, b) preferential surface localization of resistant cells is observed in spheroid culture, cells were labeled with CellTracker Green or Red prior to seeding spheroids and were imaged using multiphoton microscopy after 48h of culture

of approximately 200um diameter co-culture spheroids, consisting of a total of 2000 cells without much of the signal drop-off observed for confocal microscopy. Within 30-hours of seeding the spheroids, we observe a striking preferential localization of the BxGR-360C cells to the outer layer of the formed spheroids, see figure 5.8. In these spheroids, gemcitabine-sensitive BxPC-3 cells form a core, surrounded by a layer of BxGR-360C cells. The thickness of the layer of resistant cells was observed to correspond directly to the fraction of resistant cells in the co-cultures. Near-complete surface coverage of resistant cells was observed then the resistance cells constitute 25% or higher of cells in spheroids consisting of a total of 2000 cells. These results were consistent between live cell MPM imaging and cryosectioning followed by immunofluroescence, see figure 5.9b.

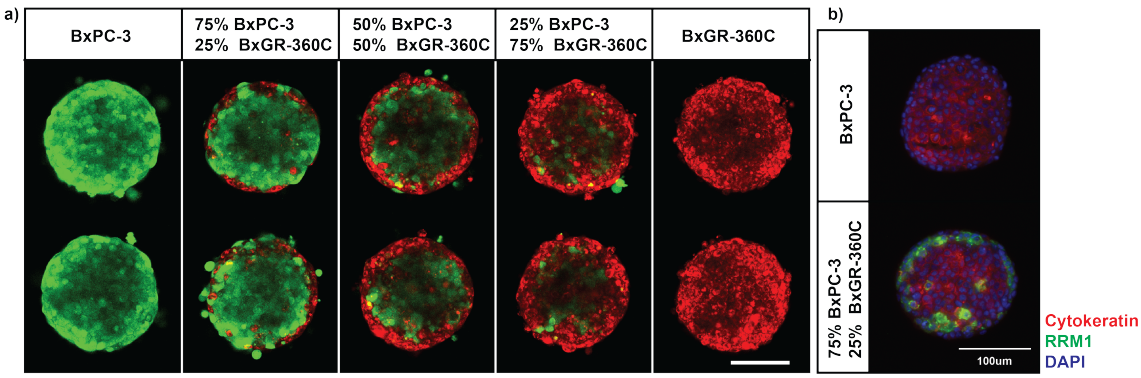

Figure 5.9: a) preferential surface localization of gemcitabine resistant cells (BxGR-360C) when cultured in spheroids with sensitive cell (BxPC-3) is observed across co-culture ratios, b) cryosectioning followed by immunofluorescent staining for RRM1 (green) reveals surface localization of BxGR-360C cells in spheroids, 8μm thick section, DAPI (blue), cytokeratin (red)

We next sought to determine if the cell-sorting behavior was consistent across both resistant sub-clones. To this end we generated co-culture spheroids with all permutations of BxPC-3, mixed together in pairs, see figure 5.10a. To our initial surprise, we found that both resistant sub-clones preferentially localize to the spheroid surface, but that no cell-sorting occurs between 80C and 360C cells. This is surprising as BxPC-3 and BxGR-80C cells are almost phenotypically indistinguishable, whereas BxGR-360C display a very different phenotype, as discussed a section above. To rule out any effect of seeding order or difference in cell settling due to presence of cell clumps we performed experiments with filtered cells and reversed the seeding order, neither of which changed the preferential localization of resistant cells to the surface.

To look closer at the dynamics of spheroid formation, we also performed MPM time-lapse studies on these spheroids, see figure 5.11. These studies indicate that a loosely associated, mostly flat, network of cells forms within 4 hours of seeding the spheroids and that spheroid formation results from the

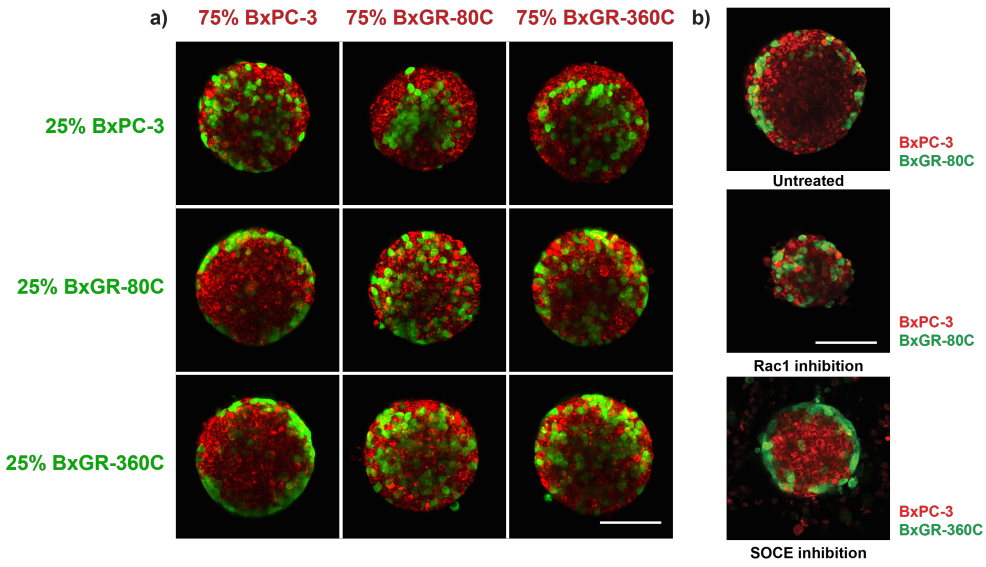

Figure 5.10: Multiphoton live-cell imaging of heterogeneous co-culture spheroids. a) Gemcitabine resistant cells BxGR-80C and BxGR-360C display preferential surface localization when co-cultured with drug-sensitive BxPC-3 cells. No cell-sorting is observed between resistant cells or in spheroids consisting of only one cell type, b) (top) representative spheroid of untreated resistant and non-resistant cells, (middle) Rac inhibition was observed to prevent cell-sorting and adversely affect spheroid formation, (bottom) inhibition of store operated calcium entry (SOCE) was observed to not effect cell-sorting, scale bar 100μm

relatively rapid contraction of this cellular network. By looking in detail at the position of resistant BxGR-360C cells over-time reveals that the BxPC-3 cells contract to form the core of the spheroids, and during this process a majority of resistant cell are deposited on the spheroid surface.

Gemcitabine resistant cells exert a chemoprotective effect on spheroid co-cultures

As discussed previously, the upregulation of RRM1 in BxGR-360C cells results in gemcitabine detoxification by supplying and excess of RRM1 for gemcitabine

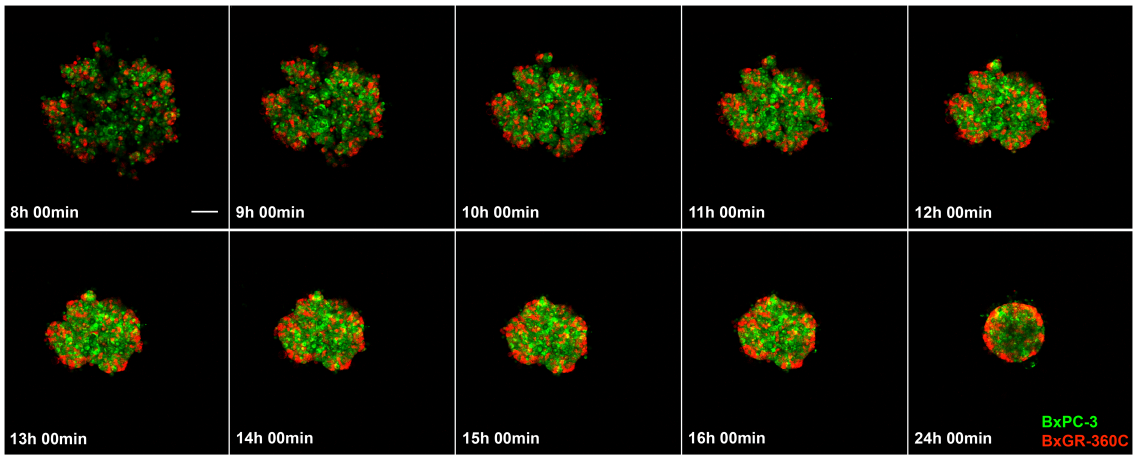

Figure 5.11: Live-cell time lapse multiphoton imaging of spheroid formation. 1500 gemcitabine sensitive BxPC-3 cells (green) were seeded with 500 gemcitabine-resistant BxGR-360C cells (red) in attachment free wells, time lapse imaging was started after 8 hours and spheroids were imaged every 30 minutes for 8 hours, complete spheroid formation was observed after 24 hours, a focal plane near the spheroid center is shown, scale bar 100μm

to react with. The presence of RRM1 over-expressing cells in a tumor may thus lead to gemcitabine depletion in the tumor microenvironment, potentially protecting not only the RRM1 over-expressing cells but also cells in the surrounding microenvironment. Given that the RRM1 over-expressing BxGR-360C cells preferentially localize to the spheroid surface when co-cultured with gemcitabine sensitive BxPC-3 cells, it is possible that the resistant cells may exert a chemoprotective effect on the spheroid as a whole. To determine if this is the case, we exposed co-cultured spheroids consisting of varying ratios of resistant and sensitive cells to a range of gemcitabine concentrations. The relative fraction of viable and dead cells was then determined.

Figure 5.12a shows that here is a marked protective effect from having a small fraction of BxGR-360C cells mixed into a population of BxPC-3. This effect is readily observable when the fraction of resistant cells is 25% or higher, the cellular fraction above which complete surface coverage of resistant cells is

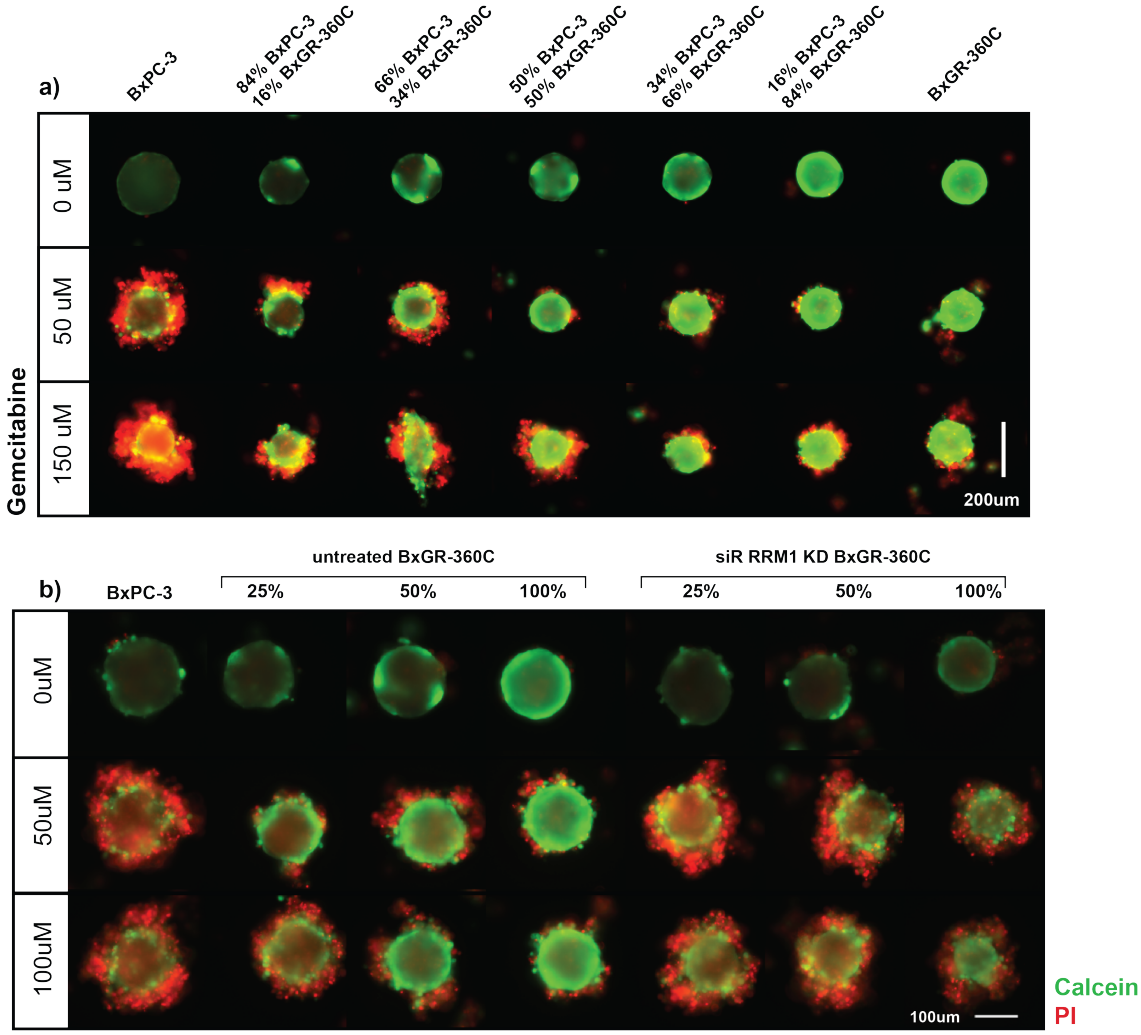

Figure 5.12: Live/dead labeling reveals a chemoprotective effect of gemcitabine resistant cells on heterogenous tumor spheroids treated with gemcitabine. a) a marked chemoprotective effect is observed when a small fraction of gemcitabine-resistant BxGR-360C are co-cultured with drug-sensitive BxPC-3 cell in the presence of gemcitabine, b) the protective effect is lost when RRM1 is knocked-down using siRNA interference in BxGR-360C cells, calcein labels live cells (green) and propidium iodide labels dead cells (red)

observed. Importantly, this protective effect was abolished when RRM1 was knocked down in the resistant cells prior to spheroid formation, see figure 5.12b. This observation thus supports the idea that a minority of cancer cells, expressing a drug resistance pathway may have a positive effect on the viability of the cancer cell population as a whole. We hypothesize this

effect results from the depletion of gemcitabine in the local environment by the RRM1-overexpressing cells, in combination with the limited mass transfer of gemcitabine into the tumor spheroids. The protective effect could thus be overcome by increasing the concentration of available gemcitabine, overflowing the RRM1 resistance mechanism and increasing the flux of drug into the spheroid.

5.5 Conclusions

In conclusion, this work shows that acquisition of genetic mutations, driven by the selection for drug resistance, can lead to changes in microscopic cancer cell phenotype that lead to altered macroscopic properties such as cell-sorting behavior, resulting in increased cell population-level drug resistance.

CHAPTER 6

CONCLUSIONS AND FUTURE DIRECTIONS

6.1 Conclusions

6.1.1 Cellular mechanisms of acquired gemcitabine chemoresistance

In our cell line models of acquired resistance to gemcitabine we have identified two, previously described, independent resistance mechanisms. Cell line subclones derived from PANC-1 and HPAF-II cells display loss of deoxycytidine kinase expression, whereas subclones derived from BxPC-3 display copy-number amplification and overexpression of the ribonucleotide reductase (RNR) subunit RRM1.

Although these resistance mechanisms lead to the same end result, i.e. increased cellular tolerance to gemcitabine, they are different in principle of molecular mechanism. Loss deoxycytidine kinase diminishes intracellular activation of gemcitabine by preventing the phosphorylation of gemcitabine into gemcitabine monophosphate. Whereas, RRM1 is a subunit in the RNR enzyme complex that catalyzes the conversion of NDPs to dNDPs, and thereby supplies building blocks for DNA synthesis. Gemcitabine diphosphate is a irreversible suicide inhibitor of RNR that inhibits the enzyme by covalently reacting to RRM1 subunits in enzymatically active RNR complexes. By overexpressing RRM1, the resistant cells are able to neutralize gemcitabine by allowing the drug to react with RNR complexes and then presumably replacing the inactivated RRM1 with active RRM1, which they have in excess.

Our results indicate that the loss of deoxycytidine expression results in a stronger induction of chemoresistance to gemcitabine than RRM1 overexpression without affecting cell proliferation and viability in any obvious way. RRM1 overexpression however, resulted in more moderate resistance to gemcitabine and significantly slower proliferation rate was observed in cells expressing very high levels of RRM1 (BxGR-360C cells). Since we have concluded that there is a stoichiometric relationship between the level of RRM1 overexpression and the ability of the cell to neutralize gemcitabine in these cells, we would predict that this would lead to a resistance mechanism with limited maximum efficiency. The cells cannot produce unlimited amounts of a particular protein to cope with the drug, and very high levels of overexpression probably have off-target effects. Furthermore, it is thought that RNR inactivation sometimes leads to inactivation of RRM2 as well as RRM1, in which case excess RRM1 alone would not be able to rescue RNR activity. As we have shown conclusively, the genetic amplification also led to the overexpression of other genes in the vicinity of RRM1 (passenger amplifications), genes that may have unpredictable or unfavorable results on cell phenotype and viability when overexpressed.

In this system, it remains unknown why different cell populations under identical conditions develop different resistance mechanism. However, despite in some cases isolating several resistant clones form the same cell line, we always observed the same resistance mechanism emerging in a particular cell line. It is interesting to note that both PANC-1 and HPAF-II are KRAS mutant and SMAD4 wild-type, whereas BxPC-3 are KRAS wild-type and SMAD4 mutant. It is thus possible that the genotype of the cells and resulting cellular state influences the likelihood of a particular resistance mechanism emerging

in the cell population. It is also possible that whichever mechanism emerges first, in a purely stochastic way, becomes the dominant resistance mechanism. Amplification of the RRM1 gene is, to our knowledge, only observed in a small fraction of pancreatic cancer patients. However, it is possible that RRM1 amplification is especially relevant in the small minority of patients (<10%) that suffer from KRAS wild-type pancreatic cancer.

It is also important to remember that conventional chemotherapy is transient. Typically, a patient is treated with a drug through intravenous administration for a relatively short period of time, with a predetermined treatment frequency. The treatment dose, infusion rate and frequency is empirically optimized to maximize the drug efficacy and minimize side effects. Cancer cells are thus only exposed to the drug for a relative short period if time. The half-life of gemcitabine in patients ranges from 30 min to 10 hours, depending on length of infusion and patient characteristics, indicating that the duration of drug-exposure is on the order of hours. This means that in order for a tumor to become clinically resistant to therapy, the cancer cells do not necessarily have to develop resistance mechanisms that allow them to proliferate in the presence of a constant drug concentration. The cells only have to avoid accumulating enough cytotoxic damage to trigger cell death while the drug is still present in the tumor microenvironment. One possible ”resistance mechanism” would thus be a slower proliferation rate. Cancer cells that divide slower are less likely to attempt cell division while the drug is present, and thus less likely to accumulate enough damage to trigger apoptosis. When administration is stopped and the drug concentration goes back down, surviving cells would then be able to repopulate the tumor. Using constant drug exposure to generate resistant cells, as we did in the projects

described in this thesis, the emerging resistance mechanisms may thus not represent mechanisms that are commonly found in patient tumors. However, the mechanisms observed offer important insights into the intracellular drug metabolism and allow for studying how cancer cells adapt to drug treatment and how it influences cell behavior.

Pancreatic cancer displays significant inherent resistance to chemotherapy, often also in the absence of acquired resistance. In most cases even the initial response to therapy is minimal. It is likely that other factors, such as penetration and retention of small molecule drugs in pancreatic tumors play a dominant role in determining the overall response to chemotherapy.

6.1.2 Relationship between cellular phenotype and chemoresistance

Previous research has suggested a strong correlation between cellular EMT-status and resistance to gemcitabine. This correlation has been observed in both directions, i.e. cells with acquired resistance to gemcitabine have been observed to display EMT characteristics, and EMT has been indicated to increase tumor resistance to therapy. It is possible that there is something fundamental about a mesenchymal cellular state that is beneficial for cancer cells in the context of drug resistance. Cancer cells in a mesenchymal state not only proliferate slower, but also engage in fewer cell-cell interactions and operate more independently from each other. It is possible that there are disadvantages associated with being part of a tightly connected epithelial colony when exposed to a cytotoxic drug. Some specialized cell-cell junctions present in epithelial tissues, such as connexins/gap junctions, are able to traffic small molecules directly between the cytoplasm of two adjacent cells and could

thus potentially increase the penetration and distribution of a cytotoxic drug into an epithelial-like cancer cell colony. Long-term exposure to the drug would in this case select agains epithelial traits.

It also well established that epithelial tissues is some cases display communal (non-autonomous) forms of cell death, where cell death-signaling is propagated from cell to cell with in a population[153]. A mesenchymal state could potentially protect against such signaling, but it is unclear how relevant these types of cell death are in the context of cancer. One can also image a protective effect of growing as a colony rather than as individual cells. Single cells will be more exposed to the surrounding media containing the drug than cells within an epithelial colony, which would result in a preference for an epithelial phenotype.

When we set out to generate cell lines with acquired resistance to gemcitabine we expected to find increased expression of EMT-makers and increased EMT-like behavior across the board. However, although we observed loss of epithelial characteristics in most of the cell lines generated, we did not find EMT to be directly implicated in all cells. The EMT-program may be one of many transcriptional programs that lead to similar effects in terms of loss of epithelial phenotype and tissue organization. This may explain why we observe loss of epithelial characteristics, but no clear EMT in the chemoresistant cells.

Formation of cohesive epithelial sheets also require coordination and correct timing cell-cell of signaling and cell-cell junction formation. We observed what appears to be dysregulation of cell-cell junctions in our resistant cells, most likely resulting from genetic aberrations, such as passenger amplifications, accumulated during the development of resistance. Dysregulation of cell-cell

junctions may directly lead to the loss of epithelial characteristics, without requiring the activation of an EMT program. This is emphasized by the fact that we observe the same level of E-cadherin expression in gemcitabine resistant BxPC-3 subclones as we do in sensitive cells, yet fewer cell-cell junctions, which indicates dysregulation of cell-cell junctions rather than downregulation of cell-cell junction components.

6.1.3 The effect of phenotypic heterogeneity on pancreatic circulating tumor cell capture and tumor spheroids

It is well recognized that cancers display significant intra-tumor heterogeneity and often consist of multiple coexisting subclones. There are many processes that can potentially increase cellular heterogeneity of tumors. The clonal development of cancer inherently leads to the development of heterogeneous tumors[154]. In addition, cancer cells are exposed to many types of growth-factor and cytokine-mediated signaling that may influence cell phenotype. Growth-factor induced epithelial-to-mesenchymal transition (EMT) is one example of signaling in the tumor microenvironment that has the potential of increasing the heterogeneity of cancer cell populations. Cancer cells receiving signaling from the microenvironment or from other cells will thus display varying phenotype, despite constituting an isogenic population. Furthermore, the signaling that takes place in the core of a tumor will differ significantly from the signaling closer to the surface, at the intersection between tumor and stroma, or in the vicinity of blood vessels. As a result the signaling networks in a tumor can be assumes to complex, noisy, and unstable, leading to significant cellular heterogeneity.

In the projects described in this thesis, we found that EMT induction and acquired resistance to gemcitabine significantly altered the phenotype and behavior of pancreatic cancer cells. Within these *in vitro* models, we determined the effect of EMT and chemoresistance on microfluidic CTC immunocapture. As immunocapture relies on being able to distinguish cancer cells from blood cells based on a difference in phenotype, processes that change the phenotype of the target cells have serious implications for these isolation platforms. In particular, we found that the loss in expression of the epithelial marker EpCAM resulted in significant loss of capture performance, an observation that has implications for the clinical implementation of positive-selection CTC technologies. In addition, we identified EGFR capture as a potentially more robust capture modality, as compared to EpCAM capture.

In a separate study, we observed striking effects of the acquisition of chemoresistance on the tissue-level organizational characteristics of some cancer cell populations. We found that acquired chemoresistance altered the cell-sorting behavior of some cells and that chemoresistant cells preferentially localize to the outside of tumor spheroids in some cases. The preferential localization of resistant cells to the outside of spheroids, in combination with the mechanism of drug resistance, results in chemoprotection of the cancer cell population as a whole.

The protective effect of resistant cancer cells on non-resistant populations we observe, suggests the possibility of cooperation between cancer cell populations in tumors. In a different context, cooperation of antibiotic resistant and non-resistant cell populations, resulting in mutually beneficial chemoprotection has been observed in bacterial co-cultures[155]. It is thus not unreasonable

to predict that this may also take place in some mammalian tumors. Indeed, cooperation between cancer subpopulations has been suggested to occur also human cancers and to potentially have clinical implications[154].

6.2 Future directions

6.2.1 Circulating epithelial cells as biomarkers for risk stratification of patients with pancreatic cystic lesions

In this thesis we have shown feasibility of using captured circulating epithelial cells (CECs) as biomarkers for risk-stratification of patients with precancerous pancreatic cyst lesions. Immediate follow up studies to the work in this thesis include, (1) comparing EpCAM, EGFR and MUC1 as targets for microfluidic immunocapture of CTCs and CECs from patients samples, (2) a longitudinal follow-up study of the patients screened in Chapter 2 to determine if CEC count and phenotype correlates with evidence of carcinogenesis upon resection and long-term survival, and (3) genetic analysis of captured CECs to determine their connection to carcinogenesis. KRAS and GNAS mutations are indicated in the progression of IPMNs to pancreatic cancer and could serve a appropriate mutations to screen for in captured CEC[94].

6.2.2 Cell-sorting in tumor spheroids

To understand the fundamental processes that control cell-sorting in tumor spheroids further work is necessary. Our results thus far indicate that cell-sorting is driven, in part, by dysregulation of cell-cell junctions and cell junction-cytoskeleton interactions.

Phenotypic characterization of cells that sort in spheroid cultures point to a potential role of Rho-familiy small GTPases. Specifically, RhoG may play a role in the sorting behavior observed in Chapter 4. Following the same logic, the potential role of STIM1 should be evaluated. siRNA-mediated knock-down of RhoG and STIM1 may clarify their potential roles in cell-sorting. Alternatively, RhoG or STIM1 could be knocked-in in naive cells. If possible, the transcriptome of resistant and non-resistant BxPC-3 clones should be analyzed and compared to rule out other potential mechanisms. It would also be interesting to see if EMT-induction leads to cell-sorting in cancer cell populations, a question we would be able to address directly using the models developed in Chapter 3 and Chapter 4.

Works should also be undertaken to determine the generality of the observation that chemoresistant cells preferentially localize to surface of spheroids, as this may be of mechanistic and pathological significance. Other cell culture systems, such as doxorubicin resistant MCF7 cultures should be tested[156].

BIBLIOGRAPHY

[1] L Rahib, B D Smith, R Aizenberg, A B Rosenzweig, J M Fleshman, and L M Matrisian. Projecting Cancer Incidence and Deaths to 2030: The Unexpected Burden of Thyroid, Liver, and Pancreas Cancers in the United States. *Cancer Research*, 74(11):2913–2921, May 2014.

[2] Rebecca L Siegel, Kimberly D Miller, and Ahmedin Jemal. Cancer statistics, 2016. *CA: a cancer journal for clinicians*, 66(1):7–30, January 2016.

[3] Audrey Vincent, Joseph Herman, Rich Schulick, Ralph H Hruban, and Michael Goggins. Pancreatic cancer. *Lancet*, 378(9791):607–620, August 2011.

[4] M Ducreux, A Sa Cuhna, C Caramella, A Hollebecque, P Burtin, D Goéré, T Seufferlein, K Haustermans, J L Van Laethem, T Conroy, and D Arnold. Cancer of the pancreas: ESMO Clinical Practice Guidelines for diagnosis, treatment and follow-up. *Annals of Oncology*, 26(suppl 5):v56–v68, August 2015.

[5] Andrew D Rhim and Ben Z Stanger. Molecular biology of pancreatic ductal adenocarcinoma progression: aberrant activation of developmental pathways. *Progress in molecular biology and translational science*, 97:41–78, 2010.

[6] S Yachida and C A Iacobuzio-Donahue. Evolution and dynamics of pancreatic cancer progression. *Oncogene*, 32(45):5253–5260, November 2013.

[7] Masao Tanaka, Carlos Fernández-del Castillo, Volkan Adsay, Suresh Chari, Massimo Falconi, Jin-Young Jang, Wataru Kimura, Philippe Levy, Martha Bishop Pitman, C Max Schmidt, Michio Shimizu, Christopher L Wolfgang, Koji Yamaguchi, and Kenji Yamao. International consensus guidelines 2012 for the management of IPMN and MCN of the pancreas. *PAN*, 12(3):183–197, May 2012.

[8] Daniel D Von Hoff, Thomas Ervin, Francis P Arena, E Gabriela Chiorean, Jeffrey Infante, Malcolm Moore, Thomas Seay, Sergei A Tjulandin, Wen Wee Ma, Mansoor N Saleh, Marion Harris, Michele Reni, Scot Dowden, Daniel Laheru, Nathan Bahary, Ramesh K Ramanathan, Josep Tabernero, Manuel Hidalgo, David Goldstein, Eric Van Cutsem, Xinyu Wei, Jose Iglesias, and Markus F Renschler. Increased Survival in Pancreatic Cancer with nab-Paclitaxel plus Gemcitabine. *The New England journal of medicine*, 369(18):1691–1703, October 2013.

[9] Klaus Pantel and Ruud H Brakenhoff. Dissecting the metastatic cascade. *Nature Reviews Cancer*, 4(6):448–456, June 2004.

[10] Scott Valastyan and Robert A Weinberg. Tumor Metastasis: Molecular Insights and Evolving Paradigms. *Cell*, 147(2):275–292, October 2011.

[11] Andrew D Rhim, Emily T Mirek, Nicole M Aiello, Anirban Maitra, Jennifer M Bailey, Florencia McAllister, Maximilian Reichert, Gregory L Beatty, Anil K Rustgi, Robert H Vonderheide, Steven D Leach, and Ben Z Stanger. EMT and Dissemination Precede Pancreatic Tumor Formation. *Cell*, 148(1-2):349–361, January 2012.

[12] Sunitha Nagrath, Rhonda M Jack, Vaibhav Sahai, and Diane M Simeone. Opportunities and Challenges for Pancreatic Circulating Tumor Cells. *Gastroenterology*, 151(3):412–426, September 2016.

[13] Yibin Kang and Joan Massagué. Epithelial-mesenchymal transitions: twist in development and metastasis. *Cell*, 118(3):277–279, August 2004.

[14] Jean Paul Thiery. Epithelial–mesenchymal transitions in tumour progression. *Nature Reviews Cancer*, 2(6):442–454, June 2002.

[15] Raghu Kalluri and Robert A Weinberg. The basics of epithelial-mesenchymal transition. *Journal of Clinical Investigation*, 119(6):1420–1428, June 2009.

[16] Raghu Kalluri and Eric G Neilson. Epithelial-mesenchymal transition and its implications for fibrosis. *Journal of Clinical Investigation*, 112(12):1776–1784, December 2003.

[17] Xiaofeng Zheng, Julienne L Carstens, Jiha Kim, Matthew Scheible, Judith Kaye, Hikaru Sugimoto, Chia-Chin Wu, Valerie S LeBleu, and Raghu Kalluri. Epithelial-to-mesenchymal transition is dispensable for metastasis but induces chemoresistance in pancreatic cancer. *Nature*, 527(7579):525–530, November 2015.

[18] V Ellenrieder, S F Hendler, W Boeck, T Seufferlein, A Menke, C Ruhland, G Adler, and T M Gress. Transforming growth factor beta1 treatment leads to an epithelial-mesenchymal transdifferentiation of pancreatic cancer cells requiring extracellular signal-regulated kinase 2 activation. *Cancer Research*, 61(10):4222–4228, May 2001.

[19] N A Bhowmick, M Ghiassi, A Bakin, M Aakre, C A Lundquist, M E Engel, C L Arteaga, and H L Moses. Transforming growth factor-beta1 mediates epithelial to mesenchymal transdifferentiation through a RhoA-dependent mechanism. *Molecular biology of the cell*, 12(1):27–36, January 2001.

[20] M Zeisberg, J Hanai, H Sugimoto, T Mammoto, D Charytan, F Strutz, and R Kalluri. BMP-7 counteracts TGF-β1–induced epithelial-to-mesenchymal

transition and reverses chronic renal injury. *Nature medicine*, 9(7):964–968, 2003.

[21] Lu Xie, Brian K Law, Anna M Chytil, Kimberly A Brown, Mary E Aakre, and Harold L Moses. Activation of the Erk Pathway Is Required for TGF-β1–Induced EMT In Vitro. *Neoplasia*, 6(5):603–610, September 2004.

[22] Hidenori Kasai, Jeremy T Allen, Roger M Mason, Takashi Kamimura, and Zhi Zhang. TGF-beta1 induces human alveolar epithelial to mesenchymal cell transition (EMT). *Respiratory research*, 6:56, June 2005.

[23] S Uttamsingh, X Bao, K T Nguyen, M Bhanot, J Gong, J L-K Chan, F Liu, T T Chu, and L-H Wang. Synergistic effect between EGF and TGF-β1 in inducing oncogenic properties of intestinal epithelial cells. *Oncogene*, 27(18):2626–2634, November 2007.

[24] Irina Kolosova, David Nethery, and Jeffrey A Kern. Role of Smad2/3 and p38 MAP kinase in TGF-β1-induced epithelial-mesenchymal transition of pulmonary epithelial cells. *Journal of cellular physiology*, 226(5):1248–1254, February 2011.

[25] Ami N Shah, Justin M Summy, Jing Zhang, Serk In Park, Nila U Parikh, and Gary E Gallick. Development and Characterization of Gemcitabine-Resistant Pancreatic Tumor Cells. *Annals of surgical oncology*, 14(12):3629–3637, October 2007.

[26] Alakesh Bera, Kolaparthi VenkataSubbaRao, Muthu Saravanan Manoharan, Ping Hill, and James W Freeman. A miRNA Signature of Chemoresistant Mesenchymal Phenotype Identifies Novel Molecular Targets Associated with Advanced Pancreatic Cancer. *PLoS ONE*, 9(9):e106343, September 2014.

[27] Betty K Samulitis, Kelvin W Pond, Erika Pond, Anne E Cress, Hitendra Patel, Lee Wisner, Charmi Patel, Robert T Dorr, and Terry H Landowski. Gemcitabine resistant pancreatic cancer cell lines acquire an invasive phenotype with collateral hypersensitivity to histone deacetylase inhibitors. *Cancer biology & therapy*, 16(1):43–51, 2014.

[28] A Lecharpentier, P Vielh, P Perez-Moreno, D Planchard, J C Soria, and F Farace. Detection of circulating tumour cells with a hybrid (epithelial/mesenchymal) phenotype in patients with metastatic non-small cell lung cancer. *British Journal of Cancer*, 105(9):1338–1341, October 2011.

[29] M Yu, A Bardia, B S Wittner, S L Stott, M E Smas, D T Ting, S J Isakoff, J C Ciciliano, M N Wells, A M Shah, K F Concannon, M C Donaldson, L V Sequist, E Brachtel, D Sgroi, J Baselga, S Ramaswamy, M Toner, D A Haber, and S Maheswaran. Circulating Breast Tumor Cells Exhibit

Dynamic Changes in Epithelial and Mesenchymal Composition. *Science*, 339(6119):580–584, January 2013.

[30] Galatea Kallergi, Maria A Papadaki, Eleni Politaki, Dimitris Mavroudis, Vassilis Georgoulias, and Sophia Agelaki. Epithelial to mesenchymal transition markers expressed in circulating tumour cells of early and metastatic breast cancer patients. *Breast Cancer Research*, 13(3):R59, June 2011.

[31] Andrew D Rhim, Fredrik I Thege, Steven M Santana, Timothy B Lannin, Trisha N Saha, Shannon Tsai, Lara R Maggs, Michael L Kochman, Gregory G Ginsberg, John G Lieb, Vinay Chandrasekhara, Jeffrey A Drebin, Nuzhat Ahmad, Yu-Xiao Yang, Brian J Kirby, and Ben Z Stanger. Detection of circulating pancreas epithelial cells in patients with pancreatic cystic lesions. *Gastroenterology*, 146(3):647–651, March 2014.

[32] C Alix-Panabieres and K Pantel. Circulating Tumor Cells: Liquid Biopsy of Cancer. *Clinical chemistry*, 59(1):110–118, January 2013.

[33] Erica D Pratt, Chao Huang, Benjamin G Hawkins, Jason P Gleghorn, and Brian J Kirby. Rare cell capture in microfluidic devices. *Chemical Engineering Science*, 66(7):1508–1522, October 2010.

[34] Sunitha Nagrath, Lecia V Sequist, Shyamala Maheswaran, Daphne W Bell, Daniel Irimia, Lindsey Ulkus, Matthew R Smith, Eunice L Kwak, Subba Digumarthy, Alona Muzikansky, Paula Ryan, Ulysses J Balis, Ronald G Tompkins, Daniel A Haber, and Mehmet Toner. Isolation of rare circulating tumour cells in cancer patients by microchip technology. *Nature*, 450(7173):1235–1239, December 2007.

[35] Shannon L Stott, Chia-Hsien Hsu, Dina I Tsukrov, Min Yu, David T Miyamoto, Belinda A Waltman, S Michael Rothenberg, Ajay M Shah, Malgorzata E Smas, George K Korir, Frederick P Floyd, Anna J Gilman, Jenna B Lord, Daniel Winokur, Simeon Springer, Daniel Irimia, Sunitha Nagrath, Lecia V Sequist, Richard J Lee, Kurt J Isselbacher, Shyamala Maheswaran, Daniel A Haber, and Mehmet Toner. Isolation of circulating tumor cells using a microvortex-generating herringbone-chip. *Proceedings of the National Academy of Sciences of the United States of America*, 107(43):18392–18397, October 2010.

[36] Elodie Sollier, Derek E Go, James Che, Daniel R Gossett, Sean O'Byrne, Westbrook M Weaver, Nicolas Kummer, Matthew Rettig, Jonathan Goldman, Nicholas Nickols, Susan McCloskey, Rajan P Kulkarni, and Dino Di Carlo. Size-selective collection of circulating tumor cells using Vortex technology. *Lab on a Chip*, 14(1):63, 2013.

[37] Nezihi Murat Karabacak, Philipp S Spuhler, Fabio Fachin, Eugene J Lim, Vincent Pai, Emre Ozkumur, Joseph M Martel, Nikola Kojic, Kyle Smith, Pin-i Chen, Jennifer Yang, Henry Hwang, Bailey Morgan, Julie Trautwein, Thomas A Barber, Shannon L Stott, Shyamala Maheswaran, Ravi Kapur, Daniel A Haber, and Mehmet Toner. Microfluidic, marker-free isolation of circulating tumor cells from blood samples. *Nature Protocols*, 9(3):694–710, February 2014.

[38] Jason P Gleghorn, Erica D Pratt, Denise Denning, He Liu, Neil H Bander, Scott T Tagawa, David M Nanus, Paraskevi A Giannakakou, and Brian J Kirby. Capture of circulating tumor cells from whole blood of prostate cancer patients using geometrically enhanced differential immunocapture (GEDI) and a prostate-specific antibody. *Lab on a Chip*, 10(1):27–29, January 2010.

[39] Brian J Kirby, Mona Jodari, Matthew S Loftus, Gunjan Gakhar, Erica D Pratt, Chantal Chanel-Vos, Jason P Gleghorn, Steven M Santana, He Liu, James P Smith, Vicente N Navarro, Scott T Tagawa, Neil H Bander, David M Nanus, and Paraskevi Giannakakou. Functional Characterization of Circulating Tumor Cells with a Prostate-Cancer-Specific Microfluidic Device. *PLoS ONE*, 7(4):e35976, April 2012.

[40] Kenneth H Yu, Mark Ricigliano, Manuel Hidalgo, Ghassan K Abou-Alfa, Maeve A Lowery, Leonard B Saltz, Joseph F Crotty, Kristen Gary, Brandon Cooper, Rena Lapidus, Mariola Sadowska, and Eileen M O'Reilly. Pharmacogenomic modeling of circulating tumor and invasive cells for prediction of chemotherapy response and resistance in pancreatic cancer. *Clinical cancer research : an official journal of the American Association for Cancer Research*, 20(20):5281–5289, October 2014.

[41] Marcia Irene Canto, Ralph H Hruban, Elliot K Fishman, Ihab R Kamel, Richard Schulick, Zhe Zhang, Mark Topazian, Naoki Takahashi, Joel Fletcher, Gloria Petersen, Alison P Klein, Jennifer Axilbund, Constance Griffin, Sapna Syngal, John R Saltzman, Koenraad J Mortele, Jeffrey Lee, Eric Tamm, Raghunandan Vikram, Priya Bhosale, Daniel Margolis, James Farrell, and Michael Goggins. Frequent Detection of Pancreatic Lesions in Asymptomatic High-Risk Individuals. *Gastroenterology*, 142(4):796–804, April 2012.

[42] Subhankar Chakraborty, Michael J Baine, Aaron R Sasson, and Surinder K Batra. Current status of molecular markers for early detection of sporadic pancreatic cancer. *BBA - Reviews on Cancer*, 1815(1):44–64, January 2011.

[43] Massimo Cristofanilli, G Thomas Budd, Matthew J Ellis, Alison Stopeck, Jeri Matera, M Craig Miller, James M Reuben, Gerald V Doyle, W Jeffrey

Allard, Leon W M M Terstappen, and Daniel F Hayes. Circulating tumor cells, disease progression, and survival in metastatic breast cancer. *The New England journal of medicine*, 351(8):781–791, August 2004.

[44] J S de Bono, H I Scher, R B Montgomery, C Parker, M C Miller, H Tissing, G V Doyle, L W W M Terstappen, K J Pienta, and D Raghavan. Circulating Tumor Cells Predict Survival Benefit from Treatment in Metastatic Castration-Resistant Prostate Cancer. *Clinical Cancer Research*, 14(19):6302–6309, October 2008.

[45] M G Krebs, R Sloane, L Priest, L Lancashire, J M Hou, A Greystoke, T H Ward, R Ferraldeschi, A Hughes, G Clack, M Ranson, C Dive, and F H Blackhall. Evaluation and Prognostic Significance of Circulating Tumor Cells in Patients With Non-Small-Cell Lung Cancer. *Journal of Clinical Oncology*, 29(12):1556–1563, April 2011.

[46] S J Cohen, C J A Punt, N Iannotti, B H Saidman, K D Sabbath, N Y Gabrail, J Picus, M A Morse, E Mitchell, M C Miller, G V Doyle, H Tissing, L W M M Terstappen, and N J Meropol. Prognostic significance of circulating tumor cells in patients with metastatic colorectal cancer. *Annals of Oncology*, 20(7):1223–1229, June 2009.

[47] Edlyn Soeth, Urte Grigoleit, Barbara Moellmann, Christian Röder, Bodo Schniewind, Bernd Kremer, Holger Kalthoff, and Ilka Vogel. Detection of tumor cell dissemination in pancreatic ductal carcinoma patients by CK 20 RT-PCR indicates poor survival. *Journal of Cancer Research and Clinical Oncology*, 131(10):669–676, September 2005.

[48] Katrin Hoffmann, Christiane Kerner, Wolfgang Wilfert, Marc Mueller, Joachim Thiery, Johann Hauss, and Helmut Witzigmann. Detection of disseminated pancreatic cells by amplification of cytokeratin-19 with quantitative RT-PCR in blood, bone marrow and peritoneal lavage of pancreatic carcinoma patients. *World journal of gastroenterology : WJG*, 13(2):257–263, January 2007.

[49] Toshio Kurihara, Takao Itoi, Atsushi Sofuni, Fumihide Itokawa, Takayoshi Tsuchiya, Shujirou Tsuji, Kentaro Ishii, Nobuhito Ikeuchi, Akihiko Tsuchida, Kazuhiko Kasuya, Takashi Kawai, Yoshihiro Sakai, and Fuminori Moriyasu. Detection of circulating tumor cells in patients with pancreatic cancer: a preliminary result. *Journal of Hepato-Biliary-Pancreatic Surgery*, 15(2):189–195, April 2008.

[50] B P Negin, N J Meropol, and R K Alpaugh. Characterization and prognostic significance of circulating tumor cells in the peripheral blood of patients with metastatic pancreatic cancer. – Negin et al. 28 (15): 4127 – ASCO Meeting Abstracts. *ASCO Meeting Abstract*, 2010.

[51] L Khoja, A Backen, R Sloane, L Menasce, D Ryder, M Krebs, R Board, G Clack, A Hughes, F Blackhall, J W Valle, and C Dive. A pilot study to explore circulating tumour cells in pancreatic cancer as a novel biomarker. *British Journal of Cancer*, 106(3):508–516, January 2012.

[52] Andreia de Albuquerque, Ilja Kubisch, Georg Breier, Gudrun Stamminger, Nikos Fersis, Astrid Eichler, Sepp Kaul, and Ulrich Stölzel. Multimarker gene analysis of circulating tumor cells in pancreatic cancer patients: a feasibility study. *Oncology*, 82(1):3–10, 2012.

[53] F C Bidard, F Huguet, C Louvet, L Mineur, O Bouche, B Chibaudel, P Artru, F Desseigne, J B Bachet, C Mathiot, J Y Pierga, and P Hammel. Circulating tumor cells in locally advanced pancreatic adenocarcinoma: the ancillary CirCe 07 study to the LAP 07 trial. *Annals of Oncology*, 24(8):2057–2061, July 2013.

[54] Yujuan Zhang, Fei Wang, Ning Ning, Qian Chen, Zhuo Yang, Ye Guo, Danfei Xu, Donghong Zhang, Ting Zhan, and Wei Cui. Patterns of circulating tumor cells identified by CEP8, CK and CD45 in pancreatic cancer. *International journal of cancer*, 136(5):1228–1233, March 2015.

[55] Yuko Mataki, Sonshin Takao, Kousei Maemura, Shinichiro Mori, Hiroyuki Shinchi, Shoji Natsugoe, and Takashi Aikou. Carcinoembryonic antigen messenger RNA expression using nested reverse transcription-PCR in the peripheral blood during follow-up period of patients who underwent curative surgery for biliary-pancreatic cancer: longitudinal analyses. *Clinical cancer research : an official journal of the American Association for Cancer Research*, 10(11):3807–3814, June 2004.

[56] Gregory Sergeant, Tania Roskams, Jos van Pelt, François Houtmeyers, Raymond Aerts, and Baki Topal. Perioperative cancer cell dissemination detected with a real-time RT-PCR assay for EpCAM is not associated with worse prognosis in pancreatic ductal adenocarcinoma. *BMC Cancer*, 11:47, January 2011.

[57] Gregory Sergeant, Rudy van Eijsden, Tania Roskams, Victor Van Duppen, and Baki Topal. Pancreatic cancer circulating tumour cells express a cell motility gene signature that predicts survival after surgery. *BMC Cancer*, 12:527, November 2012.

[58] Chuanli Ren, Chongxu Han, Jinqing Zhang, Ping He, Daxin Wang, Buhai Wang, Ping Zhao, and Xiaohang Zhao. Detection of apoptotic circulating tumor cells in advanced pancreatic cancer following 5-fluorouracil chemotherapy. *Cancer biology & therapy*, 12(8):700–706, October 2011.

[59] Jason Klapman and Mokenge P Malafa. Early detection of pancreatic cancer: why, who, and how to screen. *Cancer control : journal of the Moffitt Cancer Center*, 15(4):280–287, October 2008.

[60] R A Weinberg. Mechanisms of malignant progression. *Carcinogenesis*, 29(6):1092–1095, April 2008.

[61] G H Sakorafas and M G Sarr. Pancreatic cancer after surgery for chronic pancreatitis. *Digestive and liver disease : official journal of the Italian Society of Gastroenterology and the Italian Association for the Study of the Liver*, 35(7):482–485, July 2003.

[62] Banke Agarwal, Arlene M Correa, and Linus Ho. Survival in pancreatic carcinoma based on tumor size. *Pancreas*, 36(1):e15–20, January 2008.

[63] Masao Tanaka, Suresh Chari, Volkan Adsay, Fernandez-Del Carlos Castillo, Massimo Falconi, Michio Shimizu, Koji Yamaguchi, Kenji Yamao, and Seiki Matsuno. International Consensus Guidelines for Management of Intraductal Papillary Mucinous Neoplasms and Mucinous Cystic Neoplasms of the Pancreas. *Pancreatology*, 6(1-2):17–32, April 2006.

[64] Stefan Fritz, Miriam Klauss, Frank Bergmann, Thilo Hackert, Werner Hartwig, Oliver Strobel, Bogata D Bundy, Markus W Büchler, and Jens Werner. Small (Sendai Negative) Branch-Duct IPMNs. *Annals of surgery*, 256(2):313–320, August 2012.

[65] Min Yu, David T Ting, Shannon L Stott, Ben S Wittner, Fatih Ozsolak, Suchismita Paul, Jordan C Ciciliano, Malgorzata E Smas, Daniel Winokur, Anna J Gilman, Matthew J Ulman, Kristina Xega, Gianmarco Contino, Brinda Alagesan, Brian W Brannigan, Patrice M Milos, David P Ryan, Lecia V Sequist, Nabeel Bardeesy, Sridhar Ramaswamy, Mehmet Toner, Shyamala Maheswaran, and Daniel A Haber. RNA sequencing of pancreatic circulating tumour cells implicates WNT signalling in metastasis. *Nature*, 487(7408):510–513, July 2012.

[66] T Riall, W Nealon, J Goodwin, D Zhang, Y Kuo, C Townsend, and J Freeman. Pancreatic Cancer in the General Population: Improvements in Survival Over the Last Decade. *Journal of Gastrointestinal Surgery*, 10(9):1212–1224, November 2006.

[67] Rahul Pannala, Ananda Basu, Gloria M Petersen, and Suresh T Chari. New-onset diabetes: a potential clue to the early diagnosis of pancreatic cancer. *The Lancet Oncology*, 10(1):88–95, January 2009.

[68] Shyamala Maheswaran and Daniel A Haber. Circulating tumor cells: a window into cancer biology and metastasis. *Current opinion in genetics & development*, 20(1):96–99, February 2010.

[69] V Zieglschmid, C Hollmann, and O Böcher. Detection of disseminated tumor cells in peripheral blood. *Critical reviews in clinical laboratory sciences*, 42(2):155–196, 2005.

[70] E Racila, D Euhus, A J Weiss, C Rao, J McConnell, L W Terstappen, and J W Uhr. Detection and characterization of carcinoma cells in the blood. *Proceedings of the National Academy of Sciences*, 95(8):4589–4594, April 1998.

[71] David R Parkinson, Nicholas Dracopoli, Brenda Gumbs Petty, Carolyn Compton, Massimo Cristofanilli, Albert Deisseroth, Daniel F Hayes, Gordon Kapke, Prasanna Kumar, Jerry SH Lee, Minetta C Liu, Robert McCormack, Stanislaw Mikulski, Larry Nagahara, Klaus Pantel, Sonia Pearson-White, Elizabeth A Punnoose, Lori T Roadcap, Andrew E Schade, Howard I Scher, Caroline C Sigman, and Gary J Kelloff. Considerations in the development of circulating tumor cell technology for clinical use. *Journal of Translational Medicine*, 10(1):1–1, July 2012.

[72] James P Smith, Timothy B Lannin, Yusef Syed, Steven M Santana, and Brian J Kirby. Parametric control of collision rates and capture rates in geometrically enhanced differential immunocapture (GEDI) microfluidic devices for rare cell capture. *Biomedical Microdevices*, 16(1):143–151, February 2014.

[73] Siyang Zheng, Henry Lin, Jing-Quan Liu, Marija Balic, Ram Datar, Richard J Cote, and Yu-Chong Tai. Membrane microfilter device for selective capture, electrolysis and genomic analysis of human circulating tumor cells. *Journal of Chromatography A*, 1162(2):154–161, August 2007.

[74] Christopher M Earhart, Casey E Hughes, Richard S Gaster, Chin Chun Ooi, Robert J Wilson, Lisa Y Zhou, Eric W Humke, Lingyun Xu, Dawson J Wong, Stephen B Willingham, Erich J Schwartz, Irving L Weissman, Stefanie S Jeffrey, Joel W Neal, Rajat Rohatgi, Heather A Wakelee, and Shan X Wang. Isolation and mutational analysis of circulating tumor cells from lung cancer patients with magnetic sifters and biochips. *Lab on a Chip*, 14(1):78–88, January 2014.

[75] AmirAli H Talasaz, Ashley A Powell, David E Huber, James G Berbee, Kyung-Ho Roh, Wong Yu, Wenzhong Xiao, Mark M Davis, R Fabian Pease, and Michael N Mindrinos. Isolating highly enriched populations of circulating epithelial cells and other rare cells from blood using a magnetic sweeper device. *Proceedings of the National Academy of Sciences*, 106(10):3970–3975, 2009.

[76] Giuseppe Galletti, Matthew S Sung, Linda T Vahdat, Manish A Shah, Steven M Santana, Giuseppe Altavilla, Brian J Kirby, and Paraskevi Giannakakou. Isolation of breast cancer and gastric cancer circulating tumor cells by use of an anti HER2-based microfluidic device. *Lab on a Chip*, 14(1):147–156, January 2014.

[77] Steven M Santana, He Liu, Neil H Bander, Jason P Gleghorn, and Brian J Kirby. Immunocapture of prostate cancer cells by use of anti-PSMA antibodies in microdevices. *Biomedical Microdevices*, 14(2):401–407, December 2011.

[78] S L Stott, R J Lee, S Nagrath, M Yu, D T Miyamoto, L Ulkus, E J Inserra, M Ulman, S Springer, Z Nakamura, A L Moore, D I Tsukrov, M E Kempner, D M Dahl, C L Wu, A J Iafrate, M R Smith, R G Tompkins, L V Sequist, M Toner, D A Haber, and S Maheswaran. Isolation and Characterization of Circulating Tumor Cells from Patients with Localized and Metastatic Prostate Cancer. *Science Translational Medicine*, 2(25):25ra23–25ra23, March 2010.

[79] Sendurai A Mani, Wenjun Guo, Mai-Jing Liao, Elinor Ng Eaton, Ayyakkannu Ayyanan, Alicia Y Zhou, Mary Brooks, Ferenc Reinhard, Cheng Cheng Zhang, Michail Shipitsin, Lauren L Campbell, Kornelia Polyak, Cathrin Brisken, Jing Yang, and Robert A Weinberg. The epithelial-mesenchymal transition generates cells with properties of stem cells. *Cell*, 133(4):704–715, May 2008.

[80] Kornelia Polyak and Robert A Weinberg. Transitions between epithelial and mesenchymal states: acquisition of malignant and stem cell traits. *Nature Reviews Cancer*, 9(4):265–273, March 2009.

[81] Michael A Hollingsworth and Benjamin J Swanson. Mucins in cancer: protection and control of the cell surface. *Nature Reviews Cancer*, 4(1):45–60, January 2004.

[82] Kohji Nagata, Michiko Horinouchi, Miyuki Saitou, Michiyo Higashi, Mitsuharu Nomoto, Masamichi Goto, and Suguru Yonezawa. Mucin expression profile in pancreatic cancer and the precursor lesions. *Journal of Hepato-Biliary-Pancreatic Surgery*, 14(3):243–254, May 2007.

[83] L D Roy, M Sahraei, D B Subramani, D Besmer, S Nath, T L Tinder, E Bajaj, K Shanmugam, Y Y Lee, S I L Hwang, S J Gendler, and P Mukherjee. MUC1 enhances invasiveness of pancreatic cancer cells by inducing epithelial to mesenchymal transition. *Oncogene*, 30(12):1449–1459, November 2010.

[84] N Remmers, J M Anderson, E M Linde, D J DiMaio, A J Lazenby, H H Wandall, U Mandel, H Clausen, F Yu, and M A Hollingsworth.

Aberrant Expression of Mucin Core Proteins and O-Linked Glycans Associated with Progression of Pancreatic Cancer. *Clinical Cancer Research*, 19(8):1981–1993, April 2013.

[85] W Qi, B C Schultes, D Liu, M Kuzma, W Decker, and R Madiyalakan. Characterization of an anti-MUC1 monoclonal antibody with potential as a cancer vaccine. *Hybridoma and hybridomics*, 20(5-6):313–324, 2001.

[86] Ravibhushan Singh and Dilip Bandyopadhyay. MUC1: a target molecule for cancer therapy. *Cancer biology & therapy*, 6(4):481–486, April 2007.

[87] Yue Geng, Tait Takatani, Kimberly Yeh, Jong-Wei Hsu, and Michael R King. Targeting Underglycosylated MUC1 for the Selective Capture of Highly Metastatic Breast Cancer Cells Under Flow. *Cellular and Molecular Bioengineering*, 6(2):148–159, May 2013.

[88] B Agrawal, M J Krantz, J Parker, and B M Longenecker. Expression of MUC1 mucin on activated human T cells: implications for a role of MUC1 in normal immune regulation. *Cancer Research*, 58(18):4079–4081, September 1998.

[89] Isabel Correa, Tim Plunkett, Anda Vlad, Arron Mungul, Jessica Candelora Kettel, Joy M Burchell, Joyce Taylor papadimitriou, and Olivera J Finn. Form and pattern of MUC1 expression on T cells activated in vivo or in vitro suggests a function in Tcell migration. *Immunology*, 108(1):32–41, 2003.

[90] Angela Gradilone, Cristina Raimondi, Chiara Nicolazzo, Arianna Petracca, Orietta Gandini, Bruno Vincenzi, Giuseppe Naso, Anna Maria Aglianò, Enrico Cortesi, and Paola Gazzaniga. Circulating tumour cells lacking cytokeratin in breast cancer: the importance of being mesenchymal. *Journal of Cellular and Molecular Medicine*, 15(5):1066–1070, May 2011.

[91] Michael J Swartz, Surinder K Batra, Grish C Varshney, Michael A Hollingsworth, Charles J Yeo, John L Cameron, Robb E Wilentz, Ralph H Hruban, and Pedram Argani. MUC4 expression increases progressively in pancreatic intraepithelial neoplasia. *American journal of clinical pathology*, 117(5):791–796, May 2002.

[92] Hee-Ug Park, Jong-Woo Kim, Grace E Kim, Han-Ik Bae, Suzanne C Crawley, Stacey C Yang, James R Gum, Surinder K Batra, Karine Rousseau, and Dallas M Swallow. Aberrant expression of MUC3 and MUC4 membrane-associated mucins and sialyl lex antigen in pancreatic intraepithelial neoplasia. *Pancreas*, 26(3):e48–e54, 2003.

[93] Shyamala Maheswaran, Lecia V Sequist, Sunitha Nagrath, Lindsey Ulkus, Brian Brannigan, Chey V Collura, Elizabeth Inserra, Sven Diederichs, A John Iafrate, Daphne W Bell, Subba Digumarthy, Alona Muzikansky, Daniel Irimia, Jeffrey Settleman, Ronald G Tompkins, Thomas J Lynch, Mehmet Toner, and Daniel A Haber. Detection of Mutations in EGFRin Circulating Lung-Cancer Cells. *The New England journal of medicine*, 359(4):366–377, July 2008.

[94] J WU, H Matthaei, A Maitra, M Dal Molin, L D Wood, J R Eshleman, M Goggins, M I Canto, R D Schulick, B H Edil, C L Wolfgang, A P Klein, L A Diaz, P J Allen, C M Schmidt, K W Kinzler, N Papadopoulos, R H Hruban, and B Vogelstein. Recurrent GNAS Mutations Define an Unexpected Pathway for Pancreatic Cyst Development. *Science Translational Medicine*, 3(92):92ra66–92ra66, July 2011.

[95] N S Pellegata, F Sessa, B Renault, M Bonato, B E Leone, E Solcia, and G N Ranzani. K-ras and p53 Gene Mutations in Pancreatic Cancer: Ductal and Nonductal Tumors Progress through Different Genetic Lesions. *Cancer Research*, 1994.

[96] Nicholas Navin, Jude Kendall, Jennifer Troge, Peter Andrews, Linda Rodgers, Jeanne McIndoo, Kerry Cook, Asya Stepansky, Dan Levy, Diane Esposito, Lakshmi Muthuswamy, Alex Krasnitz, W Richard McCombie, James Hicks, and Michael Wigler. Tumour evolution inferred by single-cell sequencing. *Nature*, 472(7341):90–94, March 2011.

[97] Emily L Deer, Jessica González-Hernández, Jill D Coursen, Jill E Shea, Josephat Ngatia, Courtney L Scaife, Matthew A Firpo, and Sean J Mulvihill. Phenotype and genotype of pancreatic cancer cell lines. *Pancreas*, 39(4):425–435, May 2010.

[98] M A Hollingsworth, J M Strawhecker, T C Caffrey, and D R Mack. Expression of MUC1, MUC2, MUC3 and MUC4 mucin mRNAs in human pancreatic and intestinal tumor cell lines. *International journal of cancer. Journal international du cancer*, 57(2):198–203, April 1994.

[99] W J Allard. Tumor Cells Circulate in the Peripheral Blood of All Major Carcinomas but not in Healthy Subjects or Patients With Nonmalignant Diseases. *Clinical Cancer Research*, 10(20):6897–6904, October 2004.

[100] James P Smith, Alexander C Barbati, Steven M Santana, Jason P Gleghorn, and Brian J Kirby. Microfluidic transport in microdevices for rare cell capture. *ELECTROPHORESIS*, 33(21):3133–3142, November 2012.

[101] Ashley A Powell, AmirAli H Talasaz, Haiyu Zhang, Marc A Coram, Anupama Reddy, Glenn Deng, Melinda L Telli, Ranjana H Advani,

Robert W Carlson, Joseph A Mollick, Shruti Sheth, Allison W Kurian, James M Ford, Frank E Stockdale, Stephen R Quake, R Fabian Pease, Michael N Mindrinos, Gyan Bhanot, Shanaz H Dairkee, Ronald W Davis, and Stefanie S Jeffrey. Single Cell Profiling of Circulating Tumor Cells: Transcriptional Heterogeneity and Diversity from Breast Cancer Cell Lines. *PLoS ONE*, 7(5):e33788, May 2012.

[102] Zhiwei Wang, Yiwei Li, Aamir Ahmad, Sanjeev Banerjee, Asfar S Azmi, Dejuan Kong, and Fazlul H Sarkar. Pancreatic cancer: understanding and overcoming chemoresistance. *Nature Reviews Gastroenterology and Hepatology*, 8(1):27–33, 2011.

[103] Christopher L Wolfgang, Joseph M Herman, Daniel A Laheru, Alison P Klein, Michael A Erdek, Elliot K Fishman, and Ralph H Hruban. Recent progress in pancreatic cancer. *CA: a cancer journal for clinicians*, 63(5):318–348, July 2013.

[104] Fredrik I Thege, Timothy B Lannin, Trisha N Saha, Shannon Tsai, Michael L Kochman, Michael A Hollingsworth, Andrew D Rhim, and Brian J Kirby. Microfluidic immunocapture of circulating pancreatic cells using parallel EpCAM and MUC1 capture: characterization, optimization and downstream analysis. *Lab on a Chip*, 14(10):1775–1784, May 2014.

[105] Daniel L Adams, Steingrimur Stefansson, Christian Haudenschild, Stuart S Martin, Monica Charpentier, Saranya Chumsri, Massimo Cristofanilli, Cha-Mei Tang, and R Katherine Alpaugh. Cytometric characterization of circulating tumor cells captured by microfiltration and their correlation to the CellSearch(®) CTC test. *Cytometry. Part A : the journal of the International Society for Analytical Cytology*, 87(2):137–144, February 2015.

[106] Abhisek Mitra, Lopa Mishra, and Shulin Li. EMT, CTCs and CSCs in tumor relapse and drug-resistance. *Oncotarget*, 6(13):10697–10711, May 2015.

[107] Mats Grände, Asa Franzen, Jan-Olof Karlsson, Lars E Ericson, Nils-Erik Heldin, and Mikael Nilsson. Transforming growth factor-beta and epidermal growth factor synergistically stimulate epithelial to mesenchymal transition (EMT) through a MEK-dependent mechanism in primary cultured pig thyrocytes. *Journal of Cell Science*, 115(Pt 22):4227–4236, November 2002.

[108] Bahriye Aktas, Mitra Tewes, Tanja Fehm, Siegfried Hauch, Rainer Kimmig, and Sabine Kasimir-Bauer. Stem cell and epithelial-mesenchymal transition markers are frequently overexpressed in circulating tumor cells of metastatic breast cancer patients. *Breast Cancer Research*, 11(4):R46, 2009.

[109] Lars Petter Jordheim, Pascal Sève, Olivier Trédan, and Charles Dumontet. The ribonucleotide reductase large subunit (RRM1) as a predictive factor in patients with cancer. *The Lancet Oncology*, 12(7):693–702, July 2011.

[110] Yuriko Saiki, Yuki Yoshino, Hiroko Fujimura, Tatsuya Manabe, Yuki Kudo, Miki Shimada, Nariyasu Mano, Tomohiro Nakano, Yoonha Lee, Shinjiro Shimizu, Shinya Oba, Sho Fujiwara, Hideyuki Shimizu, Na Chen, Zhaleh Kashkouli Nezhad, Guo Jin, Shinichi Fukushige, Makoto Sunamura, Masaharu Ishida, Fuyuhiko Motoi, Shinichi Egawa, Michiaki Unno, and Akira Horii. Biochemical and Biophysical Research Communications. *Biochemical and Biophysical Research Communications*, 421(1):98–104, April 2012.

[111] Michael Pickup, Sergey Novitskiy, and Harold L Moses. The roles of TGFβ in the tumour microenvironment. *Nature Reviews Cancer*, 13(11):788–799, November 2013.

[112] Hideaki Ijichi, Motoyuki Otsuka, Keisuke Tateishi, Tsuneo Ikenoue, Takayuki Kawakami, Fumihiko Kanai, Yoshihiro Arakawa, Naohiko Seki, Kiyoshi Shimizu, Kohei Miyazono, Takao Kawabe, and Masao Omata. Smad4-independent regulation of p21/WAF1 by transforming growth factor-β. *Oncogene*, 23(5):1043–1051, February 2004.

[113] Ying E Zhang. Non-Smad pathways in TGF-beta signaling. *Cell Research*, 19(1):128–139, January 2009.

[114] Timothy B Lannin, Fredrik I Thege, and Brian J Kirby. Comparison and optimization of machine learning methods for automated classification of circulating tumor cells. *Cytometry Part B: Clinical Cytometry*, 89(10):922–931, October 2016.

[115] Nicholas McGranahan and Charles Swanton. Biological and therapeutic impact of intratumor heterogeneity in cancer evolution. *Cancer Cell*, 27(1):15–26, January 2015.

[116] Nicholas C Turner and Jorge S Reis-Filho. Genetic heterogeneity and cancer drug resistance. *The Lancet Oncology*, 13(4):e178–85, April 2012.

[117] Peter J Campbell, Shinichi Yachida, Laura J Mudie, Philip J Stephens, Erin D Pleasance, Lucy A Stebbings, Laura A Morsberger, Calli Latimer, Stuart McLaren, Meng-Lay Lin, David J McBride, Ignacio Varela, Serena A Nik-Zainal, Catherine Leroy, Mingming Jia, Andrew Menzies, Adam P Butler, Jon W Teague, Constance A Griffin, John Burton, Harold Swerdlow, Michael A Quail, Michael R Stratton, Christine Iacobuzio-Donahue, and P Andrew Futreal. The patterns and dynamics of genomic instability in metastatic pancreatic cancer. *Nature*, 467(7319):1109–1113, October 2010.

[118] R Maddipati and B Z Stanger. Pancreatic Cancer Metastases Harbor Evidence of Polyclonality. *Cancer Discovery*, 5(10):1086–1097, September 2015.

[119] C Li, D G Heidt, P Dalerba, C F Burant, L Zhang, V Adsay, M Wicha, M F Clarke, and D M Simeone. Identification of Pancreatic Cancer Stem Cells. *Cancer Research*, 67(3):1030–1037, February 2007.

[120] Patrick C Hermann, Stephan L Huber, Tanja Herrler, Alexandra Aicher, Joachim W Ellwart, Markus Guba, Christiane J Bruns, and Christopher Heeschen. Distinct Populations of Cancer Stem Cells Determine Tumor Growth and Metastatic Activity in Human Pancreatic Cancer. *Cell Stem Cell*, 1(3):313–323, September 2007.

[121] Anke Van den broeck, Lies Gremeaux, Baki Topal, and Hugo Vankelecom. Human pancreatic adenocarcinoma contains a side population resistant to gemcitabine. *BMC Cancer*, 12:354, August 2012.

[122] G Wayne Brodland. The Differential Interfacial Tension Hypothesis (DITH): A Comprehensive Theory for the Self-Rearrangement of Embryonic Cells and Tissues. *Journal of Biomechanical Engineering*, 124(2):188, March 2002.

[123] M Krieg, Y Arboleda-Estudillo, P H Puech, J Käfer, F Graner, D J Müller, and C P Heisenberg. Tensile forces govern germ-layer organization in zebrafish. *Nature Cell Biology*, 10(4):429–436, March 2008.

[124] A Kicheva, M Cohen, and J Briscoe. Developmental Pattern Formation: Insights from Physics and Biology. *Science*, 338(6104):210–212, October 2012.

[125] Steve Pawlizak, Anatol W Fritsch, Steffen Grosser, Dave Ahrens, Tobias Thalheim, Stefanie Riedel, Tobias R Kießling, Linda Oswald, Mareike Zink, M Lisa Manning, and Josef A Käs. Testing the differential adhesion hypothesis across the epithelial mesenchymal transition. *New Journal of Physics*, 17(8):1–17, August 2015.

[126] Sean Curran, Marguerite M Vantangoli, Kim Boekelheide, and Jeffrey R Morgan. Architecture of Chimeric Spheroids Controls Drug Transport. *Cancer Microenvironment*, 8(2):101–109, August 2015.

[127] Marielena Gamboa Castro, Susan E Leggett, and Ian Y Wong. Clustering and jamming in epithelial-mesenchymal co-cultures. *Soft Matter*, 12(40):8327–8337, October 2016.

[128] Thomas Lecuit and Alpha S Yap. E-cadherin junctions as active mechanical integrators in tissue dynamics. *Nature Cell Biology*, 17(5):533–539, May 2015.

[129] Sandra Citi, Domenica Spadaro, Yann Schneider, Jeffrey Stutz, and Pamela Pulimeno. Regulation of small GTPases at epithelial cell-cell junctions. *Molecular Membrane Biology*, 28(7-8):427–444, July 2011.

[130] Sandra Citi, Diego Guerrera, Domenica Spadaro, and Jimit Shah. Epithelial junctions and Rho family GTPases: the zonular signalosome. *Small GTPases*, 5(4):1–15, 2014.

[131] L P Jordheim. Increased expression of the large subunit of ribonucleotide reductase is involved in resistance to gemcitabine in human mammary adenocarcinoma cells. *Molecular Cancer Therapeutics*, 4(8):1268–1276, August 2005.

[132] Jennifer D Davidson, Liandong Ma, Michael Flagella, Sandaruwan Geeganage, Lawrence M Gelbert, and Christopher A Slapak. An increase in the expression of ribonucleotide reductase large subunit 1 is associated with gemcitabine resistance in non-small cell lung cancer cell lines. *Cancer Research*, 64(11):3761–3766, June 2004.

[133] Gerold Bepler, Zhong Zheng, Ashish Gautam, Swati Sharma, Alan Cantor, Anupama Sharma, W Douglas Cress, Young-Chul Kim, Rafael Rosell, Colleen McBride, Lary Robinson, Eric Sommers, and Eric Haura. Ribonucleotide reductase M1 gene promoter activity, polymorphisms, population frequencies, and clinical relevance. *Lung Cancer*, 47(2):183–192, February 2005.

[134] Jun Wang, Gregory J S Lohman, and JoAnne Stubbe. Enhanced subunit interactions with gemcitabine-5′-diphosphate inhibit ribonucleotide reductases. *Proceedings of the National Academy of Sciences*, 104(36):14324–14329, September 2007.

[135] Zhengming Chen, Jun Zhou, Yingtao Zhang, and Gerold Bepler. Modulation of the ribonucleotide reductase M1-gemcitabine interaction in vivo by N-ethylmaleimide. *Biochemical and Biophysical Research Communications*, 413(2):383–388, September 2011.

[136] Y Aye, M Li, M J C Long, and R S Weiss. Ribonucleotide reductase and cancer: biological mechanisms and targeted therapies. *Oncogene*, 34(16):2011–2021, April 2015.

[137] S Vincent, P Jeanteur, and P Fort. Growth-regulated expression of rhoG, a new member of the ras homolog gene family. *Molecular and Cellular Biology*, 12(7):3138–3148, July 1992.

[138] Hironori Katoh and Manabu Negishi. RhoG activates Rac1 by direct interaction with the Dock180-binding protein Elmo. *Nature*, 424(6947):461–464, July 2003.

[139] H Katoh. Activation of Rac1 by RhoG regulates cell migration. *Journal of Cell Science*, 119(1):56–65, January 2006.

[140] J Meller, L Vidali, and M A Schwartz. Endogenous RhoG is dispensable for integrin-mediated cell spreading but contributes to Rac-independent migration. *Journal of Cell Science*, 121(12):1981–1989, June 2008.

[141] Elena Vigorito, Daniel D Billadeu, Doris Savoy, Simon McAdam, Gina Doody, Phillipe Fort, and Martin Turner. RhoG regulates gene expression and the actin cytoskeleton in lymphocytes. *Oncogene*, 22(3):330–342, January 2003.

[142] Jaap D van Buul, Michael J Allingham, Thomas Samson, Julia Meller, Etienne Boulter, Rafael García-Mata, and Keith Burridge. RhoG regulates endothelial apical cup assembly downstream from ICAM1 engagement and is involved in leukocyte trans-endothelial migration. *The Journal of Cell Biology*, 178(7):1279–1293, September 2007.

[143] Shawn M Ellerbroek, Krister Wennerberg, William T Arthur, Jill M Dunty, Dan R Bowman, Kris A DeMali, Channing Der, and Keith Burridge. SGEF, a RhoG guanine nucleotide exchange factor that stimulates macropinocytosis. *Molecular biology of the cell*, 15(7):3309–3319, July 2004.

[144] Dong Tian, Min Diao, Yuxiang Jiang, Lingfei Sun, Yan Zhang, Zhucheng Chen, Shanjin Huang, and Guangshuo Ou. Anillin Regulates Neuronal Migration and Neurite Growth by Linking RhoG to the Actin Cytoskeleton. *Current Biology*, 25(9):1135–1145, May 2015.

[145] Nao Hiramoto-Yamaki, Shingo Takeuchi, Shuhei Ueda, Kohei Harada, Satoshi Fujimoto, Manabu Negishi, and Hironori Katoh. Ephexin4 and EphA2 mediate cell migration through a RhoG-dependent mechanism. *The Journal of Cell Biology*, 190(3):461–477, August 2010.

[146] Aneta Kwiatkowska, Sebastien Didier, Shannon Fortin, Yayu Chuang, Timothy White, Michael E Berens, Elisabeth Rushing, Jennifer Eschbacher, Nhan L Tran, Amanda Chan, and Marc Symons. The small GTPase RhoG mediates glioblastoma cell invasion. *Molecular cancer*, 11:65, September 2012.

[147] H E Collins, X Zhu-Mauldin, R B Marchase, and J C Chatham. STIM1/Orai1-mediated SOCE: current perspectives and potential roles in cardiac function and pathology. *AJP: Heart and Circulatory Physiology*, 305(4):H446–H458, August 2013.

[148] Jianwei Sun, Fujian Lu, Huifang He, Junling Shen, Jane Messina, Rahel Mathew, Dapeng Wang, Amod A Sarnaik, Wei-Chiao Chang, Minjung

Kim, Heping Cheng, and Shengyu Yang. STIM1- and Orai1-mediated Ca 2+oscillation orchestrates invadopodium formation and melanoma invasion. *The Journal of Cell Biology*, 207(4):535–548, November 2014.

[149] Yih-Fung Chen, Wen-Tai Chiu, Ying-Ting Chen, Pey-Yun Lin, Huey-Jy Huang, Cheng-Yang Chou, Hsien-Chang Chang, Ming-Jer Tang, and Meng-Ru Shen. Calcium store sensor stromal-interaction molecule 1-dependent signaling plays an important role in cervical cancer growth, migration, and angiogenesis. *Proceedings of the National Academy of Sciences of the United States of America*, 108(37):15225–15230, September 2011.

[150] Feng-Chiao Tsai, Akiko Seki, Hee Won Yang, Arnold Hayer, Silvia Carrasco, Seth Malmersjö, and Tobias Meyer. A polarized Ca2+, diacylglycerol and STIM1 signalling system regulates directed cell migration. *Nature Cell Biology*, 16(2):133–144, January 2014.

[151] Y T Chen, Y F Chen, W T Chiu, Y K Wang, H C Chang, and M R Shen. The ER Ca2+ sensor STIM1 regulates actomyosin contractility of migratory cells. *Journal of Cell Science*, 126(5):1260–1267, April 2013.

[152] Shengyu Yang, J Jillian Zhang, and Xin-Yun Huang. Orai1 and STIM1 Are Criticalfor Breast Tumor Cell Migration and Metastasis. *Cancer Cell*, 15(2):124–134, February 2009.

[153] M Eroglu and W B Derry. Your neighbours matter - non-autonomous control of apoptosis in development and disease. *Cell death and differentiation*, 23(7):1110–1118, July 2016.

[154] Kirill S Korolev, Joao B Xavier, and Jeff Gore. Turning ecology and evolution against cancer. *Nature Reviews Cancer*, 14(5):371–380, April 2014.

[155] Eugene Anatoly Yurtsev, Arolyn Conwill, and Jeff Gore. Oscillatory dynamics in a bacterial cross-protection mutualism. *Proceedings of the National Academy of Sciences of the United States of America*, 113(22):6236–6241, May 2016.

[156] X Ma, Z Chen, D Hua, D He, L Wang, P Zhang, J Wang, Y Cai, C Gao, X Zhang, F Zhang, T Wang, T Hong, L Jin, X Qi, S Chen, X Gu, D Yang, Q Pan, Y Zhu, Y Chen, D Chen, L Jiang, X Han, Y Zhang, J Jin, and X Yao. Essential role for TrpC5-containing extracellular vesicles in breast cancer with chemotherapeutic resistance. *Proceedings of the National Academy of Sciences of the United States of America*, 111(17):6389–6394, April 2014.